

**PERFORMANCE STUDY OF OPTICAL COHERENT
AND DIRECT DETECTION DPSK SYSTEMS IN
PRESENCE OF FIBER CHROMATIC DISPERSION**



A Thesis submitted to the Electrical and Electronic
Engineering Department of BUET, Dhaka,
in partial fulfillment of
the requirements for the degree of
Master of Science in Engineering
(Electrical and Electronic)

MOHAMMAD JAHANGIR ALAM



August 1996

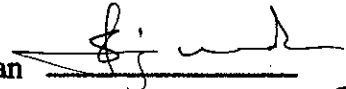
DEDICATED TO MY BELOVED PARENTS

APPROVAL

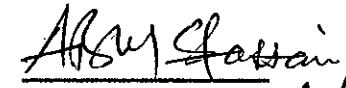
The thesis titled "Performance study of optical coherent and direct detection DPSK systems in presence of fiber chromatic dispersion" submitted by Mohammad Jahangir Alam, Roll no. 921305P, Session 1990-91-92 to the Electrical and Electronic Engineering Department of B.U.E.T has been accepted as satisfactory for partial fulfilment of the requirements for the degree of Master of Science in Engineering (Electrical and Electronic).

Board of Examiners

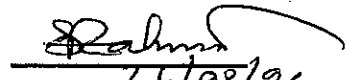
1. Dr. Satya Prasad Majumder
Associate Professor
Department of E.E.E
B.U.E.T, Dhaka- 1000.

Chairman 
(Supervisor) 26.8.96

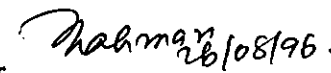
2. Dr. A. B. M. Siddique Hossain
Professor and Head
Department of E.E.E
B.U.E.T, Dhaka- 1000.

Member 
(Ex-officio) 26/08/96

3. Dr. Md. Saifur Rahman
Associate Professor
Department of E.E.E
B.U.E.T, Dhaka- 1000.

Member 
26/08/96

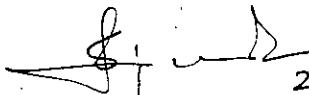
4. Md. Mujibur Rahman
Divisional Engineer
Gulshan Exchange
BTTB, Dhaka- 1000.

Member 
(External) 26/08/96

DECLARATION

This work has been done by me and it has not been submitted elsewhere for the award of any degree or diploma.

Countersigned


26.8.96
(Dr. Satya Prasad Majumder)

Supervisor

Jalam
26.8.96
(Mohammad Jahangir Alam)

CONTENTS

ACKNOWLEDGMENTS	viii
ABSTRACT	ix
LIST OF FIGURES	x
LIST OF PRINCIPAL SYMBOLS	xvii
LIST OF ABBREVIATIONS	xix
1. INTRODUCTION	1
1.1 Introduction to optical communication	1
1.1.1 Advantage of optical communication	3
1.1.2 Limitations of optical communication	6
1.2 Modulation and detection schemes	8
1.3 Review of previous works	10
1.4 Objective of the thesis	11
1.5 Organization of the thesis	12

2.	PERFORMANCE ANALYSIS OF DIRECT DETECTION OPTICAL DPSK SYSTEM IN THE PRESENCE OF FIBRE CHROMATIC DISPERSION	13
2.1	Introduction	13
2.2	The receiver model	14
2.3	Mach-Zehnder Interferometer	16
	2.3.1 MZI configuration and operation	16
	2.3.2 MZI Characteristics	18
2.4	Theoretical analysis	20
	2.4.1 Power spectral densities of the phase noise components	24
	2.4.2 Bit error rate expression	26
2.4	Results and discussions	27
3.	PERFORMANCE ANALYSIS OF OPTICAL HETERODYNE DPSK SYSTEM IN PRESENCE OF LASER PHASE NOISE AND FIBRE CHROMATIC DISPERSION	45
3.1	Introduction	45
3.2	The receiver model	47
3.3	Theoretical analysis	47
3.4	Results and discussions	53

4.	CONCLUSIONS AND SUGGESTIONS FOR FUTURE WORK	77
4.1	Conclusions	77
4.2	Suggestions for future work	79
	REFERENCES	81
APPENDIX A	Expressions of $W_{\phi}^c(f)$ and $W_{\phi}^l(f)$	A-1

ACKNOWLEDGEMENTS

The author would like to acknowledge his profound indebtedness and deep sense of gratitude to his supervisor Dr. Satya Prasad Majumder, Associate Professor of the department of Electrical and Electronic Engineering, B.U.E.T for his sincere guidance, friendly supervision, constant encouragement and valuable suggestions during the vital period of the work.

The author wishes to express his thanks and regards to Dr. A.B.M Siddique Hossain, Professor and Head of the department of Electrical and Electronic Engineering, B.U.E.T for his support to complete this work successfully.

The author also wishes to express his thanks to Dr. Mohammad Ali Choudhury and Dr. Saifur Rahman for their helpful comments and suggestions.

Lastly, the author likes to thank his friends and colleagues for their continuous support and encouragement during the entire progress of the work.

ABSTRACT

A theoretical analysis is provided for optical DPSK transmission system considering the effects of laser phase noise and chromatic dispersion of optical fibre. The analysis is carried out for correlation receivers with direct detection as well as heterodyne detection schemes. The single-mode fibre is modeled as a bandpass filter with flat amplitude response and linear group delay over the optical bandwidth of the modulated optical signal. The statistics of the signal phase fluctuations at the output of the fibre caused by non-linear filtering due to fibre chromatic dispersion are determined in terms of its moments and the probability density function (pdf) of the random phase fluctuation due to laser phase noise and fibre chromatic dispersion is evaluated. The total phase noise power at the output of the receiver photodetector is also expressed in terms of the powers of the cross-modulation and intermodulation frequency noise components.

The expressions for the conditional bit error rates, conditioned on a given value of random phase error and a given transmitted bit is derived as a function of the SNR for both types of detection schemes. The average bit error rate (BER) is then computed numerically by averaging the conditional BER over the probability distribution of the random phase error at a bit error rate of 10 Gb/s. The receiver sensitivities are determined at $BER=10^{-9}$ for dispersion shifted (DS) and nondispersion shifted (NDS) fibres at wavelength of 1.3 μm and 1.55 μm for different values of receiver and system parameters. The penalty due to phase noise and chromatic dispersion suffered by the system is then determined. At a BER of 10^{-9} , the maximum allowable fibre span for a specified power penalty of 1 dB is determined for different values of the fibre dispersion coefficients and normalized laser linewidth.

LIST OF FIGURES

- Fig. 1.1 The spectrum of electromagnetic waves and their applications.
- Fig. 1.2 Block diagram of optical communication system.
- Fig. 1.3 Essentials of a point-to-point fibre optic link.
- Fig. 2.1 Block diagram of optical direct detection DPSK receiver.
- Fig. 2.2 (a) An MZI with large ΔL or narrow wavelength spacing, (b) Transmittance characteristics of MZI and, (c) Differential output of the balanced receiver.
- Fig. 2.3 Bit error rate vs. receiver input power of direct detection optical DPSK transmission system at a bit rate of 10 Gb/s without fibre chromatic dispersion ($D_c=0.0$) for several values of normalized laser linewidth $\Delta\nu T$.
- Fig. 2.4 Bit error rate vs. receiver input power of direct detection optical DPSK transmission system at a bit rate of 10 Gb/s with fibre chromatic dispersion $D_c=1.0$ ps/Km.nm, fibre length $L=25$ Km, at an wavelength $\lambda=1550$ nm for several values of normalized laser linewidth $\Delta\nu T$.
- Fig. 2.5 Bit error rate vs. receiver input power of direct detection optical DPSK transmission system at a bit rate of 10 Gb/s with fibre chromatic dispersion $D_c=1.0$ ps/Km.nm, fibre length $L=50$ Km, at an

wavelength $\lambda=1550$ nm for several values of normalized laser linewidth $\Delta\nu T$.

Fig. 2.6 Bit error rate vs. receiver input power of direct detection optical DPSK transmission system at a bit rate of 10 Gb/s with fibre chromatic dispersion $D_c=3.0$ ps/Km.nm, fibre length $L=25$ Km, at an wavelength $\lambda=1550$ nm for several values of normalized laser linewidth $\Delta\nu T$.

Fig. 2.7 Bit error rate vs. receiver input power of direct detection optical DPSK transmission system at a bit rate of 10 Gb/s with fibre chromatic dispersion $D_c=4.0$ ps/Km.nm, fibre length $L=25$ Km, at an wavelength $\lambda=1550$ nm for a several values of normalized laser linewidth $\Delta\nu T$.

Fig. 2.8 Bit error rate vs. receiver input power of direct detection optical DPSK transmission system at a bit rate of 10 Gb/s with fibre chromatic dispersion $D_c=1.0$ ps/Km.nm, fibre length $L=50$ Km, at an wavelength $\lambda=1300$ nm for a several values of normalized laser linewidth $\Delta\nu T$.

Fig. 2.9 Bit error rate vs. receiver input power of direct detection optical DPSK transmission system at a bit rate of 10 Gb/s with fibre chromatic dispersion $D_c=1.0$ ps/Km.nm, fibre length $L=75$ Km, at an wavelength $\lambda=1300$ nm for a several values of normalized laser linewidth $\Delta\nu T$.

Fig. 2.10 Bit error rate vs. receiver input power of direct detection optical DPSK transmission system at a bit rate of 10 Gb/s with fibre chromatic dispersion $D_c=1.0$ ps/Km.nm, fibre length $L=125$ Km, at

an wavelength $\lambda=1300$ nm for a sevsral values of normalized laser linewidth $\Delta\nu T$.

Fig. 2.11 Bit error rate vs. receiver input power of direct detection optical DPSK transmission system at a bit rate of 10 Gb/s with fibre chromatic dispersion $D_c=2.0$ ps/Km.nm, fibre length $L=50$ Km, at an wavelength $\lambda=1300$ nm for a sevsral values of normalized laser linewidth $\Delta\nu T$.

Fig. 2.12 Bit error rate vs. receiver input power of direct detection optical DPSK transmission system at a bit rate of 10 Gb/s with fibre chromatic dispersion $D_c=3.0$ ps/Km.nm, fibre length $L=50$ Km, at an wavelength $\lambda=1300$ nm for a sevsral values of normalized laser linewidth $\Delta\nu T$.

Fig. 2.13 Penalty in signal power due to combined effect of laser phase noise and fibre chromatic dispersion at $BER=10^{-9}$ versus dispersion coefficient D_c (ps/Km.nm) with fibre length $L=25$ Km for several values of normalized laser linewidth $\Delta\nu T$.

Fig. 2.14 Variation of power penalty (dB) due to combined effect of laser phase noise and fibre chromatic dispersion at $BER=10^{-9}$ with normalized laser linewidth $\Delta\nu T$ for several values of dispersion factor γ .

Fig. 2.15 Variation of power penalty (dB) due to combined effect of laser phase noise and fibre chromatic dispersion at $BER=10^{-9}$ with dispersion factor γ for several values of normalized laser linewidth $\Delta\nu T$.

Fig. 2.16 Plots of allowable fibre length corresponding to 1 dB penalty at $BER=10^{-9}$ as a function of normalized laser linewidth $\Delta\nu T$ for dispersion coefficient $D_c = 1, 2$ and 3 ps/Km.nm.

- Fig. 3.1 Block diagram of optical heterodyne DPSK receiver.
- Fig. 3.2 Bit error rate vs. receiver input power of optical heterodyne DPSK transmission system at a bit rate of 10 Gb/s without fibre chromatic dispersion ($D_c=0.0$) for several values of normalized laser linewidth $\Delta\nu T$.
- Fig. 3.3 Bit error rate vs. receiver input power of optical heterodyne DPSK transmission system at a bit rate of 10 Gb/s with fibre chromatic dispersion $D_c=1.0$ ps/Km.nm, fibre length $L=100$ Km, at an wavelength $\lambda=1550$ nm for several values of normalized laser linewidth $\Delta\nu T$.
- Fig. 3.4 Bit error rate vs. receiver input power of optical heterodyne DPSK transmission system at a bit rate of 10 Gb/s with fibre chromatic dispersion $D_c=3.0$ ps/Km.nm, fibre length $L=100$ Km, at an wavelength $\lambda=1550$ nm for several values of normalized laser linewidth $\Delta\nu T$.
- Fig. 3.5 Bit error rate vs. receiver input power of optical heterodyne DPSK transmission system at a bit rate of 10 Gb/s with fibre chromatic dispersion $D_c=6.0$ ps/Km.nm, fibre length $L=100$ Km, at an wavelength $\lambda=1550$ nm for several values of normalized laser linewidth $\Delta\nu T$.
- Fig. 3.6 Bit error rate vs. receiver input power of optical heterodyne DPSK transmission system at a bit rate of 10 Gb/s with fibre chromatic dispersion $D_c=1.0$ ps/Km.nm, fibre length $L=150$ Km, at an

wavelength $\lambda=1550$ nm for several values of normalized laser linewidth $\Delta\nu T$.

Fig. 3.7 Bit error rate vs. receiver input power of optical heterodyne DPSK transmission system at a bit rate of 10 Gb/s with fibre chromatic dispersion $D_c=1.0$ ps/Km.nm, fibre length $L=200$ Km, at an wavelength $\lambda=1550$ nm for several values of normalized laser linewidth $\Delta\nu T$.

Fig. 3.8 Bit error rate vs. receiver input power of optical heterodyne DPSK transmission system at a bit rate of 10 Gb/s with fibre chromatic dispersion $D_c=1.0$ ps/Km.nm, fibre length $L=500$ Km, at an wavelength $\lambda=1550$ nm for several values of normalized laser linewidth $\Delta\nu T$.

Fig. 3.9 Bit error rate vs. receiver input power of optical heterodyne DPSK transmission system at a bit rate of 10 Gb/s with fibre chromatic dispersion $D_c=1.0$ ps/Km.nm, fibre length $L=100$ Km, at an wavelength $\lambda=1300$ nm for several values of normalized laser linewidth $\Delta\nu T$.

Fig. 3.10 Bit error rate vs. receiver input power of optical heterodyne DPSK transmission system at a bit rate of 10 Gb/s with fibre chromatic dispersion $D_c=3.0$ ps/Km.nm, fibre length $L=100$ Km, at an wavelength $\lambda=1300$ nm for several values of normalized laser linewidth $\Delta\nu T$.

Fig. 3.11 Bit error rate vs. receiver input power of optical heterodyne DPSK transmission system at a bit rate of 10 Gb/s with fibre chromatic dispersion $D_c=9.0$ ps/Km.nm, fibre length $L=100$ Km, at an

wavelength $\lambda=1300$ nm for several values of normalized laser linewidth $\Delta\nu T$.

Fig. 3.12 Bit error rate vs. receiver input power of optical heterodyne DPSK transmission system at a bit rate of 10 Gb/s with fibre chromatic dispersion $D_c=15.0$ ps/Km.nm, fibre length $L=100$ Km, at an wavelength $\lambda=1300$ nm for several values of normalized laser linewidth $\Delta\nu T$.

Fig. 3.13 Bit error rate vs. receiver input power of optical heterodyne DPSK transmission system at a bit rate of 10 Gb/s with fibre chromatic dispersion $D_c=1.0$ ps/Km.nm, fibre length $L=200$ Km, at an wavelength $\lambda=1300$ nm for several values of normalized laser linewidth $\Delta\nu T$.

Fig. 3.14 Bit error rate vs. receiver input power of optical heterodyne DPSK transmission system at a bit rate of 10 Gb/s with fibre chromatic dispersion $D_c=1.0$ ps/Km.nm, fibre length $L=500$ Km, at an wavelength $\lambda=1300$ nm for several values of normalized laser linewidth $\Delta\nu T$.

Fig. 3.15 Penalty in signal power due to combined effect of laser phase noise and fibre chromatic dispersion at $BER=10^{-9}$ versus dispersion coefficient D_c (ps/Km.nm) with fibre length $L=100$ Km and $\lambda=1550$ nm for several values of normalized laser linewidth $\Delta\nu T$.

Fig. 3.16 Penalty in signal power due to combined effect of laser phase noise and fibre chromatic dispersion at $BER=10^{-9}$ versus dispersion coefficient D_c (ps/Km.nm) with fibre length $L=100$ Km and $\lambda=1300$ nm for several values of normalized laser linewidth $\Delta\nu T$.

- Fig. 3.17 Variation of power penalty (dB) due to combined effect of laser phase noise and fibre chromatic dispersion at $BER=10^{-9}$ with normalized laser linewidth $\Delta\nu T$ at $\lambda=1550$ nm for several values of dispersion factor γ .
- Fig. 3.18 Variation of power penalty (dB) due to combined effect of laser phase noise and fibre chromatic dispersion at $BER=10^{-9}$ with normalized laser linewidth $\Delta\nu T$ at $\lambda=1300$ nm for several values of dispersion factor γ .
- Fig. 3.19 Variation of power penalty (dB) due to combined effect of laser phase noise and fibre chromatic dispersion at $BER=10^{-9}$ with dispersion factor γ for several values of normalized laser linewidth $\Delta\nu T$.
- Fig. 3.20 Plots of allowable fibre length corresponding to 1 dB penalty at $BER=10^{-9}$ as a function of normalized laser linewidth $\Delta\nu T$ for dispersion coefficient $D_c = 1, 2$ and 3 ps/Km.nm.

LIST OF PRINCIPAL SYMBOLS

T_b	Bit period
R_b	Bit rate
σ^2	Noise variance
$n(t)$	Complex additive Gaussian noise
Δf	Frequency deviation of FSK signal
ϕ_s	Angle modulation
ϕ_n	Phase noise of the transmitting laser
h	Modulation index
R_d	Photon responsivity
P_s	Input signal power
f_c	Optical carrier frequency
$H(f)$	Optical fibre transfer function
$\Gamma(f)$	Normalized transfer function
λ	Optical wavelength
ν	Frequency of optical carrier
$\Delta\nu$	Normalized linewidth of transmitting laser
τ	Delay occurred due to path difference in MZI
l_1, l_2	Lengths of arms I and II of MZI
T_I, T_{II}	Transmittance of arms I and II of MZI
ΔL	Path difference of MZI
η_{eff}	Effective refractive index of MZI
$E(t)$	Signal input to MZI
$D(\lambda)$	Fibre chromatic dispersion
γ	Dispersion factor

F	Fourrier transform
F^{-1}	Inverse fourrier transform
c	Velocity of light
K	Boltzman's constant
$\delta(t)$	Delta function of time
$W_{\theta}^c(f)$	PSD of cross-power component
$W_{\theta}^I(f)$	PSD of intermodulation power component
$P(\Delta\theta)$	PSD of $\Delta\theta$
N_{shot}	Shot noise power
N_{th}	Thermal noise power
N_{excess}	Excess noise power
α	linewidth enhancement factor
Ω	angular frequency
Γ	damping rate of relaxation oscillations

LIST OF ABBREVIATIONS

ASK	Amplitude shift keying
APD	Avalanche photo diode
BER	Bit error rate
BPPM	Binary PPM
BPSK	Binary PSK
BPF	Bandpass filter
BW	Bandwidth
CPFSK	Continuous phase FSK
CPFSK-DD	CPFSK differential detection
dBm	Decibel relative to 1 mW
DFB	Distributed feedback
DPFSK	Discontinuous phase FSK
DPSK	Differential phase shift keying
erfc	Complementary error function
EMI	Electromagnetic interference
FM	Frequency modulation
FPP	Fabry Perot filter
FSK	Frequency shift keying
FS-SW	Frequency selection Switch
FDM	Frequency division multiplexing
FWM	Four wave mixing
IF	Intermediate frequency

IM/DD	Intensity modulation direct detection
ISI	Inter-symbol interference
LD	Laser diode
LED	Light emitting diode
LO	Local oscillator
LPF	Lowpass filter
LW	Linewidth
MSK	Minimum shift keying
MSK-FM	FM with MSK sub-carrier
MZI	Mach-Zender Interferometer
NRZ	Non-return to zero
OOK	On-off keying
OFD	Optical frequency discriminator
OFDM	Optical frequency division multiplexing
OQPSK	Orthogonal QPSK
PDF	Probability density function
PIN	Positive intrinsic negative
PPM	Pulse position modulation
PRBS	Pseudo-random bit sequence
PSD	Power spectral density
PSK	Phase shift keying
SNR	Signal to noise ratio
WDM	Wavelength division multiplexing

CHAPTER 1

INTRODUCTION



1.1 Introduction to Optical Communication

The modern era of optical communication may be said to have originated with the invention of laser in 1958 and the first developments soon followed the realization of the first lasers in 1961. Compared to the conventional sources of optical frequency, laser radiation is highly monochromatic, coherent and very intense. In fact, it is much more like the radiation generated by a normal microwave transmitter. It is thus a natural step to think of its potential as a carrier for telecommunications. Initially the principal motivation was the enormous bandwidth that would be available, if it were possible to modulate the laser light at only a few percent of its fundamental frequency.

The electromagnetic spectrum shown in fig. 1.1 indicates that visible light extends from 0.4 to 0.7 μm . An appreciable portion of the electromagnetic spectrum is occupied by the optical frequency band. The inquisitive idea of guiding light through a dielectric media strikes human mind to investigate the viability of using this wide optical band for reliable and economical communication with large information capacity.

In 1960, Maiman [1] reported about a ruby laser capable of providing an intense, coherent light source operating at a single wavelength. This development started a number of research activity in optical communication. In 1966, Kao and Hockman [2] reported about an optical fibre of low transmission loss.

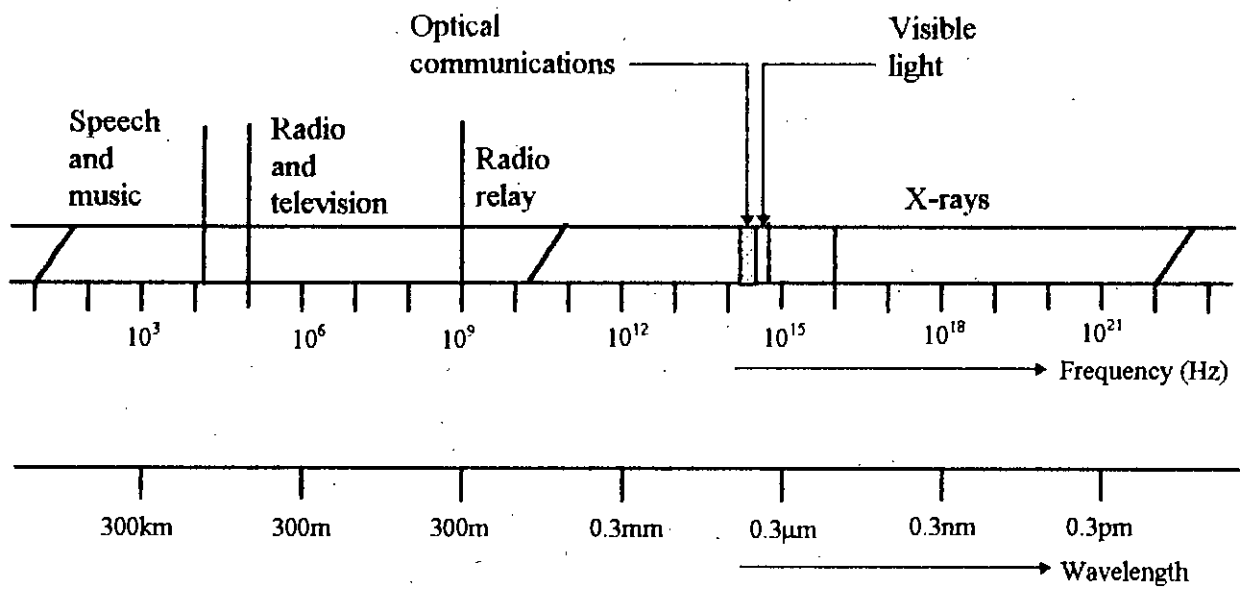


Fig. 1.1 The spectrum of electromagnetic waves and their applications.

Subsequently, sufficient progress has been made in the area of optical fibre communication in various fields. In 1968, the loss in optical fibre was extremely large, about 1000 dB/km at $\lambda=0.82 \mu\text{m}$ [3]. In 1970, Corning Glass Works developed a new fibre of transmission loss of 20 dB/km. At present, single mode fibre of transmission loss of 0.2 dB/km allowing a transmission distance of 850 km is available [3].

In optical communication system electrical signals are first converted into optical signals by means of an optical transducer, such as light emitting diode (LED) or laser diode (LD) and transmitted over long distance via silica glass fibre and then optical signals are again converted to electrical signal by another transducer such as Avalanche photodetector (APD) or PIN photodetector.

1.1.1 Advantages of optical communication

Optical fibre offers some attractive advantages over conventional microwave and RF waveguides. Some important advantages of optical fibre communications are given below [4].

- 1. Very low line attenuation:** Compared to co-axial cable, the loss in optical fibre is very small. For example, a high frequency signal on a conventional co-axial cable losses half of its power after only a few hundred meters, whereas the corresponding figure for optical power in a good optical fibre is 15 Km.
- 2. Higher information capacity:** Since the frequency of the optical carrier is of the order of 10^{14} Hz, which is exceedingly higher than microwave range by a factor of 10^5 , optical communication provides higher information capacity. Due to extremely large bandwidth of optical fibre (approximately 10^{14} Hz), transmission rates exceeding 10 Gbit/sec are possible [4,5]. On the other hand, about 1 Gbit/sec is now achieved with co-axial cables.

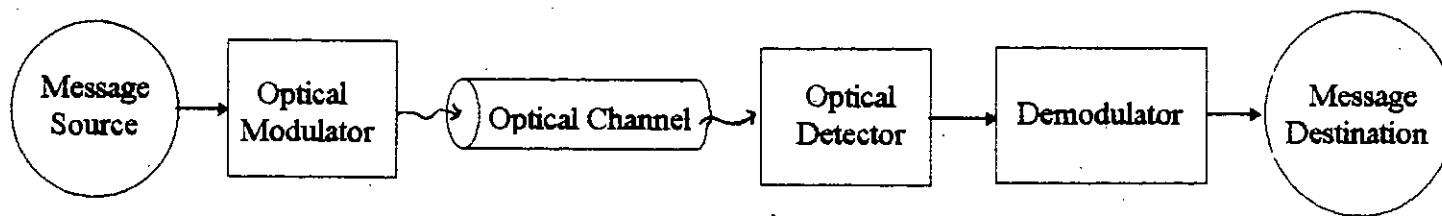


Fig. 1.2: Block diagram of optical communication System

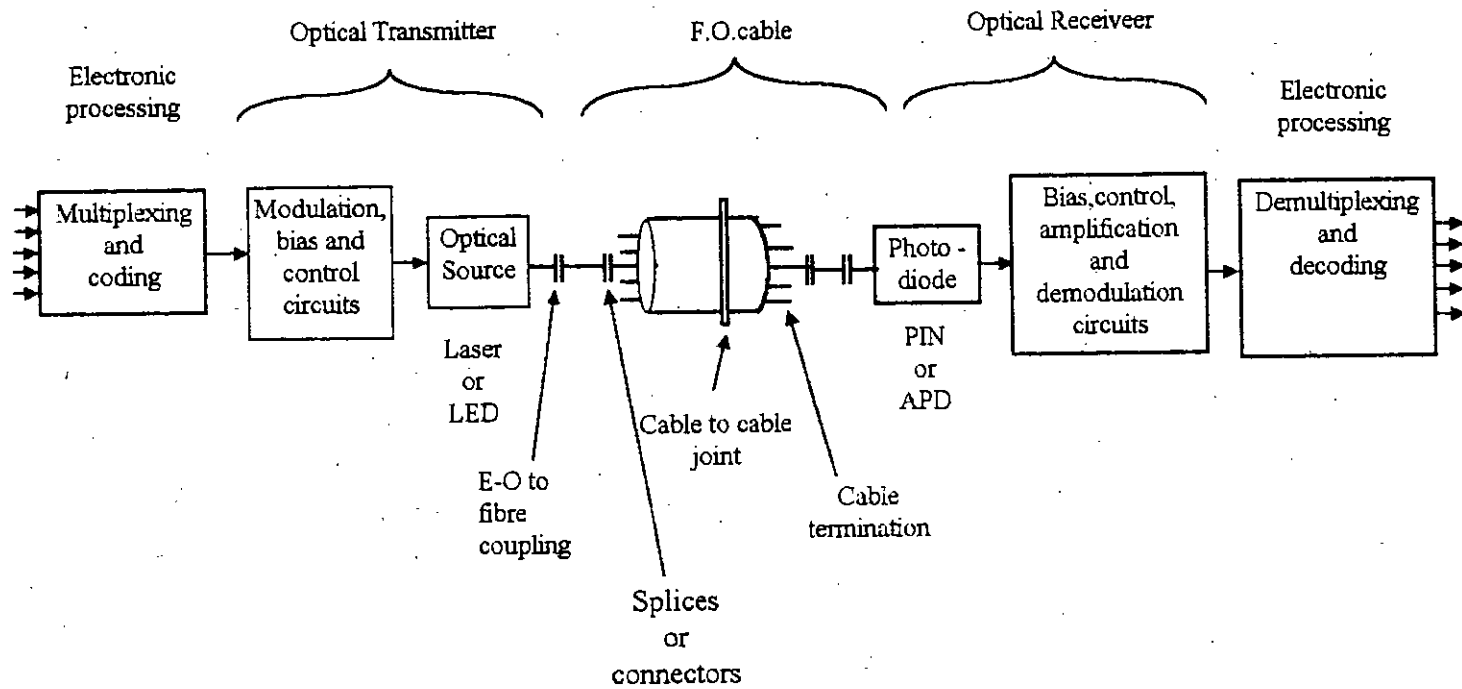


Fig.1.3 Essentials of a point-to-point fibre optic link.

3. Immunity to electromagnetic interference (EMI) and cross talk: Due to dielectric nature of the fibre, optical systems are virtually immune to cross talk and electromagnetic interference (EMI), unlike co-axial cables and microwave links.

4. Considerable reduction in cable size and weight : Due to small fibre diameter (together with a protective plastic coating of 0.25 to 0.5 mm compared to about 10 mm for copper co-axial cables) and low cable weight with considerably greater mechanical flexibility, optical communication provides the advantages of better transport, installation and the less space required in cable duct.

5. No electrical hazards : The fibres need not to be grounded or protected against lightning.

1.1.2 Limitations of optical communication

Optical communication has several difficulties. Since optical carriers have extremely small wavelengths, optical component design is more sophisticated than that of radio or microwave devices. A significant advance was made by the advent of laser as a relatively high powered optical carrier source. Further progress was made by the development of wideband optical modulators and efficient detectors.

Another drawback of optical communication is the effect of the propagation path on the optical carrier wave. This is because optical wavelengths are commensurate with molecule and particle sizes and propagation effects are generated that are uncommon to radio and microwave frequencies. Furthermore, these effects tend to be stochastic and time-varying in nature, which hinders accurate propagation modeling.

An optical signal becomes increasingly distorted as it travels along a fibre. This distortion is the consequence of intermodal dispersion and intermodal delay effects. This distortion effects can be explained by examining the behaviour of

group velocities of the guided modes, where the group velocity is the speed at which energy in a particular mode travels along the fibre. Intermodal dispersion is pulse spreading that occurs within a single mode. Since the group velocity is a function of wavelength λ , intermodal dispersion is, therefore, often referred to as chromatic dispersion. Since intermodal dispersion depends on the wavelength, its effect on signal distortion increases with the spectral width of the optical source. This spectral width is the band of wavelengths over which the source emits light. For example if the peak emission wavelength of a light emitting diode (LED) source is 850 nm, a typical source spectral width would be 40 nm; that is, the source emits most of its optical power in the 830 to 870 nm wavelength band. Laser diode optical sources have much narrower spectral widths, typical value being 1 to 2 nm.

The two main causes of intermodal dispersion are:

- (i) material dispersion, which arises from the variation of refractive index of core material as function of wavelength. This causes a wavelength dependence of the group velocity of any given mode.
- (ii) waveguide dispersion, which occurs because the modal propagation constant β is a function of r/λ (the optical fibre dimension relative to the wavelength λ , where r is the core radius).

The other factor giving rise to pulse spreading is intersymbol delay which is a result of each mode having a different value of group velocity at a single frequency. Of these three, waveguide dispersion usually can be ignored in multimode fibres. However, this effect can be significant in single mode fibres. The full effects tend to be mitigated by other factors, such as nonideal index profiles, optical power launching conditions (different amounts of optical power launched into the various modes), nonuniform mode attenuation, mode mixing in the fibre and in splices, and by statistical variations of these effects along the fibre.

1.3 Modulation and Detection Schemes

Depending on the specific application, various modulation and demodulation formats similar to those of traditional radio frequency communication are also employed in coherent lightwave transmission. These includes: binary PSK (BPSK), quadri PSK (QPSK), orthogonal QPSK (OQPSK), continuous phase FSK (CPFSK), discontinuous phase FSK (DPFSK), minimum shift keying (MSK), differential PSK (DPSK), binary pulse position modulation (BPPM), etc. Each of the modulation schemes viz. ASK, FSK, DPSK, etc. combination thereof, with homodyne, heterodyne or diversity receivers has its own merits and weaknesses and none has emerged as absolutely preferable. However, in optical communication, FSK systems are more promising than ASK or PSK for the following reasons [5]

- (i) modulation can be easily performed using direct modulation of laser diode (LD) through its injection current,
- (ii) direct FSK modulation gives large transmitting power without external modulator loss,
- (iii) distributed feedback (DFB) LDs without external cavities achieve stable operation,
- (iv) optical frequency division multiplexing is possible.

In optical communication system, broadly categorizing, two important detection strategies are normally employed, viz. direct detection and coherent detection. In direct detection reception, the intensity of the received optical field is directly converted to a current by a photodetector while in coherent detection, the received optical field is combined with the light output from a local oscillator (LO) laser and the mixed optical field is converted to an intermediate frequency (IF)

signal by heterodyning or directly to the baseband by homodyning. The first optical communication system employed intensity modulation direct detection (IMDD) technique and in spite of low receiver sensitivity, this scheme is still very popular for commercial application due to its low cost and simplicity [2,6]. However, the direct detection technique has the limitation in data rate for application in power limited free space optical channels due to relatively low optical power output of semiconductor laser diode [6]. To increase the data rate throughput of all semiconductor free space optical channels, extensive research for bandwidth, power efficient coding and modulation scheme were carried out in the last decade. Direct detection optical communication systems are very promising for future deep space application, inter-satellite links and terrestrial line of sight communication [6,7].

Coherent optical transmission systems using heterodyne or homodyne detection are attractive due to their improved receiver sensitivity compared to conventional IMDD systems and its enhanced frequency selectivity in optical frequency division multiplexing (OFDM) system [8]. Heterodyne detection systems have 10-20 dB performance improvement over direct detection system because of the use of local oscillator (LO). Significant progress has been made on coherent optical systems during the last decade and it has become more than just a promise for future application. Although some technical and financial difficulties have still to be completely overcome before coherent systems become of common use, field trials have begun to be successfully reported upon by the most important industries in the world for long-haul (point-to-point) transmission and also for multi-channel applications [9].

To achieve high receiver sensitivity using coherent detection, there are a number of practical problems which one encounters. The performance of coherent receiver can be severely degraded by i) the intensity fluctuation of the receiver's local oscillator (LO), ii) the phase noise of transmitting laser, iii) the transmission

medium limitations such as the polarization problems and chromatic dispersion of the optical fibres in a coherent transmission system.

1.4 Review of previous works

Considerable progress accomplished in the last few years in the development of very high speed optical fibre systems has resulted successful transmission experiments at bit rates of about and above 10 Gb/sec [10]. However, at these bit rates direct intensity modulation of semiconductor lasers produces significant linewidth broadening. A sufficient amount of research works have been reported, which encounters the degrading effects of laser phase noise, nonuniform FM response of distributed feedback (DFB) laser, nonlinear effects of optical fibre etc. on coherent and direct detection optical transmission systems. A key problem for high speed (>5Gb/sec) lightwave systems at 1550 NM wavelength is a high chromatic dispersion of conventional single mode fibres which are optimized for transmission at 1310 nm. When distributed feedback (DFB) lasers are intensity modulated for direct detection (IM/DD) systems, they are normally driven with current that swing from near threshold to well above threshold, producing significant chirp along with the desired intensity modulation, which causes severe system degradations when fibre dispersion is present [11]. DFB lasers can be directly modulated to produce frequency shift keying (FSK) and differential phase shift keying (DPSK) signals by driving them with a bias current far above threshold and adding a relatively small modulation current[12].

In single-mode fibre transmission systems operated at high modulation rates over long fibre spans, chromatic dispersion can produce distortion in the demodulated waveform, resulting in intersymbol interference in the received signal and a reduction of transmission system performance. Using computer simulation and laboratory experiments the chromatic dispersion limitations for direct detection

and coherent optical frequency shift keying (FSK) and differential phase shift keying (DPSK) transmission systems are determined from eye-closure penalties [13]. The chromatic dispersion limitations were also studied by considering the effect of PM to AM conversion for a sinusoidally phase-modulated source [14,15]. The dispersion penalty associated with this effect for random data sequence was not evaluated because of the complexity involved in solving the problem analytically. Prior to this work, the chromatic dispersion limitations for FSK transmission systems with direct detection have been evaluated [10]. In order to quantify the effects of chromatic dispersion on optical DPSK in presence of laser phase noise, an accurate analysis is required.

1.5 Objectives of the Thesis.

The main objective of this thesis is to analyze optical DPSK transmission system with random non-return to zero (NRZ) data taking into account the effects of laser phase noise and fibre chromatic dispersion. The analysis will be carried out for both Mach-Zehnder interferometer (MZI) based direct detection receiver and delay demodulation heterodyne receiver.

Further objective is to develop an analytical expression for the probability density function (pdf) of the random phase function due to combined effect of chromatic dispersion and phase noise and to derive the bit error rate (BER) expressions for both direct detection and heterodyne DPSK receivers. Following the theoretical development, the bit error rate performance results will be evaluated at a bit rate of 10 Gb/sec for dispersion shifted (DS) fibres at an wavelength of 1.3 μm and NDS fibres at 1.55 μm for several dispersion coefficients. The degradations of the system performance in terms of power penalty due to above effects will also be estimated for a specified bit error rate and the maximum allowable fibre length for a specified system penalty will be determined.

1.6 Organization of the thesis

In chapter 1, a brief introduction to optical communication is presented. The major features of optical communication system are discussed in brief. A review of the research works currently going on in the related field is also presented in this chapter.

In chapter 2, a theoretical analysis for optical DPSK system is presented to evaluate the bit error rate (BER) performance with MZI based direct detection receiver including the effects of laser phase noise and fibre chromatic dispersion. The results are presented for a bit rate of 10 Gb/s with several sets of receiver and fibre parameters.

In chapter 3, a theoretical analysis is presented to evaluate the bit error rate (BER) performance of heterodyne optical DPSK receiver taking into account the above system imperfections and the results are presented at a bit rate of 10 Gb/s for different values of receiver and fibre parameters.

In chapter 4, concluding remarks on this work and some recommendations for future work are presented.

CHAPTER 2

PERFORMANCE ANALYSIS OF DIRECT DETECTION OPTICAL DPSK SYSTEM IN THE PRESENCE OF FIBRE CHROMATIC DISPERSION

2.1 Introduction

Differential phase shift keying (DPSK) is one of the most attractive modulation scheme in direct detection and coherent optical communication system due to the fact that it has a compact spectrum and it can take the advantage of direct frequency modulation characteristics of distributed feedback (DFB) laser [16]. However, the performance of the system is highly degraded due to the laser phase noise and fibre chromatic dispersion. Coherent systems, in general, offer 10-20 dB performance gain over direct detection systems [17]. However, the whole system is more complex and costly compared to the direct detection system, because of the requirement of the narrow line width (LW) laser at both transmitter

and receiver for the coherent case and the additional circuits for polarization matching between the received optical field and locally generated optical field.

The direct detection systems, on the other hand, are less sensitive to laser phase noise because the detection does not utilize the phase information. Although the direct detection systems are less sensitive than heterodyne detection system, they provide the advantage of low cost and simplicity. As a result, there has been a growing research interest in direct detection for optical DPSK systems. Recently a direct detection DPSK receiver which utilizes a Mach-Zehnder Interferometer as an optical discriminator is reported [16]. However, performance degradation of this type of receiver due to fibre chromatic dispersion is yet to be determined analytically.

In this chapter, we provide the theoretical analysis of direct detection optical receiver with Mach-Zehnder Interferometer (MZI) as an optical frequency discriminator (OFD) considering the effects of laser phase noise and fibre chromatic dispersion. This chapter begins with an introduction of the receiver model which is followed by a brief description of the OFD, the Mach-Zehnder interferometer. The theoretical analysis of the receiver is provided to evaluate the bit error rate (BER) considering the effects of laser phase noise and fibre chromatic dispersion. The chapter has been concluded with results and discussion.

2.2 The receiver model

The block diagram of the DPSK direct detection receiver with MZI considered for analysis is shown in Fig. 2.1. The MZI acts as an optical filter and differentially detects the 'mark' and 'space' of received DPSK signal which are then directly fed to a pair of photodetectors. The difference of the two photocurrents is applied to the amplifier whose output is then passed through a baseband filter. The output of the baseband filter is sampled periodically and then compared with a

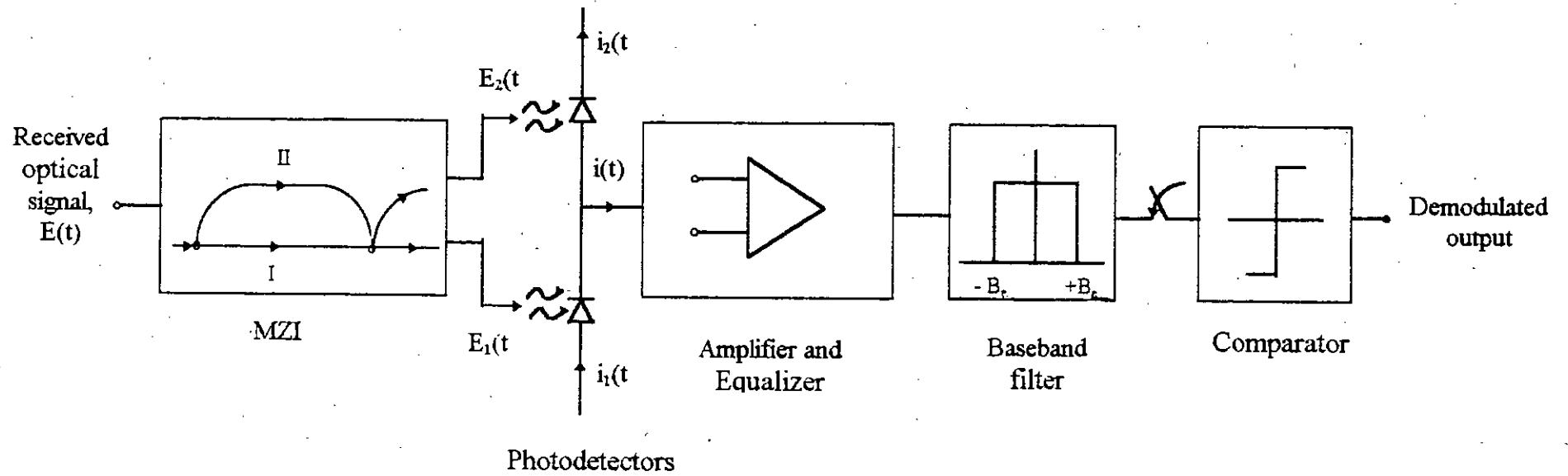


Fig.2.1 Block diagram of a DPSK direct detection receiver.

threshold of zero value in order to determine whether the transmitted symbol corresponds to a ONE or a ZERO.

2.3 Mach-Zehnder Interferometer (MZI)

The most common interference filters are designed to transmit a narrow band of wavelengths and blocks all wavelengths outside the band. Two common filters used as OFD are Mach-Zehnder interferometer (MZI) and Fabry Perot interferometer (FPI). In our receiver model, the first one, MZI is employed. Integrated MZI, consisting of silica based waveguide, is a very promising device in wavelength division multiplexing (WDM) and frequency division multiplexing (FDM) systems and extensive work is now going on employing MZI as OFD, channel selective filter and modulator [18]. Recently an experimental demonstration employing 10 Gbit/s modulation using a III-V semiconductor MZ interferometer has been reported [19].

2.3.1 MZI configuration and operation

The basic configuration of MZI is shown in Fig. 2.2. They have two input ports, two output ports, two 3 dB couplers and two waveguide arms with length difference ΔL . A thin film heater is placed in one of the arms. It acts as a phase shifter because the light path length of the heated waveguide arm changes due to the change of refractive index. The phase shifter is used for precise frequency tuning. These outputs are differentially detected by the photodetectors with balanced configuration.

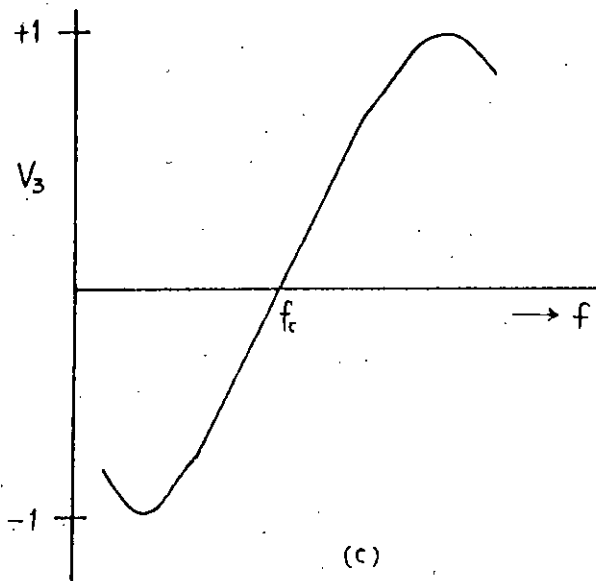
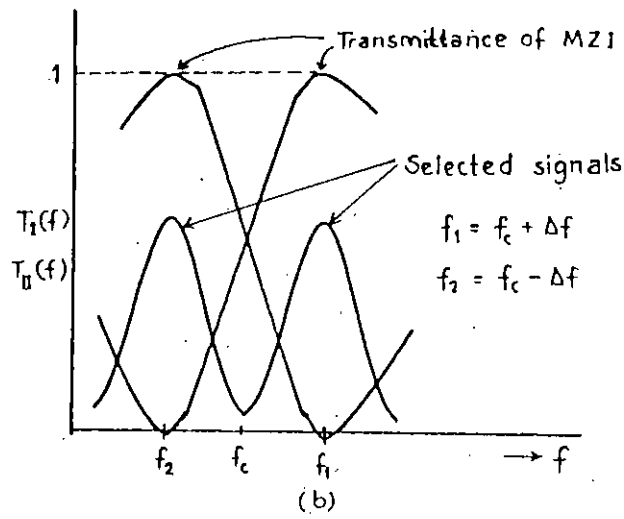
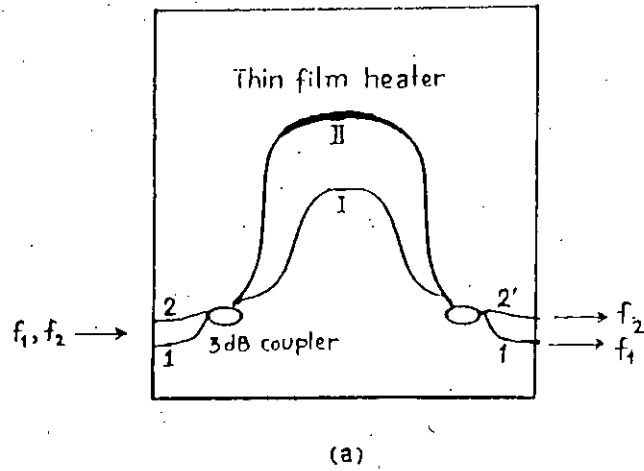


Fig. 2.2

(a) An MZI with large ΔL or more narrow wavelength spacing,
 (b) Transmittance characteristics of MZI and (c) Differential output
 of the balanced receiver.

2.3.2 MZI Characteristics

If $E(t)$ represents the signal input to the MZI, then the signals received at the output ports can be expressed as[20,21]

$$|E_2(t)| = |E(t)| \sin \left[\frac{k(l_2 - l_1)}{2} \right] \quad (2.1)$$

and

$$|E_1(t)| = |E(t)| \cos \left[\frac{k(l_2 - l_1)}{2} \right] \quad (2.2)$$

where l_1 and l_2 are the length of two arms of MZI and k is the wave number which can be expressed as

$$k = \frac{w}{v} = \frac{2\pi}{\lambda} = \frac{2\pi f \eta_{\text{eff}}}{c} \quad (2.3)$$

η_{eff} , f and c are the effective refractive index of the wave guide, frequency of optical input signal and velocity of light in vacuum, respectively.

The transmittance of arm II of MZI

$$T_{\text{II}}(f) = \frac{|E_2(t)|^2}{|E(t)|^2} = \sin^2 \left[\frac{k(l_2 - l_1)}{2} \right] = \sin^2 \theta \quad (2.4)$$

and that of arm I of MZI is

$$T_{\text{I}}(f) = \frac{|E_1(t)|^2}{|E(t)|^2} = \cos^2 \left[\frac{k(l_2 - l_1)}{2} \right] = \cos^2 \theta \quad (2.5)$$

where, θ is the phase factor related to the arm path difference $\Delta L = l_2 - l_1$ and can be expressed as

$$\theta = \frac{k\Delta L}{2} = \frac{\pi f \eta_{\text{eff}} \Delta L}{c} \quad (2.6)$$

Normally ΔL is chosen as

$$\Delta L = \frac{c}{4\eta_{\text{eff}} \Delta f} \quad (2.7)$$

Therefore,

$$\theta = \frac{\pi f}{4\Delta f} \quad (2.8)$$

Then we get

$$T_{\text{II}}(f) = \sin^2\left(\frac{\pi f}{4\Delta f}\right) \quad (2.9)$$

and,

$$T_{\text{I}}(f) = \cos^2\left(\frac{\pi f}{4\Delta f}\right) \quad (2.10)$$

The outputs of the MZI are therefore anti-symmetric and are shown in fig. 2.2

For an MZI used as an OFD, Δf is so chosen that [20,21], $\Delta f = \frac{f_c}{2n+1}$, f_c is the carrier frequency of the DPSK signal and n is an integer.

The MZI is used in our analysis only as optical delay line discriminator as our analysis is based on single channel operation. The complete potential of an MZI can be extracted when a multiplexer/ demultiplexer or a frequency selection

switch for a multi channel WDM/ FDM system is fabricated utilizing the periodicity of the transmittance versus frequency characteristic of an MZI[20,21].

2.4 Theoretical analysis

An schematic diagram of a DPSK direct detection system using a dual detector optical receiver is shown in fig.2.1. The DPSK modulated optical signal at the output of DFB laser is given by

$$\chi_i(t) = \sqrt{2P_s} \exp \{j[\omega_c t + \phi_s(t) + \Phi_n(t)]\} \quad (2.11)$$

where, P_s = average optical power at the input of fibre

ω_c = optical carrier angular frequency

$\theta(t)$ = modulating phase, and

$\Phi_n(t)$ = instantaneous laser phase noise due to the transmitter laser

The modulated phase $\phi_s(t)$ is modeled by

$$\phi_s(t) = \sum_i \phi_i u_T(t - iT) \quad (2.12)$$

where, u_T = unit amplitude rectangular pulse of duration T

ϕ_i = data phase transmitted during the interval $iT \leq t \leq (i-1)T$

which is given by

$$\phi_i = \phi_{i-1} + \Delta\phi_i = \phi_{i-1} + \pi(1 - a_i) / 2 \quad (2.13)$$

where $\{a_i\}$ is the binary data sequence, which assumes values +1 and -1, corresponding to symbol ONE and ZERO, with equal probability of occurrence.

The low-pass equivalent model for single-mode fibre transfer function which includes the chromatic dispersion effect can be modeled as [13],

$$H(f) = e^{-j\alpha f^2} = \exp\left[-j\left\{\alpha B^2 \left(\frac{f}{B}\right)^2\right\}\right] \quad (2.14)$$

where, $\alpha = \pi D(\lambda)L \frac{\lambda^2}{c}$; $D(\lambda)$ is the fibre chromatic dispersion factor, λ is the wavelength of optical carrier, c is the speed of light and L is the length of fibre, B is the data rate.

The optical signal at the output of the fibre can be obtained as

$$\begin{aligned} \chi_o(t) &= \int_0^\infty h(\tau) \chi_i(t-\tau) d\tau \\ &= \sqrt{2P_S} \left[\int_0^\infty h(\tau) e^{-j2\pi f_c \tau} e^{j\phi(t-\tau)} \right] e^{j2\pi f_c t} d\tau \end{aligned} \quad (2.15)$$

The total output phase of the optical signal at the fibre output is given by the argument of the modulation factor in equation (2.15). Thus, output phase

$$\begin{aligned} \theta_o(t) &= \text{Im} \left[\log \int_0^\infty h(\tau) e^{-j2\pi f_c \tau} e^{j\phi(t-\tau)} d\tau \right] \\ &= \text{Im} \left[\log \int_0^\infty h(\tau) e^{j\phi(t-\tau)} d\tau \right] + \text{Im} \log \{ e^{-2\pi f_c \tau} \} \end{aligned}$$

$$= \theta(t) + \beta_0 \quad (2.16)$$

where, $\theta(t)$ is the time-dependent component of the output phase $\theta_0(t)$ and β_0 is the carrier phase shift. Following Ref. [13], it is shown in Appendix that the output phase $\theta(t)$ can be expanded as

$$\begin{aligned} \theta(t) &= \text{Re}\{\phi_0(t)\} + \sum_{n=2}^{\infty} \frac{1}{n!} \text{Im}(i^n f_n) \\ &= \theta_s(t) + \theta_n(t) \end{aligned} \quad (2.17)$$

$$\text{where, } \phi_0(t) = \int_0^{\infty} h(\tau) \phi(t-\tau) d\tau \quad (2.18)$$

and the coefficients f_n are given by [22]

$$f_2 = F_2$$

$$f_3 = F_3$$

$$f_4 = F_4 - 3F_2^2$$

$$f_5 = F_5 - 10F_3F_2$$

$$f_6 = F_6 - 15F_4F_2 - 10F_3^2 + 30F_2^3$$

$$f_7 = F_7 - 21F_5F_2 - 35F_4F_2 + 210F_3F_2^2$$

$$\text{and, } F_n = \int_0^{\infty} h(\tau) [\phi_0(t-\tau) - \phi_0(t)]^n d\tau \quad (2.19)$$

In equation (2.17), $\theta_s(t)$ represents the output phase due to linear filtering and $\theta_n(t)$ represents the phase arising out due to non-linear filtering effects of fibre dispersion, and consists of cross-modulation and intermodulation phase noise terms.

The fibre output signal can be rewritten as

$$\begin{aligned} \chi_o(t) &= \sqrt{2P_s} e^{j\theta(t) + j2\pi f_c t} \\ &= \sqrt{2P_s} e^{j2\pi f_c t + j\theta_s(t) + j\theta_n(t)} \end{aligned} \quad (2.20)$$

The linear phase $\theta_s(t)$ can be expressed as

$$\begin{aligned}
\theta_s(t) &= \text{Re} \left[\int_0^\infty h(\tau) \phi(t-\tau) d\tau \right] \\
&= \text{Re} \left[\int_0^\infty h(\tau) \{ \phi_s(t-\tau) + \phi_n(t-\tau) \} d\tau \right] \\
&= \text{Re} \left[\int_0^\infty h(\tau) \phi_s(t-\tau) d\tau \right] + \text{Re} \left[\int_0^\infty h(\tau) \phi_n(t-\tau) d\tau \right] \\
&= \theta_s'(t) + \theta_n'(t) \tag{2.21}
\end{aligned}$$

where $\theta_s'(t)$ and $\theta_n'(t)$ represents the output phase corresponding to modulated phase $\phi_s(t)$ and laser phase noise $\phi_n(t)$ respectively.

The optical signal at the input to the balanced photodetector is now given by

$$\begin{aligned}
E_0(t) &= \sqrt{2P_S} \exp[j\{2\pi f_c t + \theta_s'(t) + \theta_n'(t) + \theta_n(t)\}] \\
&= \sqrt{2P_S} \exp[j\{\omega_c t + \theta_s'(t) + \theta_{nt}(t)\}] \tag{2.22}
\end{aligned}$$

$$\text{where, } \theta_m(t) = \theta_n'(t) + \theta_n(t)$$

The output current of upper photodetector is given by

$$\begin{aligned}
i_2(t) &= R_d |E_2(t)|^2 \\
&= \frac{R_d P_S}{2} [1 - \cos\{2\pi f_c \tau + \Delta\theta_s'(t, \tau) + \Delta\theta_m(t, \tau)\}] + n_2(t) \tag{2.23}
\end{aligned}$$

where, R_d is the responsivity of the photodetector, $n_2(t)$ represents the photodetector shot noise and pre-amplifier thermal noise.

$$\Delta\theta_s'(t, \tau) = \theta_s'(t) - \theta_s'(t-\tau) \text{ and,} \tag{2.25}$$

$$\Delta\theta_m(t, \tau) = \theta_m(t) - \theta_m(t-\tau) \tag{2.26}$$

Similarly, the output current at the lower photodetector can be expressed as

$$\begin{aligned}
i_1(t) &= R_d |E_1(t)|^2 \\
&= \frac{R_d P_S}{2} [1 + \cos\{2\pi f_c \tau + \Delta\theta_s'(t, \tau) + \Delta\theta_m(t, \tau)\}] + n_1(t) \tag{2.27}
\end{aligned}$$

The output of the balanced photodetector is then found as

$$\begin{aligned} i(t) &= i_2(t) - i_1(t) \\ &= R_d P_s \sum u_T(t - iT) \cos[\omega_c \tau + \Delta\theta'_s(t, \tau) + \Delta\theta_{nt}(t, \tau)] + n_0(t) \end{aligned} \quad (2.28)$$

For DPSK demodulation, $\tau = T$ and, $\omega_c \tau = 2n\pi$

For a 'mark' transmission, $a_i = +1$, $\Delta\theta'_s = 0.0$, we get

$$\begin{aligned} i_m(t) &= R_d P_s \sum u_T(t - iT) \cos[(2n\pi + \Delta\theta'_s(t, T) + \Delta\theta_{nt}(t, T))] \\ &= R_d P_s [x(t)] \end{aligned} \quad (2.29)$$

where, $x(t) = \cos[\Delta\theta_m(t)]$

2.4.1 Power spectral densities of the phase noise components

The psd of the balanced photodetector output noise $n_0(t)$ is given by [21]

$$S_{pd}(f) = eR_d P_s + 0.5R_d P_s^2 [S_X - \bar{X}^2 \delta(f)] \quad (2.30)$$

where,

$$S_X(f) = W_{\Delta\theta_m}(f)$$

$$\text{and, } W_{\Delta\theta_m}(f) = W_{\Delta\theta'_s}(f) \otimes W_{\Delta\theta_n}(f)$$

where, $W_{\Delta\theta_n}(f)$ is the psd of laser phase noise and is given by [23]

$$W_{\Delta\theta_n}(f) = 4\pi\Delta\nu_0 \left(\frac{1 - \cos\omega T}{\omega^2} \right) \left\{ 1 + \frac{\alpha^2 \Omega^4}{[(\omega - \Omega)^2 + \Gamma^2][(\omega + \Omega)^2 + \Gamma^2]} \right\} \quad (2.31)$$

where, $\Delta\nu_0 = \text{Schawlow-Tones linewidth}$

$\alpha = \text{linewidth enhancement factor}$

$\Omega = \text{angular frequency}$

$\Gamma = \text{damping rate of relaxation oscillations}$

Total noise power at the LPF output is

$$\sigma_m^2 = \sigma_s^2 = \int_{-\infty}^{\infty} [S_{pd}(f) + S_{th}(f)] |H_{LPF}(f)|^2 df \quad (2.32)$$

$$\text{Here, } S_{th}(f) = \frac{4KT}{R_L}$$

where, K is the Boltzman's constant, T is receiver temperature in $^{\circ}$ K and R_L is the receiver load resistance.

The psd of non-linear signal component is

$$W_{\Delta\theta'_n}(f) = W_{\theta}^C(f) + W_{\theta}^I(f) \quad (2.33)$$

where, $W_{\theta}^C(f)$ and $W_{\theta}^I(f)$ represent the psd of the cross-power components and inter-modulation components and are given by [Appendix A]

$$W_{\theta}^C(f) = 2W_{\phi}(f) \int_{-\infty}^{\infty} W_{\phi}(\rho) [\cos\{2\alpha(f^2 + f\rho + \rho^2)\} - 1] d\rho \quad (2.34)$$

$$W_{\theta}^I(f) = \frac{1}{6} \int_{-\infty}^{\infty} d\rho \int_{-\infty}^{\infty} d\sigma W_{\phi}(\rho) W_{\phi}(\sigma) W_{\phi}(f - \rho - \sigma) |S(f)|^2 \quad (2.35)$$

where,

$$|S(f)|^2 = |S_1(f)|^2 + |S_2(f)|^2 \quad (2.36)$$

$$S_1(f) = 2\cos(\alpha a) - \cos(\alpha b) - \cos(\alpha c) - \cos(\alpha d) + \cos(\alpha e) \quad (2.37)$$

$$S_2(f) = 2\sin(\alpha a) + \sin(\alpha b) + \sin(\alpha c) + \sin(\alpha d) - \sin(\alpha e) \quad (2.38)$$

with,

$$a = 2\rho^2 + 2\sigma^2 + f^2 - 2f\rho + 2\rho\sigma - 2f\sigma$$

$$b = f^2 + 2\rho^2 + 2\sigma^2 - 2f\rho + 4\rho\sigma - 2f\sigma$$

$$c = f^2 + 2\rho^2 - 2f\rho$$

$$d = f^2 + 2\sigma^2 - 2f\sigma$$

$$e = f^2$$

The final form of $|S(f)|^2$ is found to be

$$\begin{aligned}
 |S(f)|^2 = & 8 - 4\cos\alpha (a+b) - 4\cos\alpha (a+c) - 4\cos\alpha (a+d) + 4\cos\alpha (a-e) \\
 & + 2\cos\alpha (b-d) - 2\cos\alpha (b+e) + 2\cos\alpha (b-c) + 2\cos\alpha (c-d) \\
 & - 2\cos\alpha (c+e) - 2\cos\alpha (d+e)
 \end{aligned} \tag{2.39}$$

2.4.2 Bit error rate expression

The expression for the average bit error rate is given by [23]

$$\text{BER} = \frac{1}{2} \int_{-\infty}^{\infty} \text{erfc} \left[\frac{2R_d P_s \cos \Delta\theta_{nt}}{\sqrt{2\sigma_m^2}} \right] P(\Delta\theta_{nt}) d(\Delta\theta_{nt}) \tag{2.40}$$

where $P(\Delta\theta_{nt})$ is the pdf of $\Delta\theta_{nt}$ which have a zero mean Gaussian distribution with variance σ_x^2 and is given by

$$P(\Delta\theta_{nt}) = \frac{1}{\sqrt{2\pi\sigma_x^2}} e^{-\frac{\Delta\theta_{nt}^2}{2\sigma_x^2}} \tag{2.41}$$

Here, total phase noise variance is given by

$$\sigma_x^2 = \int_{-\frac{B_c}{2}}^{\frac{B_c}{2}} \left[W_{\Delta\theta_n}(f) \otimes W_{\Delta\theta_n}(f) \right] |H_{LPF}(f)|^2 df \tag{2.42}$$

2.5 Results and discussion

Following the theoretical analysis, the bit error rate performance of DPSK direct detection system is computed at a bit rate of 10 Gb/sec with different sets of receiver and system parameters. Bit error rate performances are evaluated for dispersion shifted (DS) fibres at an wavelength of 1300 nm and nondispersion shifted (NDS) fibres at an wavelength of 1550 nm for several dispersion coefficients D_c .

The bit error rate (BER) performance of direct detection DPSK system is shown in fig. 2.3 without considering the effect of fibre chromatic dispersion i.e. $D_c = 0.0$. The BER is plotted as a function of the received optical power P_s (dBm) for several values of normalized linewidth $\Delta\nu T$ and the receiver sensitivity is defined as the optical power required to obtain a BER of 10^{-9} . The figure shows that the BER decreases with the increase in the input power. For $\Delta\nu T = 0.0$ the receiver sensitivity is found to be -19.65 dBm. At increased value of laser linewidth, the required amount of signal power is higher to achieve the same BER. The additional signal power compared to the case of zero linewidth ($\Delta\nu T = 0.0$) may be termed as the power penalty at BER = 10^{-9} due to the effect of laser phase noise caused by non-zero linewidth. Phase noise causes the spectrum of the DPSK signal to be broadened and for a given receiver bandwidth, the signal power is less at the output of the receiver baseband filter. As a result, more signal power is required to obtain the same BER. The effect of phase noise is more at higher values of linewidth.

In presence of fibre chromatic dispersion, the BER performance of DPSK direct detection transmission system is shown in fig.2.4 for fibre length $L=25$ Km, chromatic dispersion factor $D_c=1.0$ ps/Km.nm, wavelength $\lambda=1550$ nm for several values of laser linewidth $\Delta\nu T$. Comparing this figure with fig.2.3, we notice that

the performance of the system is degraded due to the effect of fibre chromatic dispersion. At a given input power, the BER is higher in the presence of dispersion compared to the case when there is no dispersion. The receiver sensitivity thus degrades and there is an additional power penalty due to the effect of dispersion. For example, in absence of laser phase noise ($\Delta\nu T = 0.0$), the receiver sensitivity to achieve $BER = 10^{-9}$ is -19.65 dBm when there is no dispersion ($D_c = 0.0$) whereas in presence of dispersion with $D_c = 1.0$, the receiver sensitivity is found to be -19.60 dBm. For $\Delta\nu T = 0.005$, the receiver sensitivity is -19.1 dBm when $D_c = 0.0$ (from fig.2.3) and it is found to be -19.04 dBm when $D_c = 1.0$ (from fig.2.4).

It is also observed that the penalty due to the combined effect of laser phase noise and chromatic dispersion is higher at higher values of normalized linewidth $\Delta\nu T$.

When the dispersion coefficient D_c is increased to 3.0 ps/Km.nm, the bit error rate performance is shown in fig. 2.6 for several values of normalized laser linewidth $\Delta\nu T$. Compared to fig. 2.4, where $D_c = 1.0$, it is evident that increased dispersion factor causes the system performance to be more degraded. For the same value of fibre length BER is plotted in fig. 2.7 for higher value of dispersion coefficient. Similar conclusion can be drawn from fig. 2.7 when compared to fig. 2.3 and fig. 2.4.

It is further observed that at increased value of $\Delta\nu T$, there occurs bit error rate (BER) floor at increased signal power, i.e. BER does not decrease with increase in signal power. As seen from fig. 2.6, the BER floor occurs around 2×10^{-11} corresponding to $\Delta\nu T = 0.005$. Also, the BER floor goes upward for the same value of $\Delta\nu T$ when dispersion factor γ is increased from 0.0191 to 0.0254 as is evident by comparing fig. 2.6 with fig. 2.7. Thus we can draw the conclusion that, the system suffers BER floor at larger values of the chromatic dispersion coefficient D_c and / or larger fibre length.

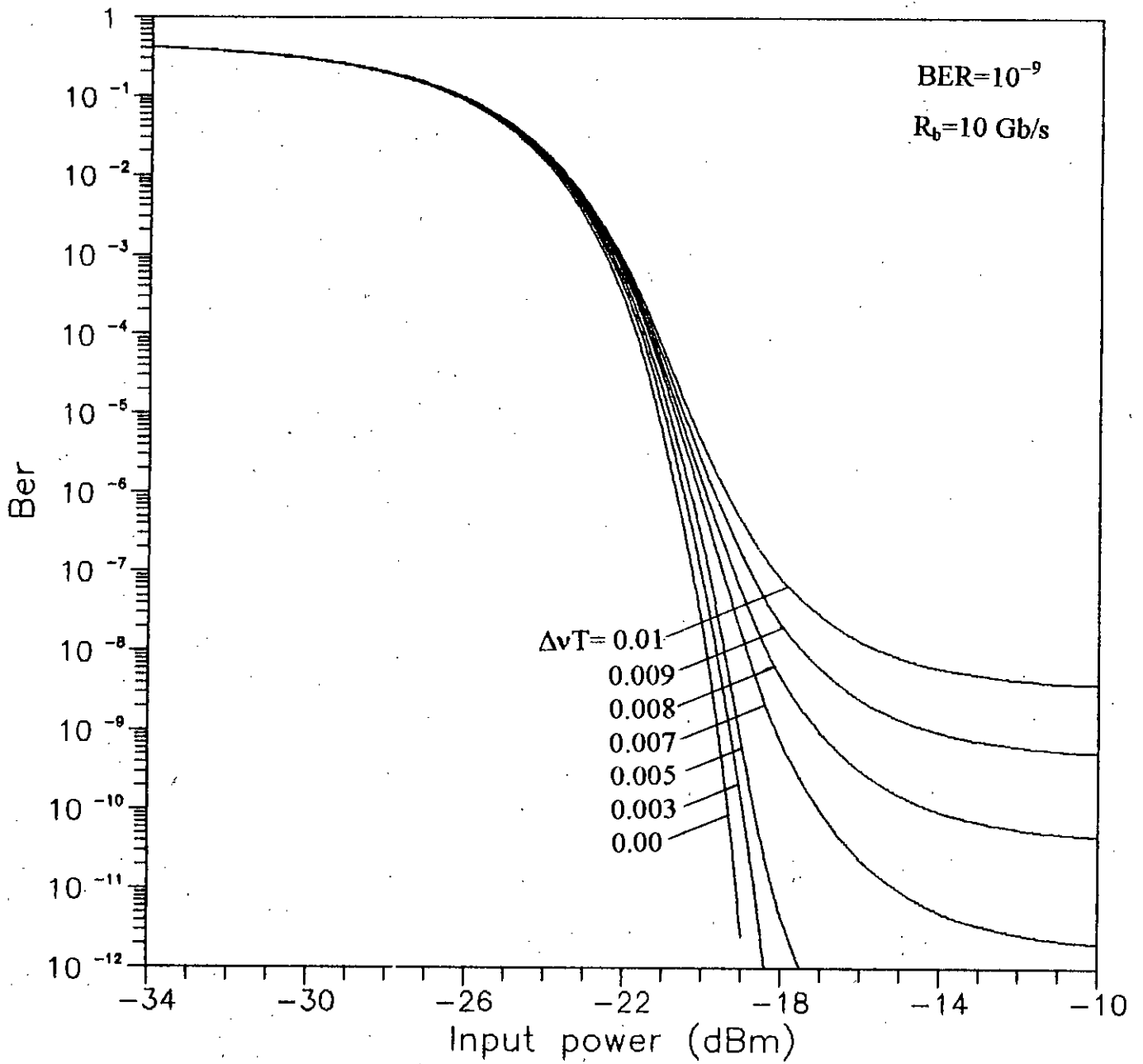


Fig. 2.3 Bit error rate vs. receiver input power of direct detection optical-DPSK transmission system at a bit rate of 10 Gb/s without fibre chromatic dispersion ($D_c=0.0$) for several values of normalized laser linewidth $\Delta\nu T$.

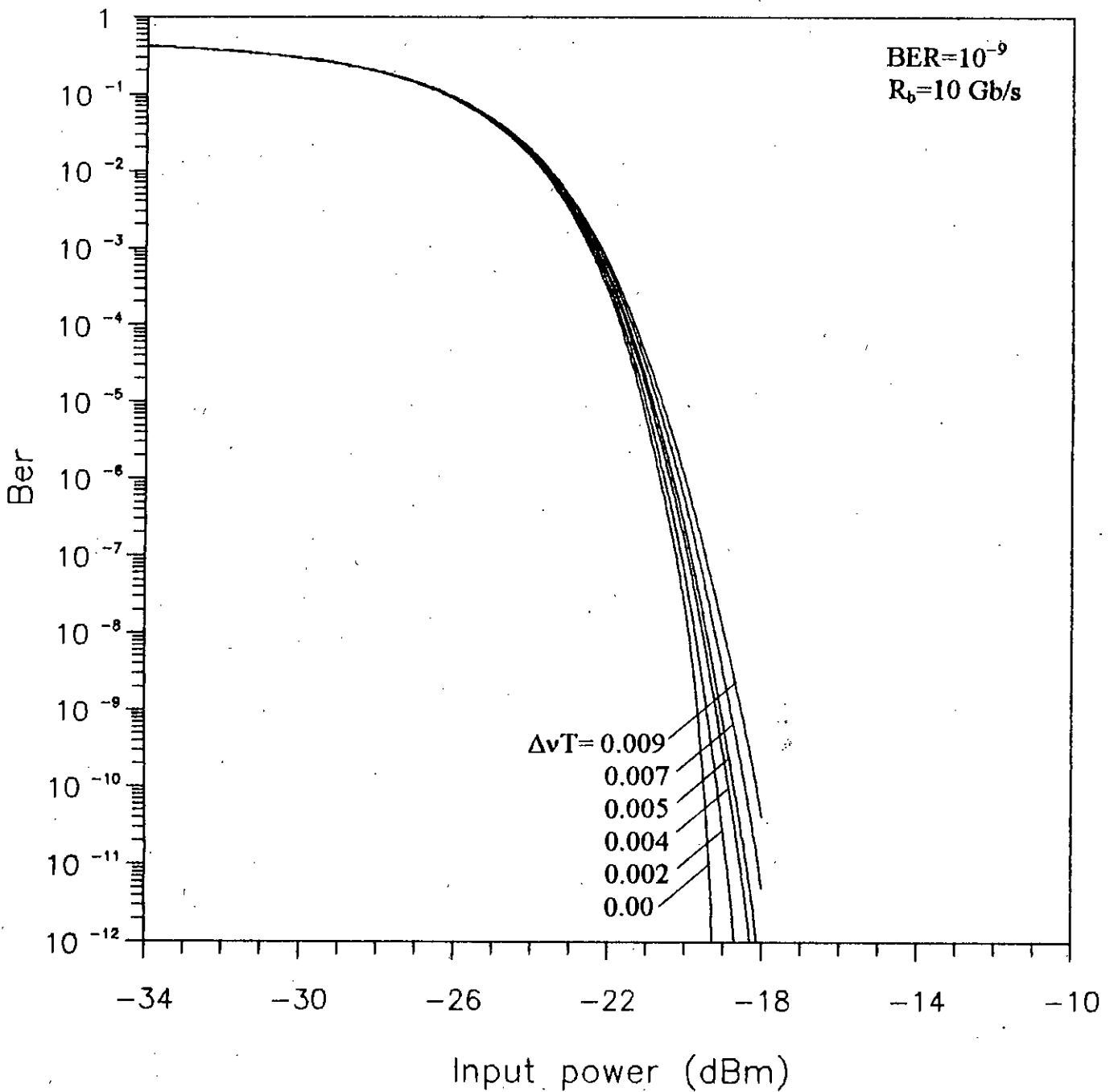


Fig. 2.4 Bit error rate vs. receiver input power of direct detection optical DPSK transmission system at a bit rate of 10 Gb/s with fibre chromatic dispersion $D_c=1.0$ ps/Km.nm, fibre length $L=25$ Km, at an wavelength $\lambda=1550$ nm for several values of normalized laser linewidth $\Delta\nu T$.

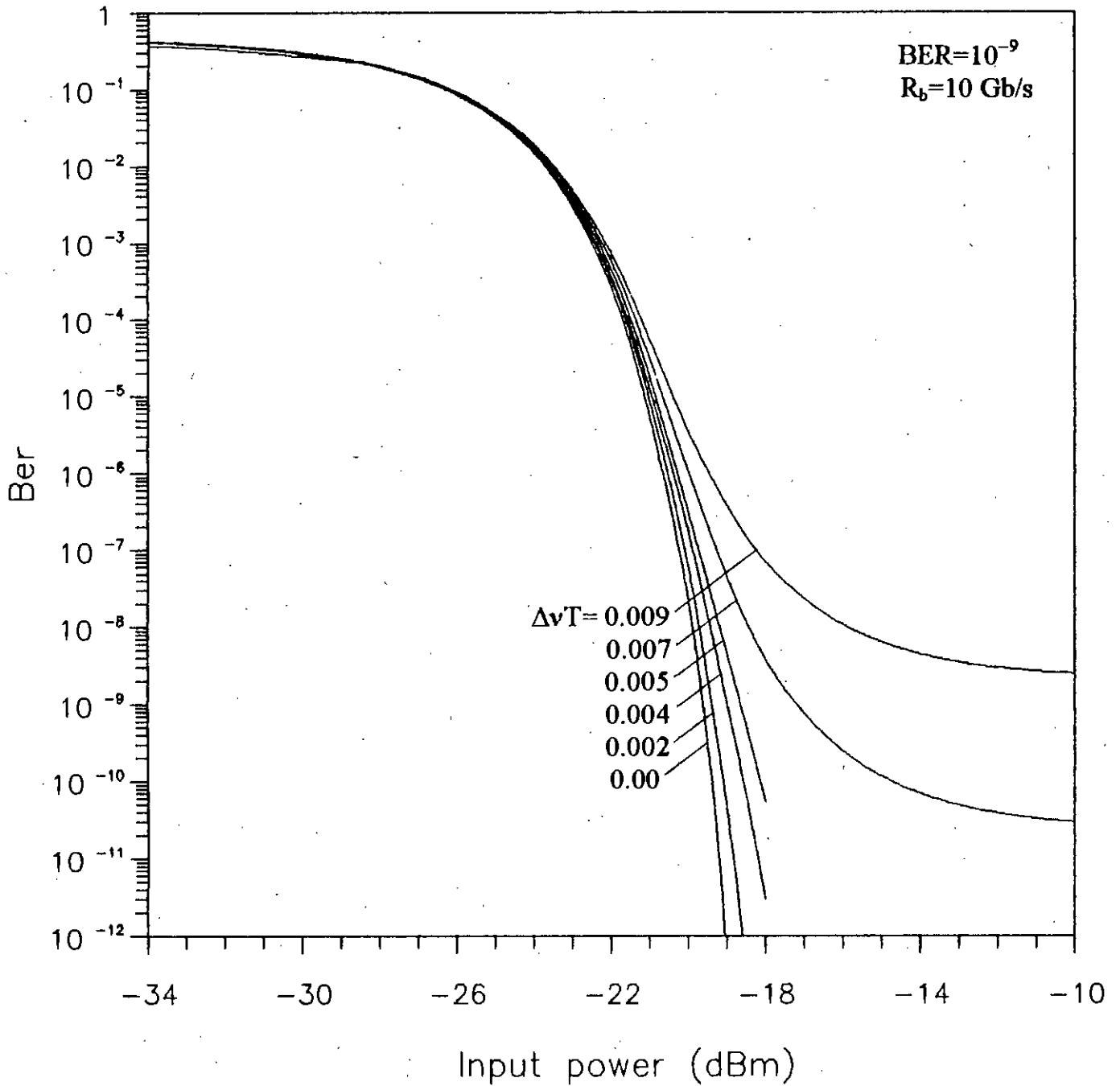


Fig. 2.5 Bit error rate vs. receiver input power of direct detection optical DPSK transmission system at a bit rate of 10 Gb/s with fibre chromatic dispersion $D_c=1.0$ ps/Km.nm, fibre length $L=50$ Km, at an wavelength $\lambda=1550$ nm for several values of normalized laser linewidth $\Delta\nu T$.

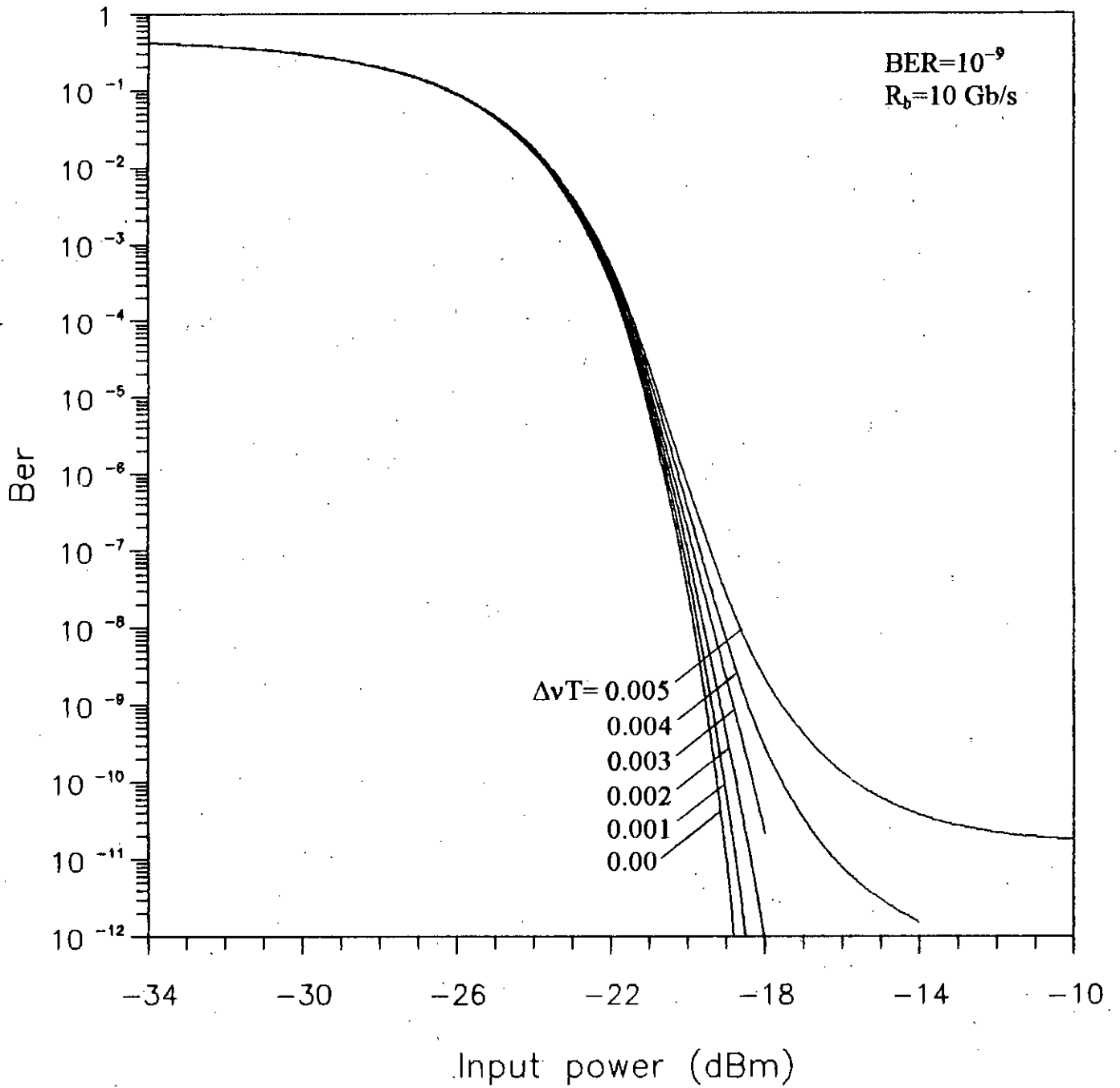


Fig. 2.6 Bit error rate vs. receiver input power of direct detection optical DPSK transmission system at a bit rate of 10 Gb/s with fibre chromatic dispersion $D_c=3.0$ ps/Km.nm, fibre length $L=25$ Km, at an wavelength $\lambda=1550$ nm for several values of normalized laser linewidth $\Delta\nu T$.

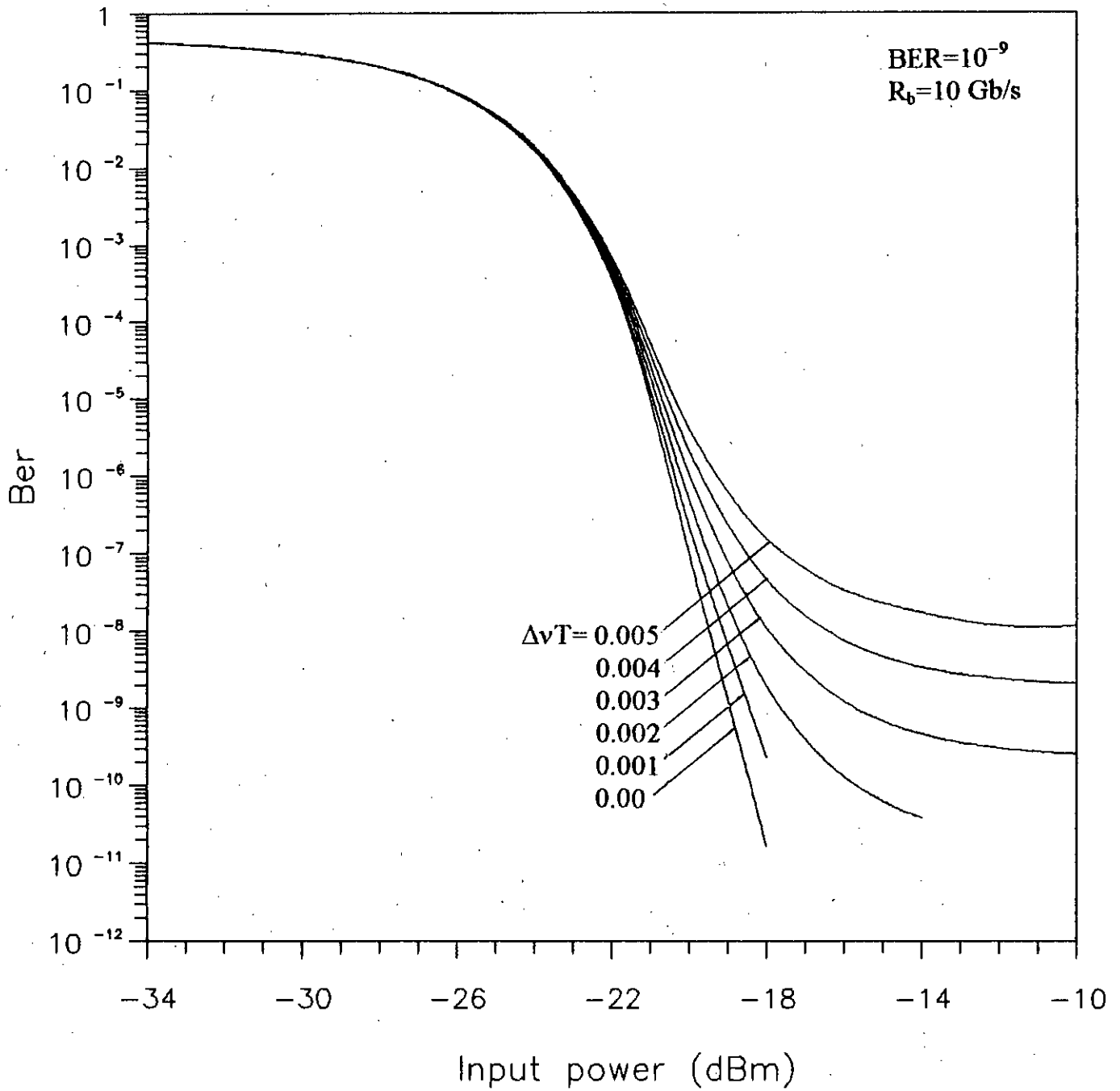


Fig. 2.7 Bit error rate vs. receiver input power of direct detection optical DPSK transmission system at a bit rate of 10 Gb/s with fibre chromatic dispersion $D_c=4.0$ ps/Km.nm, fibre length $L=25$ Km, at an wavelength $\lambda=1550$ nm. for a sevsral values of normalized laser linewidth $\Delta\nu T$.

The bit error rate performance vs. input signal power for several values of dispersion coefficients are shown in fig. 2.8 through fig. 2.12 at an wavelength $\lambda=1300$ nm. From these figures, similar conclusions can be drawn as observed from the plots for $\lambda=1550$ nm.

The penalty in signal power suffered by the system due to the combined effect of laser phase noise and fibre chromatic dispersion are determined from bit error rate (BER) curves at $BER=10^{-9}$. The plot of power penalty versus chromatic dispersion coefficient D_c (ps/Km.nm) is shown in fig. 2.13 . From the figure, it is observed that for zero and smaller values of linewidth, the penalty is below 1 dB. When the normalized linewidth $\Delta\nu T \geq 0.003$ and $D_c > 5$ ps/Km.nm, the penalty is more than 1 dB and further increases with increase in $\Delta\nu T$ and / or dispersion coefficient D_c .

To get more insight into the effect of dispersion on the system performance, the penalty in signal power at $BER=10^{-9}$ is plotted as a function of the normalized linewidth $\Delta\nu T$ in fig. 2.14 with dispersion factor as a parameter. In the absence of dispersion ($\gamma=0.0$) i.e. when only laser phase noise is present, the penalty is significantly less compared to the case of non-zero value of γ . When $\Delta\nu T=0.0$, the penalty suffered by the system is only due to chromatic dispersion and for $\Delta\nu T>0.0$ and $D_c >0.0$, the penalty is due to the combined effect of dispersion and phase noise. From the figure, it is observed that, for a given linewidth, the penalty increases with increase in the value of dispersion factor γ . For a given power penalty, say 1 dB, the allowable value of dispersion factor γ depends on the value of $\Delta\nu T$ and vice versa. For 1 dB penalty, corresponding to $\gamma =0.0127$, the allowable value of $\Delta\nu T>0.005$. For an increased value of $\gamma =0.0254$, the allowable laser linewidth $\Delta\nu T\leq 0.004$. For a fibre span of $\gamma \geq 0.0318$, the

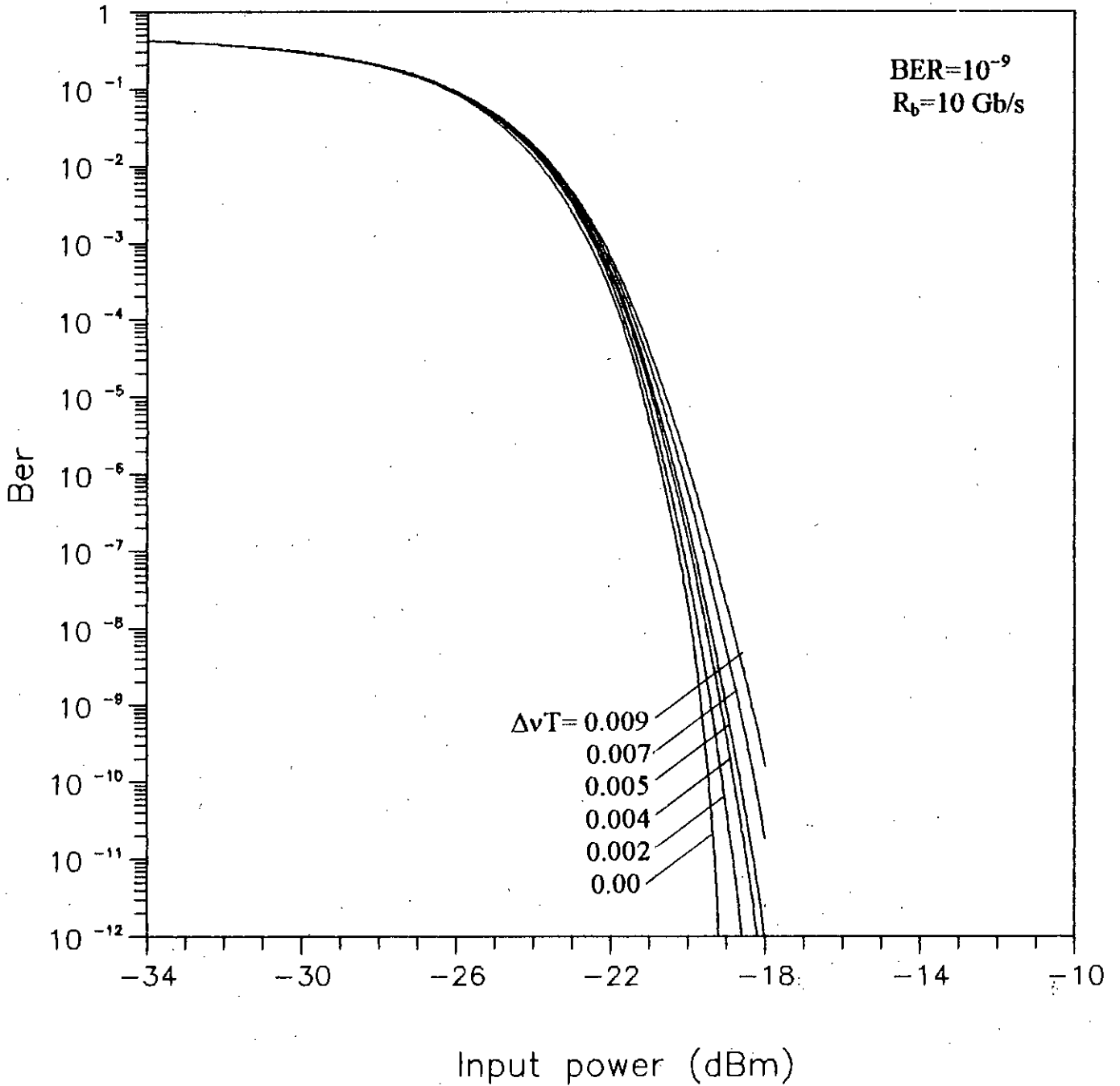


Fig. 2.8 Bit error rate vs. receiver input power of direct detection optical DPSK transmission system at a bit rate of 10 Gb/s with fibre chromatic dispersion $D_c=1.0$ ps/Km.nm, fibre length $L=50$ Km, at an wavelength $\lambda=1300$ nm for a sevsral values of normalized laser linewidth $\Delta\nu T$.

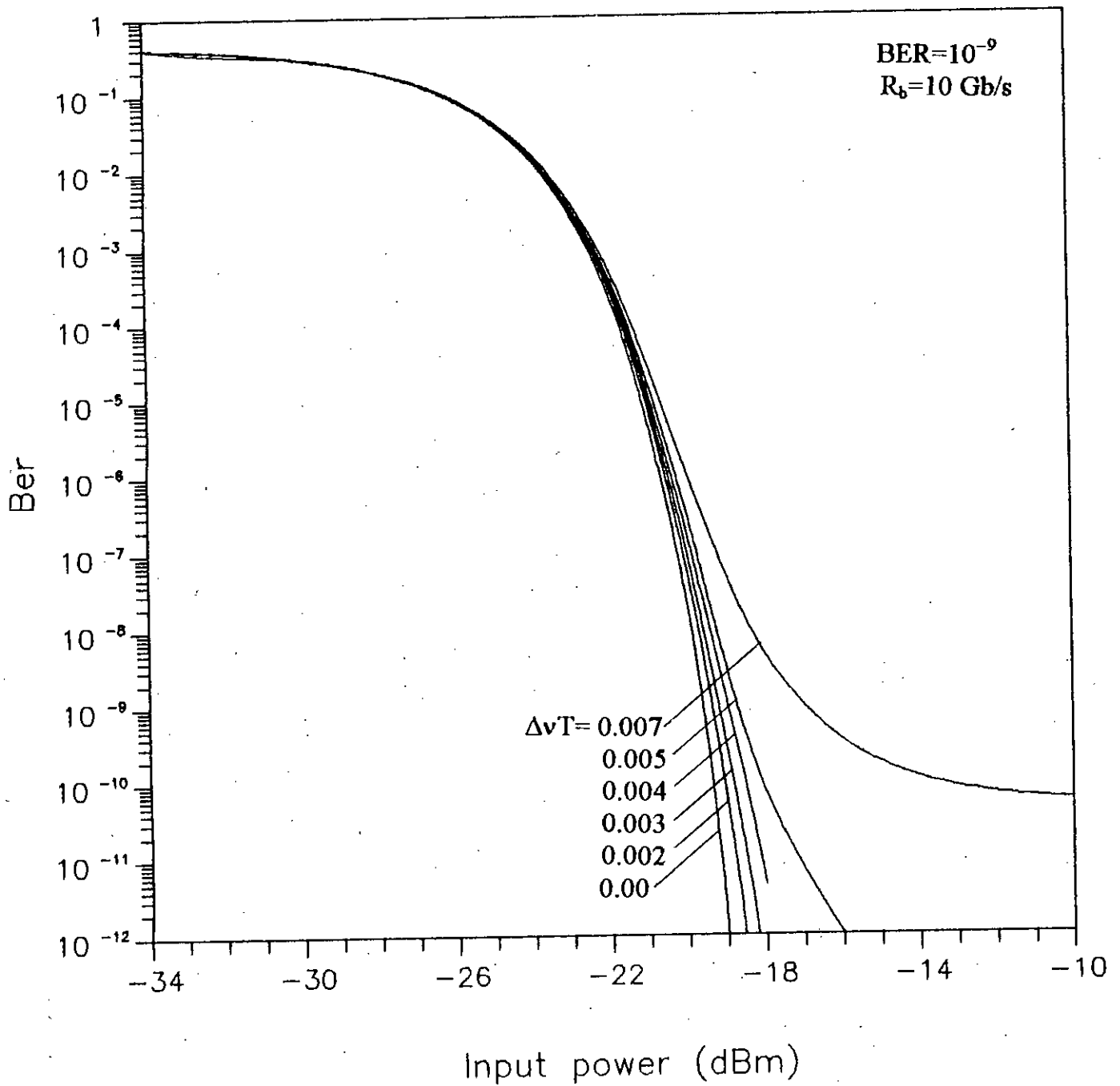


Fig. 2.9 Bit error rate vs. receiver input power of direct detection optical DPSK transmission system at a bit rate of 10 Gb/s with fibre chromatic dispersion $D_c=1.0$ ps/Km.nm, fibre length $L=75$ Km, at an wavelength $\lambda=1300$ nm for a sevsral values of normalized laser linewidth $\Delta\nu T$.

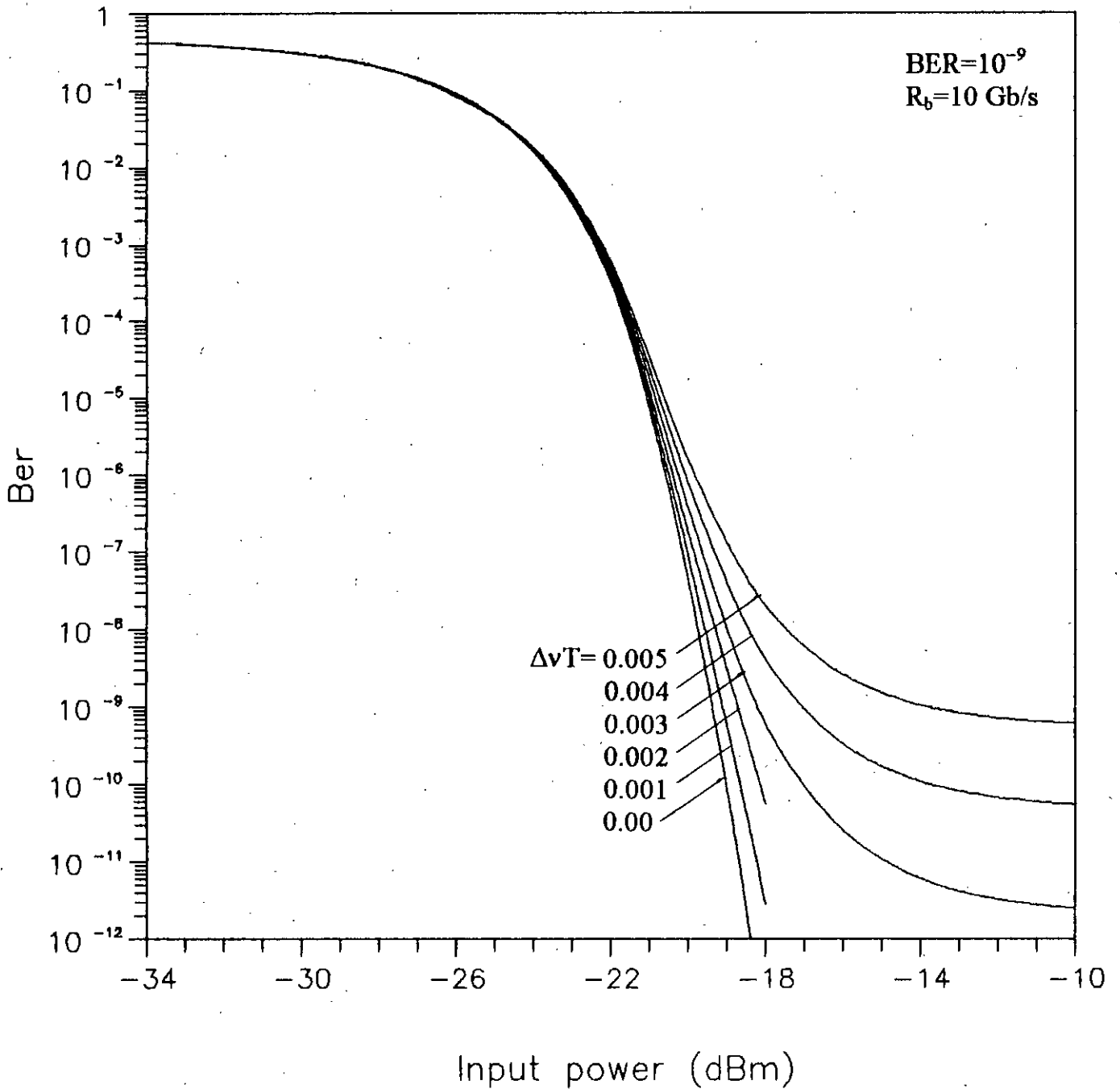


Fig. 2.10 Bit error rate vs. receiver input power of direct detection optical DPSK transmission system at a bit rate of 10 Gb/s with fibre chromatic dispersion $D_c=1.0$ ps/Km.nm, fibre length $L=125$ Km, at an wavelength $\lambda=1300$ nm for a sevsral values of normalized laser linewidth $\Delta\nu T$.

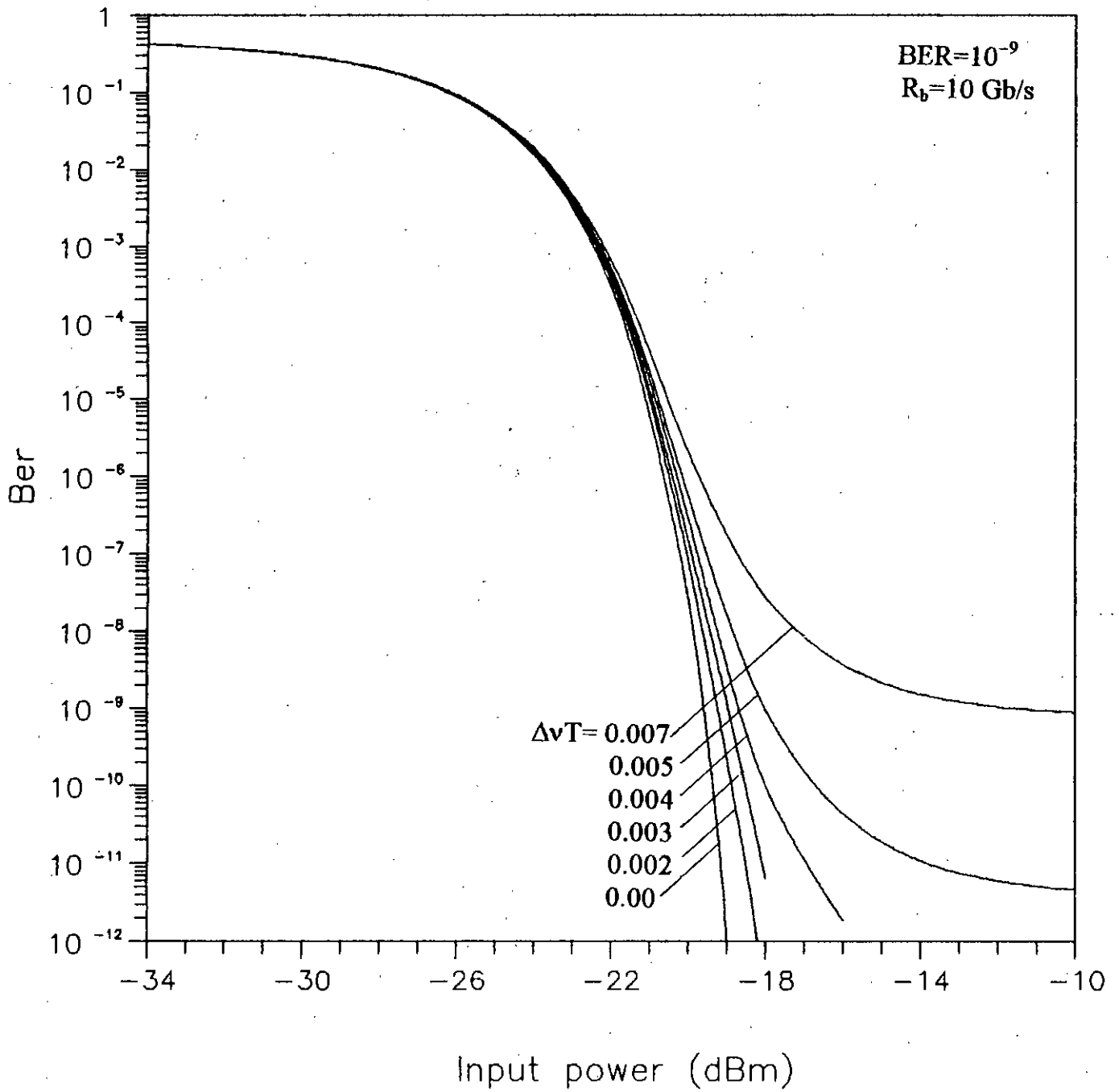


Fig. 2.11 Bit error rate vs. receiver input power of direct detection optical DPSK transmission system at a bit rate of 10 Gb/s with fibre chromatic dispersion $D_c=2.0$ ps/Km.nm, fibre length $L=50$ Km, at an wavelength $\lambda=1300$ nm for a sevsral values of normalized laser linewidth $\Delta\nu T$.

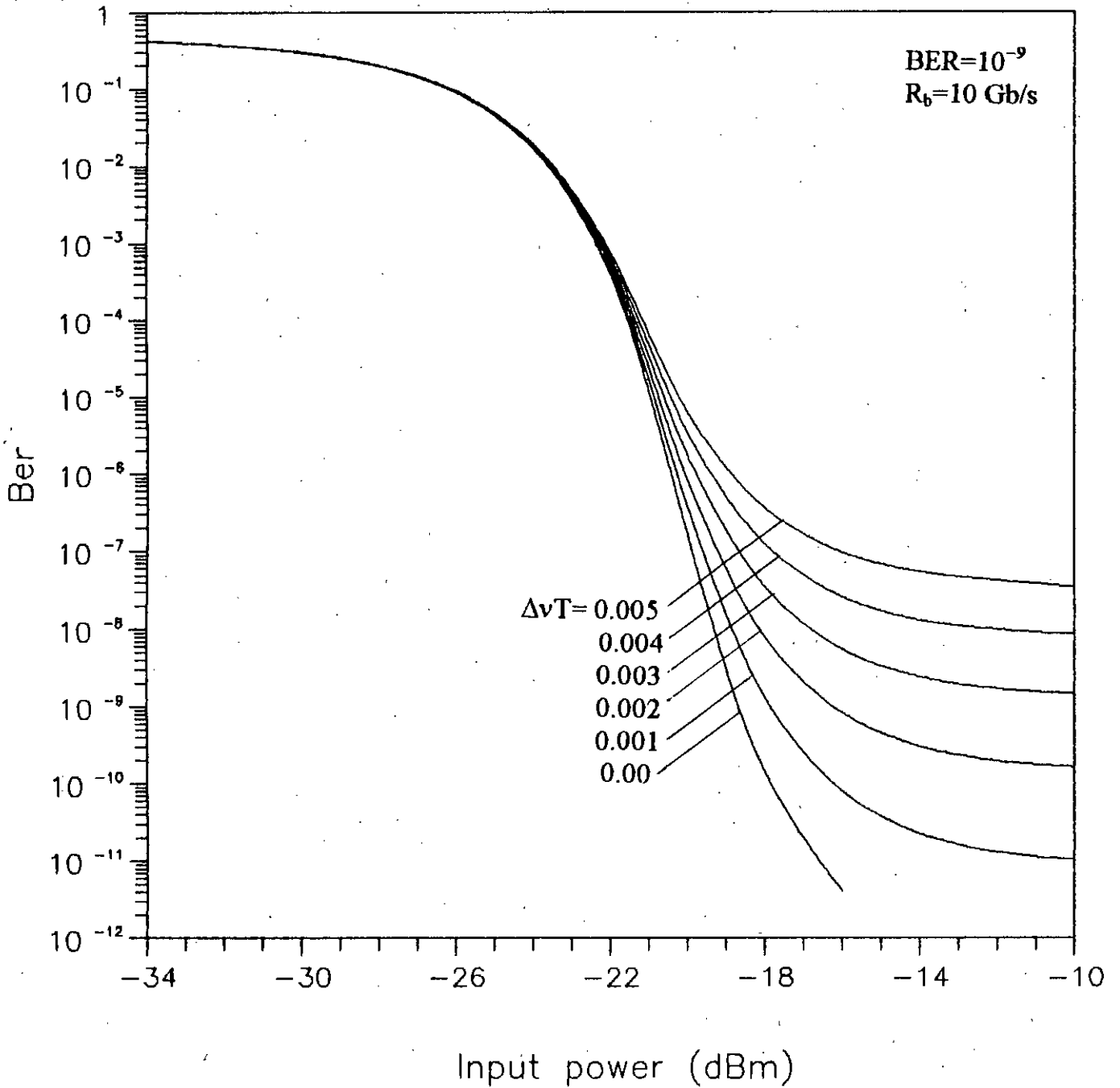


Fig. 2.12 Bit error rate vs. receiver input power of direct detection optical DPSK transmission system at a bit rate of 10 Gb/s with fibre chromatic dispersion $D_c=3.0$ ps/Km.nm, fibre length $L=50$ Km, at an wavelength $\lambda=1300$ nm for a sevsral values of normalized laser linewidth $\Delta\nu T$.

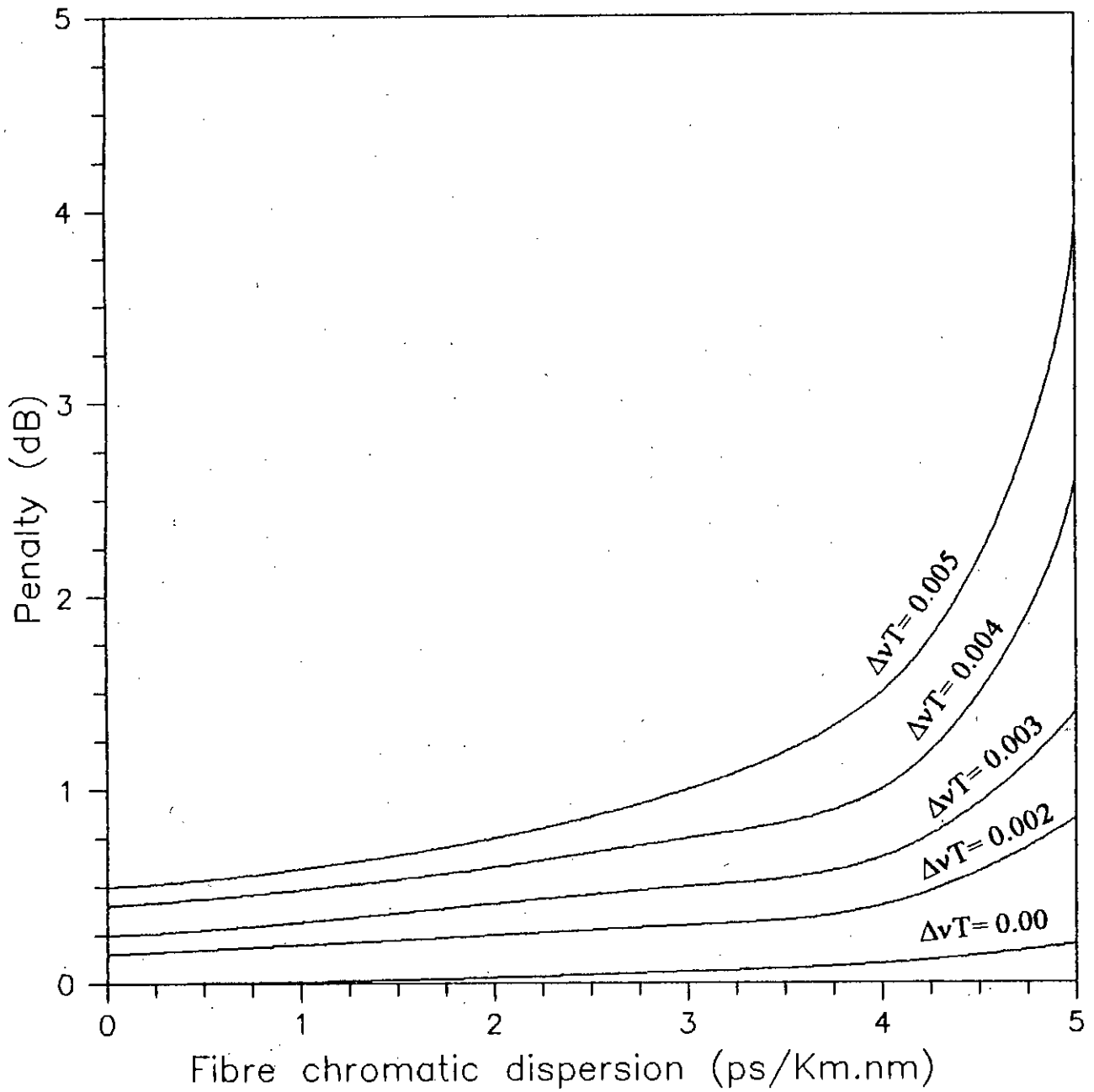


Fig. 2.13 Penalty in signal power due to combined effect of laser phase noise and fibre chromatic dispersion at $BER=10^{-9}$ versus dispersion coefficient D_c (ps/Km.nm) with fibre length $L=25$ Km for several values of normalized laser linewidth $\Delta\nu T$.

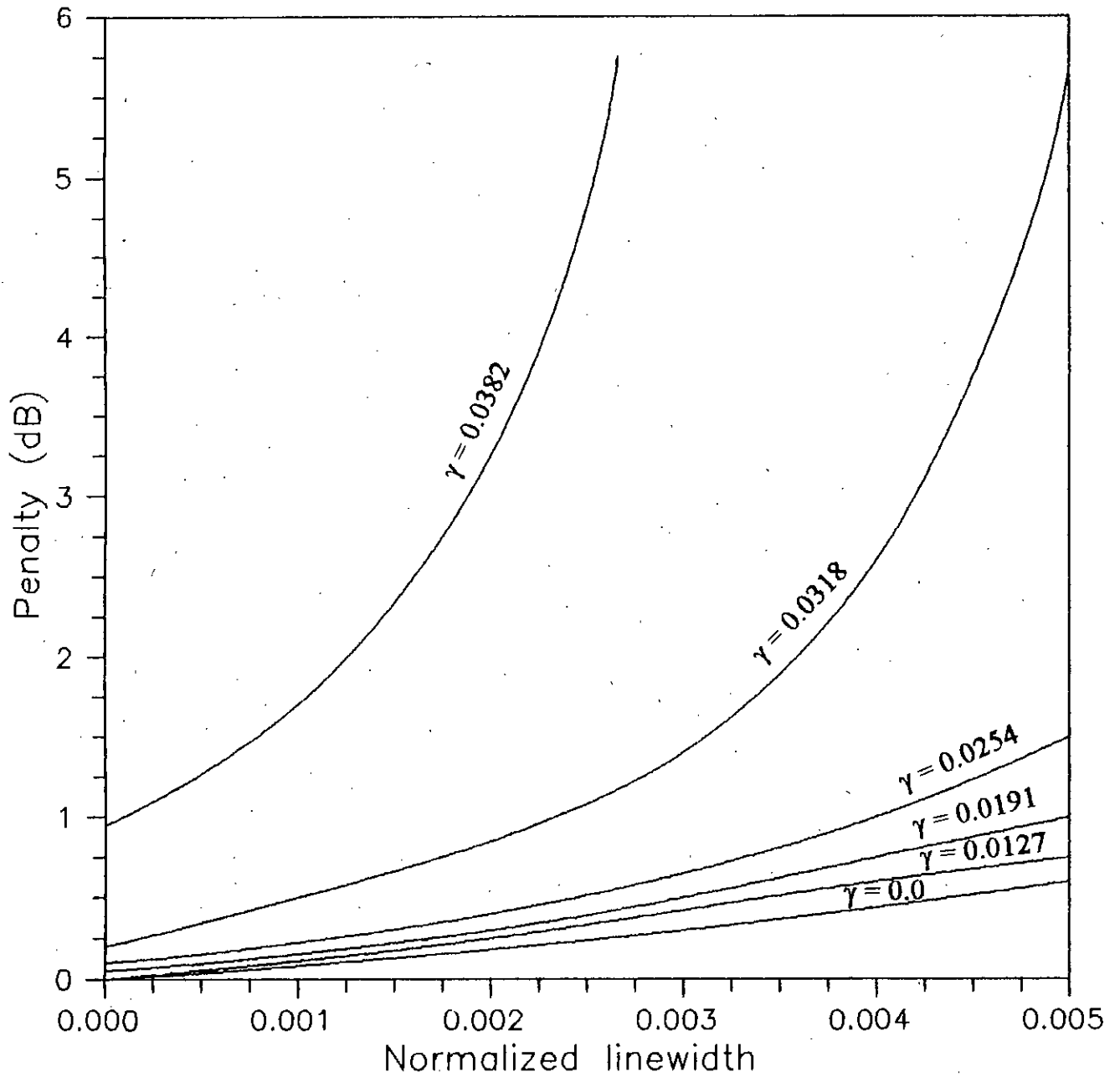


Fig. 2.14 Variation of power penalty (dB) due to combined effect of laser phase noise and fibre chromatic dispersion at $BER=10^{-9}$ with normalized laser linewidth $\Delta\nu T$ for several values of dispersion factor γ .

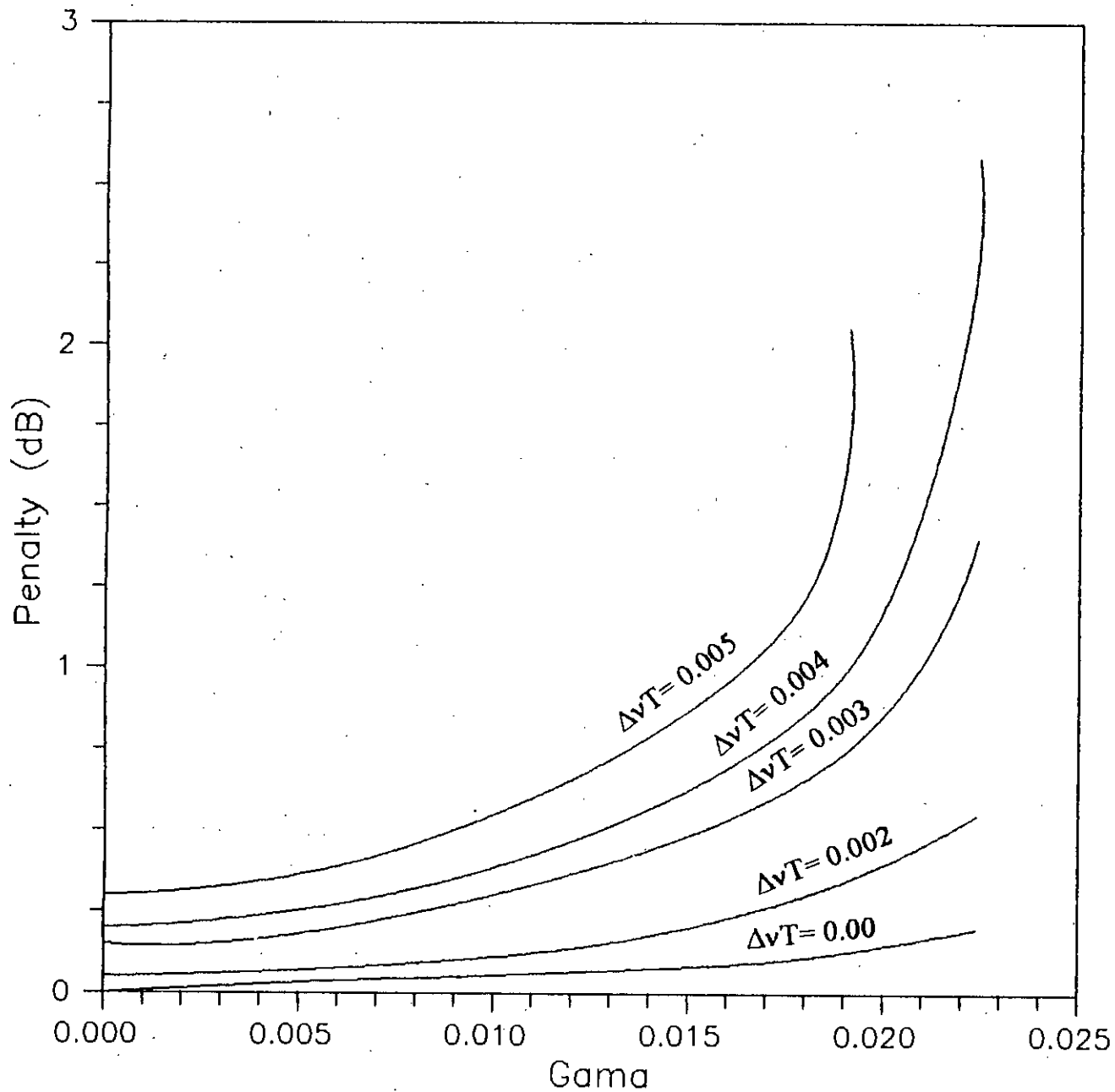


Fig. 2.15 Variation of power penalty (dB) due to combined effect of laser phase noise and fibre chromatic dispersion at $BER=10^{-9}$ with dispersion factor γ for several values of normalized laser linewidth $\Delta\nu T$.

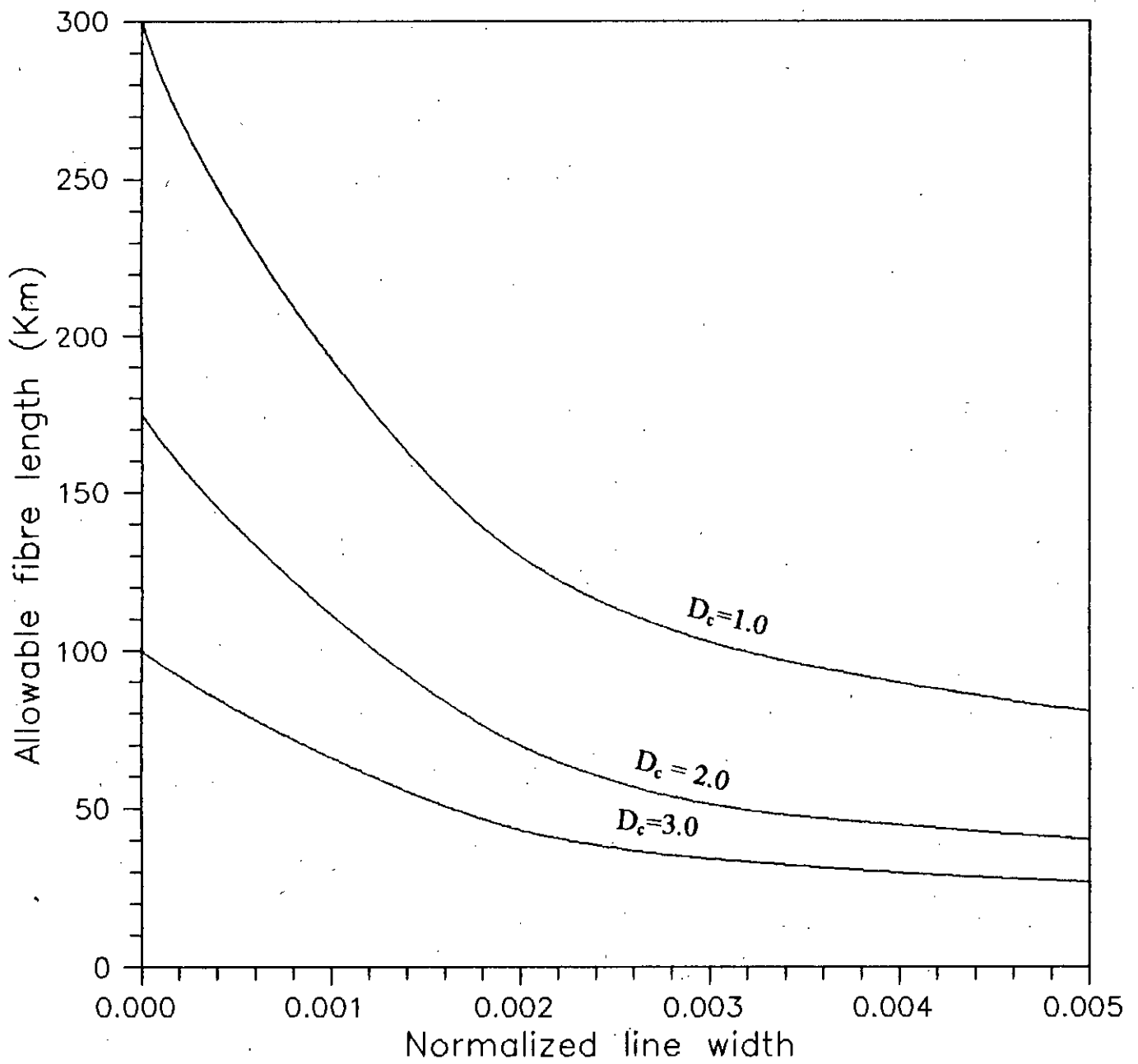


Fig. 2.16 Plots of allowable fibre length corresponding to 1 dB penalty at $BER=10^{-9}$ as a function of normalized laser linewidth $\Delta\nu T$ for dispersion coefficient $D_c = 1, 2$ and 3 ps/Km.nm.

allowable laser linewidth $\Delta\nu T \leq 0.004$. For a fibre span of $\gamma \geq 0.0318$, the allowable laser linewidth is further reduced to ≤ 0.0023 . Thus we can say that, chromatic dispersion imposes restriction on the allowable laser linewidth for a specified system penalty at a given BER.

The variation of power penalty with dispersion factor γ is plotted in fig. 2.15 for different values of normalized linewidth $\Delta\nu T$. It is observed that the penalty increases with increasing values of dispersion factor γ and normalized linewidth $\Delta\nu T$. Further, we also notice that for a given $\Delta\nu T$, at $\text{BER}=10^{-9}$ there is an upper limit on the dispersion factor γ for power penalty ≤ 1 dB. The upper limit or maximum allowable dispersion factor is less in the presence of phase noise and is significantly less at higher linewidth values. Corresponding to maximum allowable dispersion factor, we get an upper limit on the maximum fibre length for a given value of dispersion coefficient D_c corresponding to $\text{BER}=10^{-9}$ and penalty ≤ 1 dB.

For 1 dB power penalty at $\text{BER}=10^{-9}$, the allowable fibre length (Km) is plotted in fig. 2.16 as a function of normalized linewidth $\Delta\nu T$ for chromatic dispersion coefficient $D_c = 1.0, 2.0$ and 3.0 ps/Km.nm. It is observed that the allowable fibre length is about 300 Km when $\Delta\nu T=0.0$ and $D_c=1.0$. When chromatic dispersion coefficient D_c is increased to 2.0, the allowable fibre length reduces to around 175 Km and around 100 Km for $D_c=3.0$. Further, the allowable fibre length exponentially decreases with increasing linewidth.

CHAPTER 3

PERFORMANCE ANALYSIS OF OPTICAL HETERODYNE DPSK SYSTEM IN PRESENCE OF LASER PHASE NOISE AND FIBRE CHROMATIC DISPERSION

3.1 Introduction

Coherent optical communication systems offer significant improvements over direct detection in two main areas: a 10-20 dB increase in receiver sensitivity and the possibility of using frequency division multiplexing to utilize more of the fibre bandwidth [25]. The major limitations of optical transmission systems, however, are laser phase noise and fibre chromatic dispersion. The phase noise is caused by random spontaneous emission events within the laser and manifests itself as a random walk in the phase of the laser output [26]. The chromatic dispersion is caused due to the variation of group velocities within the fibre.

The effects of laser phase noise and fibre chromatic dispersion on coherent optical communication systems are to degrade the receiver sensitivity [27]. For a fixed bit error rate (BER), this necessitates an increase in received signal power compared to the ideal situation. In some cases (notably DPSK), the presence of phase noise creates a minimum BER (error floor) below which the system can not operate no matter how much signal power is available [27-31] This BER floor is a function of the ratio of the laser linewidth to the system bitrate: the higher the amount of phase noise relative to the bit rate, the higher the BER floor. Thus, systems like DPSK that suffer from this phenomena are only viable at high bitrates. Also, analysis of various modulation schemes in the presence of laser phase noise have shown that phase modulations are particularly badly degraded by even small amounts of phase noise. Despite this sensitivity, phase modulation schemes are generally attractive in that they can achieve very good receiver sensitivities [27] and are spectrally efficient [32-33] Binary DPSK has the further advantage that the receiver has a very simple structure, with only a slight performance penalty relative to coherent PSK. Previous works on the effects of fibre chromatic dispersion on the performance of optical DPSK and FSK systems were reported only for direct detection receivers [24]. The results were reported experimentally. Although computer simulation results are recently available [23] for direct detection DPSK system, no theoretical analysis is yet available which accounts for the effect of fibre chromatic dispersion and laser phase noise on the performance of such system.

In this chapter, we provide the theoretical analysis for evaluating the BER performance of an optical heterodyne DPSK transmission system considering the effects of laser phase noise and fibre chromatic dispersion. The statistics of the phase fluctuations due to chromatic dispersion in the presence of laser phase noise are determined analytically and the expression for the bit error probability of the

DPSK receiver is developed. Performance results are also computed at a bit rate of 10 Gb/s for several system parameters and fibre dispersion factors.

3.2 The receiver model

The block diagram of optical heterodyne DPSK receiver considered for the theoretical analysis is shown in fig.3.1 . The incoming optical signal of frequency f_s is mixed with the local oscillator signal of frequency f_{LO} . The photodetector output is then at an intermediate frequency (IF) given by $f_{IF} = f_s - f_{LO}$. The bandpass filter (BPS), centered at the IF and matched to the received signal , serves to limit the shot noise that is introduced by the detection process. Demodulation of the resultant IF DPSK signal is performed by splitting the signal into two, delaying one branch by the bit period T and then multiplying the two branches together. The lowpass filter (LPF) serves to remove double frequency terms introduced by the multiplication and may also further limit the noise. The LPF output is sampled at the end of each bit period and a data decision is made according to the sign of the sample: a positive output is decoded as a zero, a negative output as a one.

3.3 The theoretical analysis

The optical DPSK modulated signal input to the fibre can be expressed as

$$\chi_i(t) = \sqrt{2P_S} \exp\left\{j\left[2\pi f_c t + \varphi_n(t)\right]\right\} \sum_i u_T(t-iT) \exp(j\varphi_i) \quad (3.1)$$

where, u_T is a rectangular pulse of duration T sec

φ_n is the instantaneous phase noise of transmitting laser, and

$$\varphi_i = \varphi_{i-1} + \Delta\varphi_i = \varphi_{i-1} + \frac{\pi(1 - a_i)}{2} \quad (3.2)$$

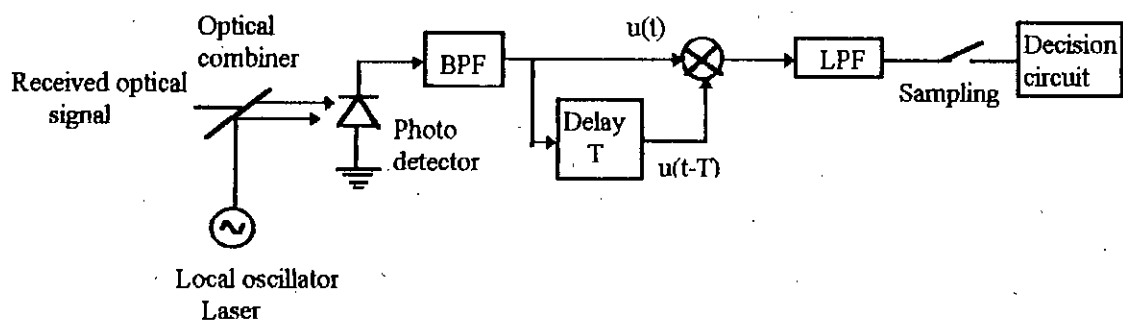


Fig. 3.1 Block diagram of optical heterodyne DPSK receiver

where, $\{a_i\}$ is the binary data sequence which assumes values $+1$ and -1 with equal probability.

Following the steps mentioned in section 2.3, considering the normalized fibre transfer function $H(f)$ as before, the optical signal at the output of the fibre in the receiving end is given by,

$$\begin{aligned}\chi_o(t) &= \sqrt{2P_s} \exp\{j[2\pi f_c t + \theta(t)]\} \\ &= \sqrt{2P_s} \exp\{j[2\pi f_c t + \theta_s(t) + \theta_n(t)]\}\end{aligned}\quad (3.3)$$

where, $\theta_s(t)$ represents the linear signal term and $\theta_n(t)$ represents the non-linear filtering terms consisting of the cross-terms and the inter-modulation terms.

As in section 2.3 we can write $\theta_s(t)$ as,

$$\begin{aligned}\theta_S(t) &= \text{Re} \left[\int_0^\infty h(\tau) \varphi(t-\tau) d\tau \right] \\ &= \text{Re} \left[\int_0^\infty h(\tau) \{ \varphi_S(t-\tau) + \varphi_n(t-\tau) \} d\tau \right] \\ &= \text{Re} \left[\int_0^\infty h(\tau) \varphi_S(t-\tau) d\tau \right] + \text{Re} \left[\int_0^\infty h(\tau) \varphi_n(t-\tau) d\tau \right] \\ &= \theta'_S(t) + \theta'_{PN}(t)\end{aligned}\quad (3.4)$$

So, we can write,

$$\begin{aligned}\chi_o(t) &= \sqrt{2P_s} \exp\left[j\{2\pi f_c t + \theta'_s(t) + \theta'_{PN}(t) + \theta_n(t)\}\right] \\ &= \sqrt{2P_s} \exp\left[j\{\omega_c t + \theta'_s(t) + \theta'_t(t)\}\right]\end{aligned}\quad (3.5)$$

where, $\theta'_t(t) = \theta'_{PN}(t) + \theta_n(t)$

The IF signal at the output of photodetector is given by,

$$\begin{aligned}r(t) &= A \cos[2\pi f_{IF} t + \theta'_s(t) + \theta'_t(t)] + n(t) \\ &= A \cos[2\pi f_{IF} t + \phi'(t)] + n(t)\end{aligned}\quad (3.6)$$

where, $A = 2R_d \sqrt{P_s P_{LO}}$

R_d is the responsivity of photodetector, P_{LO} is the power of the local oscillator laser with phase noise $\theta_{LO}(t)$

$$\begin{aligned}\text{and, } \theta'_t(t) &= \theta_t(t) + \theta_{LO}(t) \\ &= \theta'_{PN}(t) + \theta_{LO}(t) + \theta_n(t) \\ &= \theta_{PN}(t) + \theta_n(t)\end{aligned}$$

The output of the IF filter can be written as,

$$\begin{aligned}y(t) &= r(t) \otimes q(t) + n_o(t) \\ &= \int_t^\infty q(t) r(t-t') dt' + n_o(t) \\ &= A \cos[2\pi f_{IF} t + \psi(t)] + n_o(t)\end{aligned}\quad (3.7)$$

where, $\psi(t)$ is the output phase and $n_o(t)$ is the filtered additive noise with variance σ^2 ,

$q(t) = F^{-1}\{Q(f)\}$ is the impulse response of the IF filter.

The IF signal-to-noise ratio (IF SNR) can be defined as

$$\text{IF SNR} = \frac{A^2}{2\sigma^2}$$

where, $\sigma^2 = P_{\text{shot}} + P_{\text{th}}$

Defining the normalized equivalent baseband filter impulse response as

$$h_{\text{IF}}(t) = \frac{q(t)}{Q(\text{IF})} e^{-j2\pi f_{\text{IF}} t} \quad (3.8)$$

the output phase $\psi(t)$ can be expressed as [28]

$$\psi(t) = \text{Re}[h_{\text{IF}}(t) \otimes \phi'(t)] + \sum_{n=2}^{\infty} \frac{1}{n!} \text{Im}[j^n f_n]$$

In the above equation, the first term represents the linear filtering of the input phase $\phi'(t)$ and the summation represents various orders of distortion introduced by the filter. Assuming that the linear filtering term dominates, we get the output phase process relative to the carrier phase at the IF filter output, as

$$\begin{aligned} \psi(t) &= h_{\text{IF}}(t) \otimes \phi'(t) \\ &= h_{\text{IF}}(t) \otimes \theta'_s(t) + h_{\text{IF}}(t) \otimes \theta'_i(t) \\ &= \psi_s(t) + \psi_{\text{PN}}(t) + \psi_n(t) \\ &= \psi_s(t) + \psi'(t) \end{aligned} \quad (3.8)$$

$$\psi_{\text{PN}}(t) = h_{\text{IF}}(t) \otimes \theta_{\text{PN}}(t)$$

$$\psi_n(t) = h_{\text{IF}}(t) \otimes \theta_n(t)$$

wher, \otimes denotes convolution.

The accumulated phase over the demodulation interval τ with respect to IF carrier phase ($2\pi f_{\text{IF}}\tau$) is given by,

$$\begin{aligned} \Delta\psi(t, \tau) &= \psi(t) - \psi(t - \tau) \\ &= \Delta\psi_s(t, \tau) + \Delta\psi'(t, \tau) \end{aligned}$$

where, $\Delta\psi_s(t, \tau) = \psi_s(t) - \psi_s(t - \tau)$

$$\Delta\psi'(t, \tau) = \psi'(t) - \psi'(t - \tau)$$

The total accumulated phase over the demodulation interval can be written as

$$\begin{aligned}\Delta\psi_T &= 2\pi f_{IF}\tau + \Delta\psi'(t, \tau) \\ &= 2\pi f_{IF}\tau + \Delta\psi_s(t, \tau) + \Delta\psi'(t, \tau)\end{aligned}\quad (3.9)$$

The IF center frequency f_{IF} is adjusted such that $2\pi f_{IF}\tau = 2n\pi$, $n = 1, 2, \dots$ we get

$$\begin{aligned}\Delta\psi_T &= 2n\pi + \Delta\psi_s(t, \tau) + \Delta\psi'(t, \tau) \\ &= 2n\pi + \Delta\psi_s(t, \tau) + \Delta\psi_{PN}(t, \tau) + \Delta\psi_n(t, \tau)\end{aligned}\quad (3.10)$$

The average probability of error can be expressed as [28],

$$P(e) = \int_{-\infty}^{\infty} P_{\Delta\psi_n}(\Delta\psi_n) P(e|\Delta\psi_n) d\Delta\psi_n \quad (3.11)$$

where, $P_{\Delta\psi_n}(\Delta\psi_n)$ is the probability density function of $\Delta\psi_n$ and Gaussian with zero mean and variance $\sigma_{\psi_n}^2$

$$P_{\Delta\psi_n}(\Delta\psi_n) = \frac{1}{2\pi\sqrt{\sigma_{\psi_n}^2}} e^{-\frac{\Delta\psi_n^2}{2\sigma_{\psi_n}^2}} \quad (3.12)$$

and,

$$\begin{aligned}P(e|\Delta\psi_n) &= \frac{1}{2} - \frac{1}{2} \sqrt{\rho_1 \rho_2} \exp\left[-\frac{1}{2}(\rho_1 + \rho_2)\right] \sum_{n=0}^{\infty} \frac{(-1)^n}{2n+1} \exp\left[-\frac{(2n+1)^2}{2} \Delta\psi_n\right] \\ &\quad \left[I_n\left(\frac{\rho_1}{2}\right) + I_{n+1}\left(\frac{\rho_1}{2}\right) \right] \left[I_n\left(\frac{\rho_2}{2}\right) + I_{n+1}\left(\frac{\rho_2}{2}\right) \right] \cos(2n+1)\Delta\psi_n\end{aligned}\quad (3.13)$$

Here, $\rho_1 = \rho_2 = \rho$

$$P(e|\Delta\psi_n) = \frac{1}{2} - \frac{\rho}{2} \exp\left[-\frac{\rho}{2} \sum_{n=0}^{\infty} \frac{(-1)^n}{2n+1} \exp\left[-\frac{(2n+1)^2}{2} \Delta\nu T\right] 2 \left[I_n\left(\frac{\rho}{2}\right) + I_{n+1}\left(\frac{\rho}{2}\right) \right] \cos(2n+1)\Delta\psi_n\right]$$

The variance $\sigma_{\Delta\psi_n}^2$ of $\Delta\psi_n(t)$ can be obtained as

$$\sigma_{\Delta\psi_n}^2 = \int_{f_F - \frac{B_F}{2}}^{f_F + \frac{B_F}{2}} W_{\Delta\psi_n}(f) |H_F(f)|^2 df \quad (3.14)$$

and, $W_{\Delta\psi_n}(f) = W_{\Delta\psi_n}^c(f) + W_{\Delta\psi_n}^I(f)$

3.4 Results and discussion

Following the theoretical analysis, the bit error rate performance of heterodyne optical DPSK transmission system is computed at a bit rate of 10 Gb/sec for different sets of receiver and system parameters. Bit error rate performances are evaluated for dispersion shifted (DS) fibres at an wavelength of 1300 nm and nondispersion shifted (NDS) fibres at an wavelength of 1550 nm for several dispersion coefficients D_c .

The bit error rate (BER) performance of heterodyne optical DPSK system is shown in fig. 3.2 without considering the effect of fibre chromatic dispersion i.e. $D_c = 0.0$. The BER is plotted as a function of the received optical power P_s (dBm) for several values of normalized linewidth $\Delta\nu T$ and the receiver sensitivity is defined as the optical power required to obtain a BER of 10^{-9} . The figure shows that the BER decreases with the increase in the input power. For $\Delta\nu T = 0.0$ the receiver sensitivity is found to be -41.96 dBm. At increased value of laser linewidth, the required amount of signal power is higher to achieve the same BER. The additional

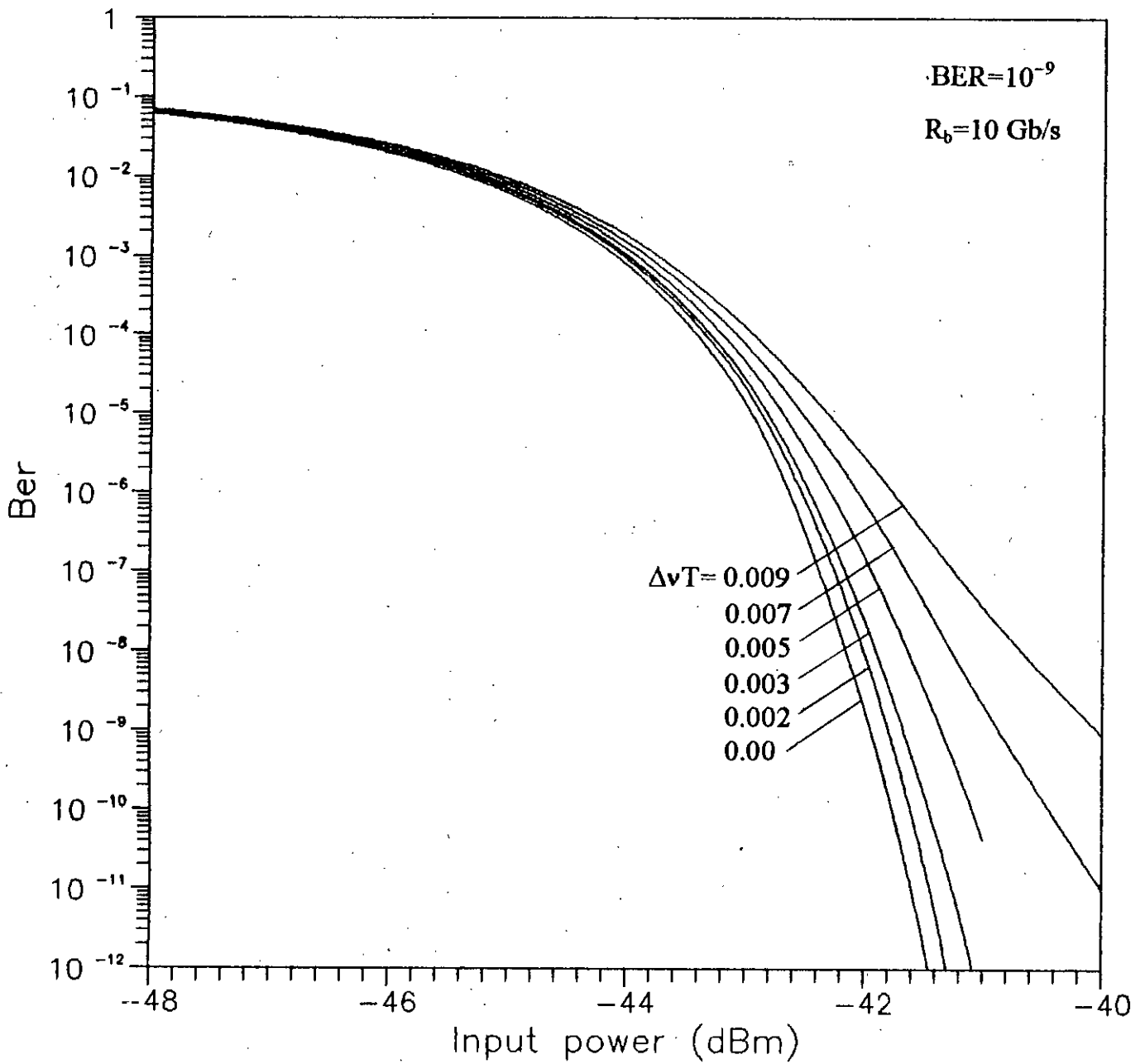


Fig. 3.2 Bit error rate vs. receiver input power of optical heterodyne DPSK transmission system at a bit rate of 10 Gb/s without fibre chromatic dispersion ($D_c=0.0$) for several values of normalized laser linewidth $\Delta\nu T$.

signal power compared to the case of zero linewidth ($\Delta\nu T = 0.0$) may be termed as the power penalty at $\text{BER} = 10^{-9}$ due to the effect of laser phase noise caused by non-zero linewidth. Phase noise causes the spectrum of the DPSK signal to be broadened and for a given receiver bandwidth, the signal power is less at the output of the receiver baseband filter. As a result, more signal power is required to obtain the same BER. The effect of phase noise is more at higher values of linewidth.

In presence of fibre chromatic dispersion, the BER performance of heterodyne optical DPSK transmission system is shown in fig. 3.3 for fibre length $L = 100$ Km, chromatic dispersion factor $D_c = 1.0$ ps/Km.nm, wavelength $\lambda = 1550$ nm for several values of laser linewidth $\Delta\nu T$. Comparing this figure with fig. 3.2, we notice that the performance of the system is degraded due to the effect of fibre chromatic dispersion. At a given input power, the BER is higher in the presence of dispersion compared to the case when there is no dispersion. The receiver sensitivity thus degrades and there is an additional power penalty due to the effect of dispersion. For example, in absence of laser phase noise ($\Delta\nu T = 0.0$), the receiver sensitivity to achieve $\text{BER} = 10^{-9}$ is -41.96 dBm when there is no dispersion ($D_c = 0.0$) whereas in presence of dispersion with $D_c = 1.0$, the receiver sensitivity is found to be -41.53 dBm. For $\Delta\nu T = 0.005$, the receiver sensitivity is -41.36 dBm when $D_c = 0.0$ (from fig. 3.2) and it is found to be -39.47 dBm when $D_c = 1.0$ (from fig. 3.3).

It is also observed that the penalty due to the combined effect of laser phase noise and chromatic dispersion is higher at higher values of normalized linewidth $\Delta\nu T$.

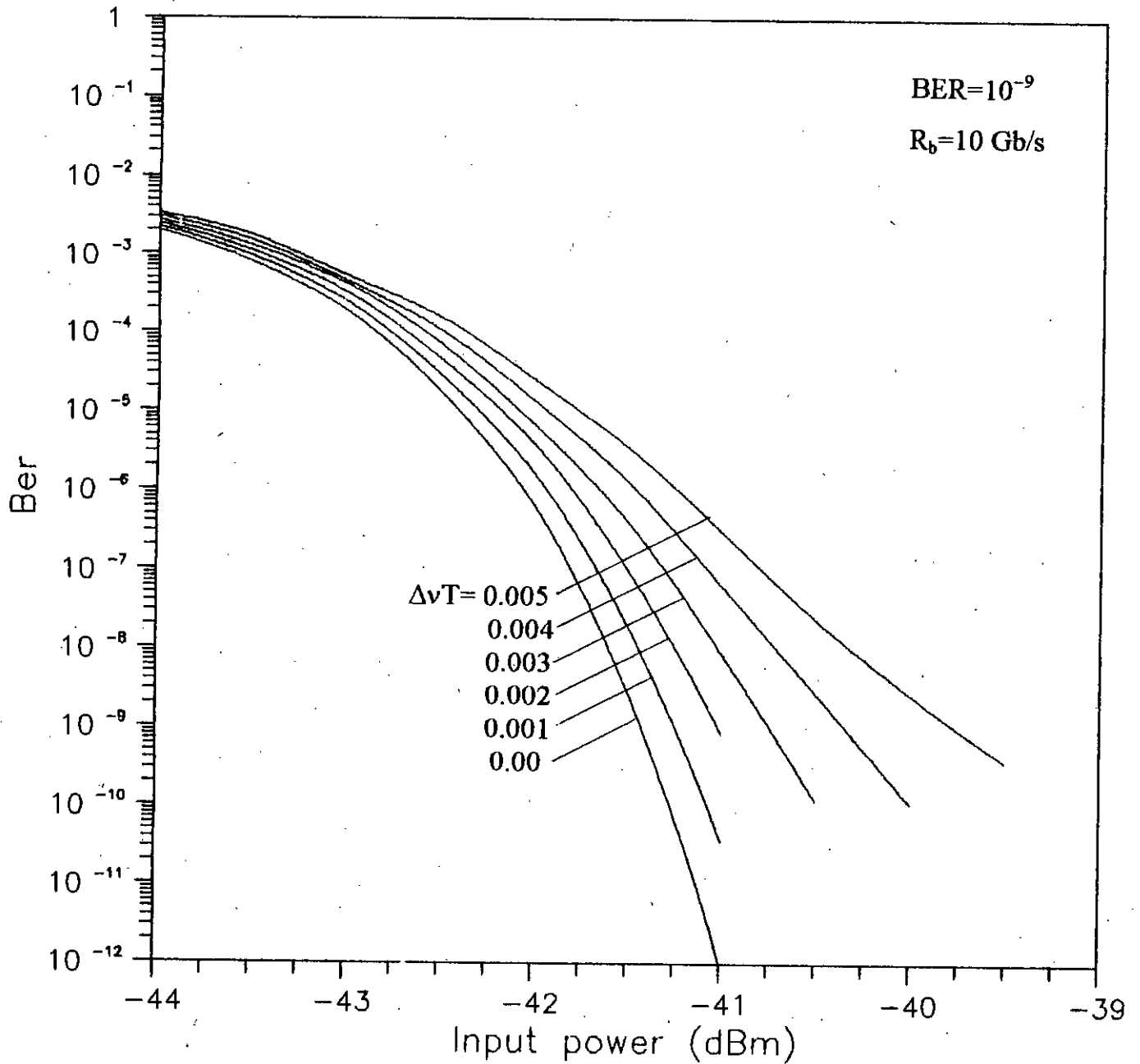


Fig. 3.3 Bit error rate vs. receiver input power of optical heterodyne DPSK transmission system at a bit rate of 10 Gb/s with fibre chromatic dispersion $D_c=1.0$ ps/Km.nm, fibre length $L=100$ Km, at an wavelength $\lambda=1550$ nm for several values of normalized laser linewidth $\Delta\nu T$.

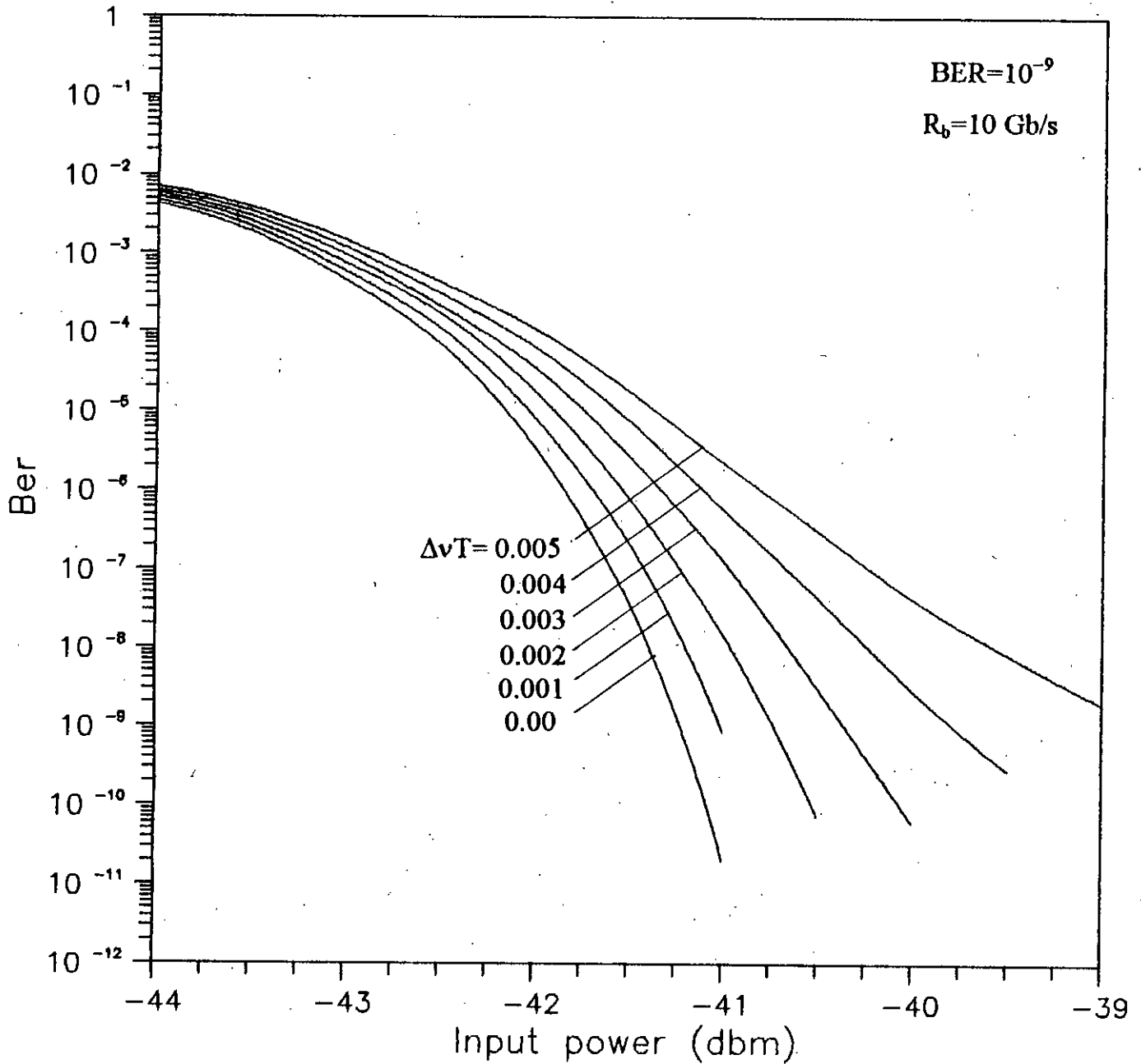


Fig. 3.4 Bit error rate vs. receiver input power of optical heterodyne DPSK transmission system at a bit rate of 10 Gb/s with fibre chromatic dispersion $D_c=3.0$ ps/Km.nm, fibre length $L=100$ Km, at an wavelength $\lambda=1550$ nm for several values of normalized laser linewidth $\Delta\nu T$.

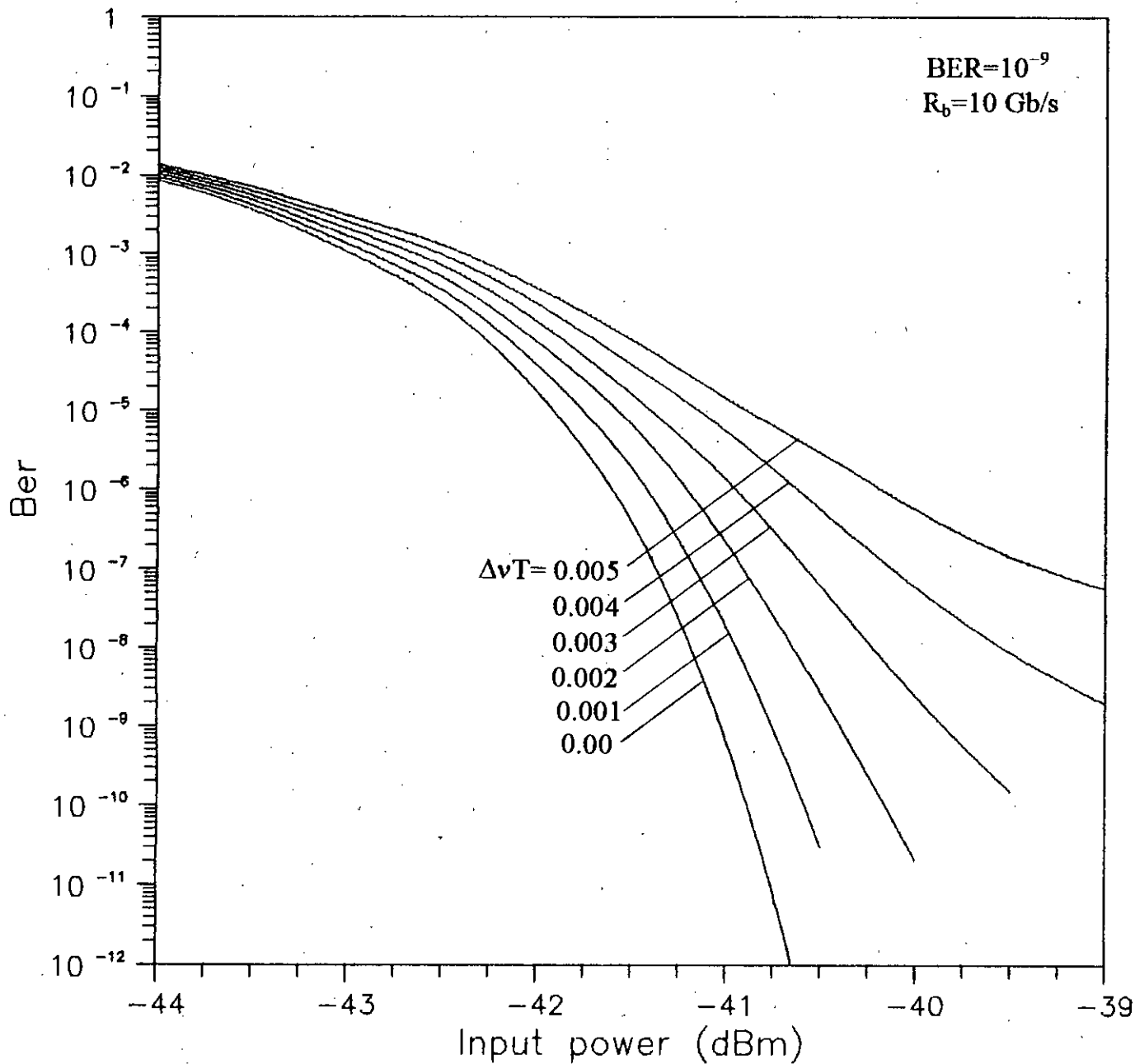


Fig. 3.5 Bit error rate vs. receiver input power of optical heterodyne DPSK transmission system at a bit rate of 10 Gb/s with fibre chromatic dispersion $D_c=6.0$ ps/Km.nm, fibre length $L=100$ Km, at an wavelength $\lambda=1550$ nm for several values of normalized laser linewidth $\Delta\nu T$.

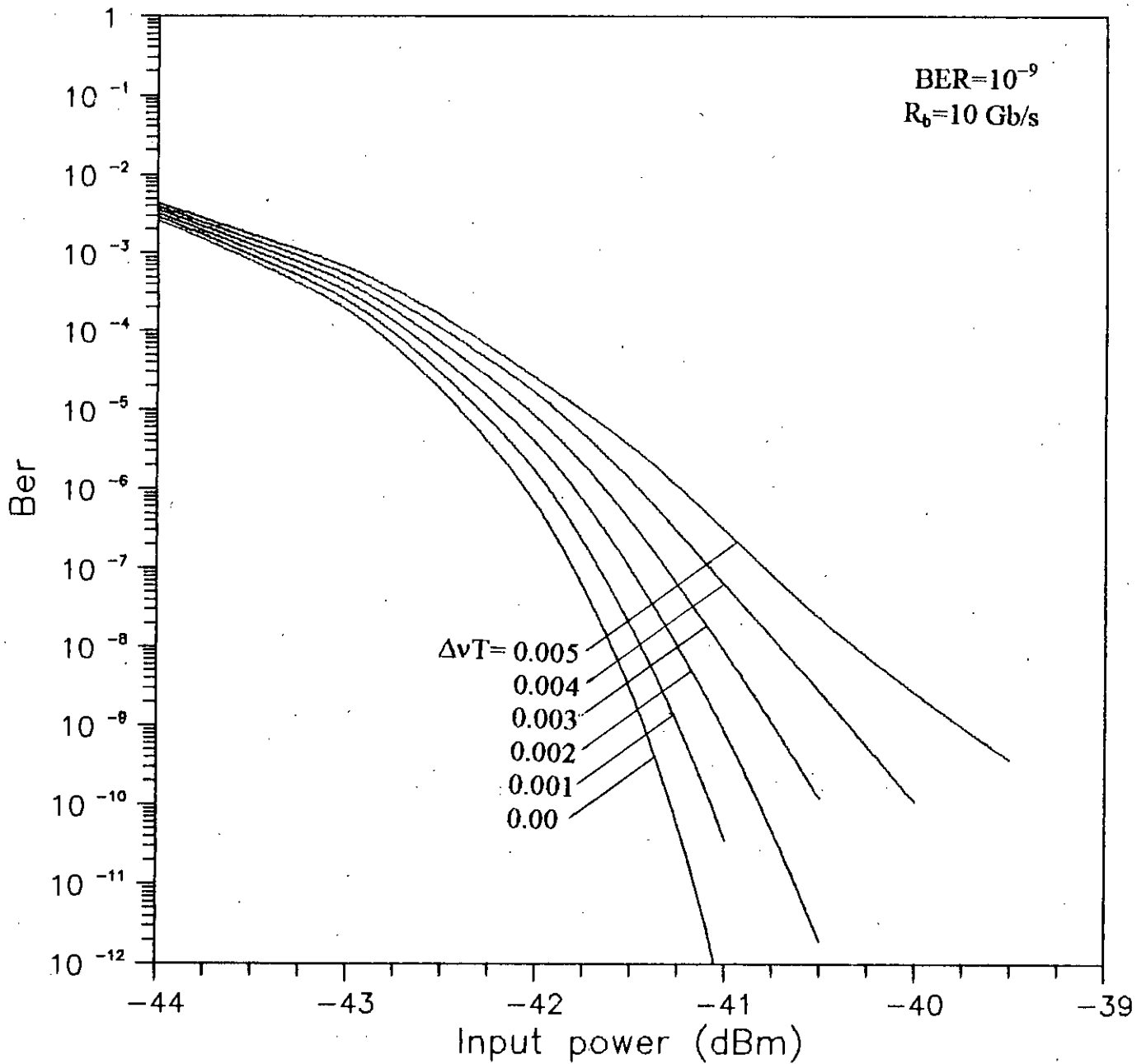


Fig. 3.6 Bit error rate vs. receiver input power of optical heterodyne DPSK transmission system at a bit rate of 10 Gb/s with fibre chromatic dispersion $D_c=1.0$ ps/Km.nm, fibre length $L=150$ Km, at an wavelength $\lambda=1550$ nm for several values of normalized laser linewidth $\Delta\nu T$.

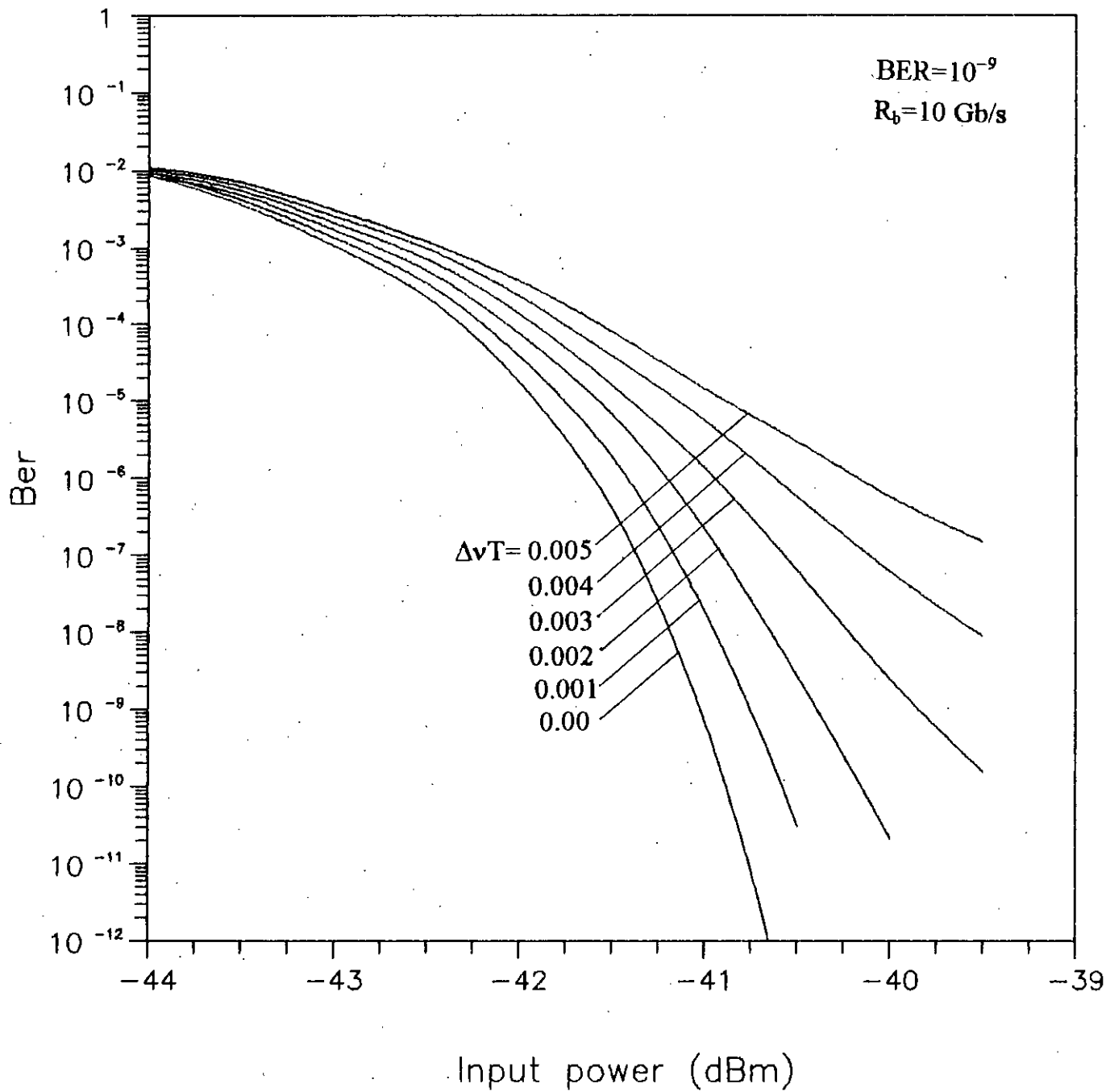


Fig. 3.7 Bit error rate vs. receiver input power of optical heterodyne DPSK transmission system at a bit rate of 10 Gb/s with fibre chromatic dispersion $D_c=1.0$ ps/Km.nm, fibre length $L=200$ Km, at an wavelength $\lambda=1550$ nm for several values of normalized laser linewidth $\Delta\nu T$.

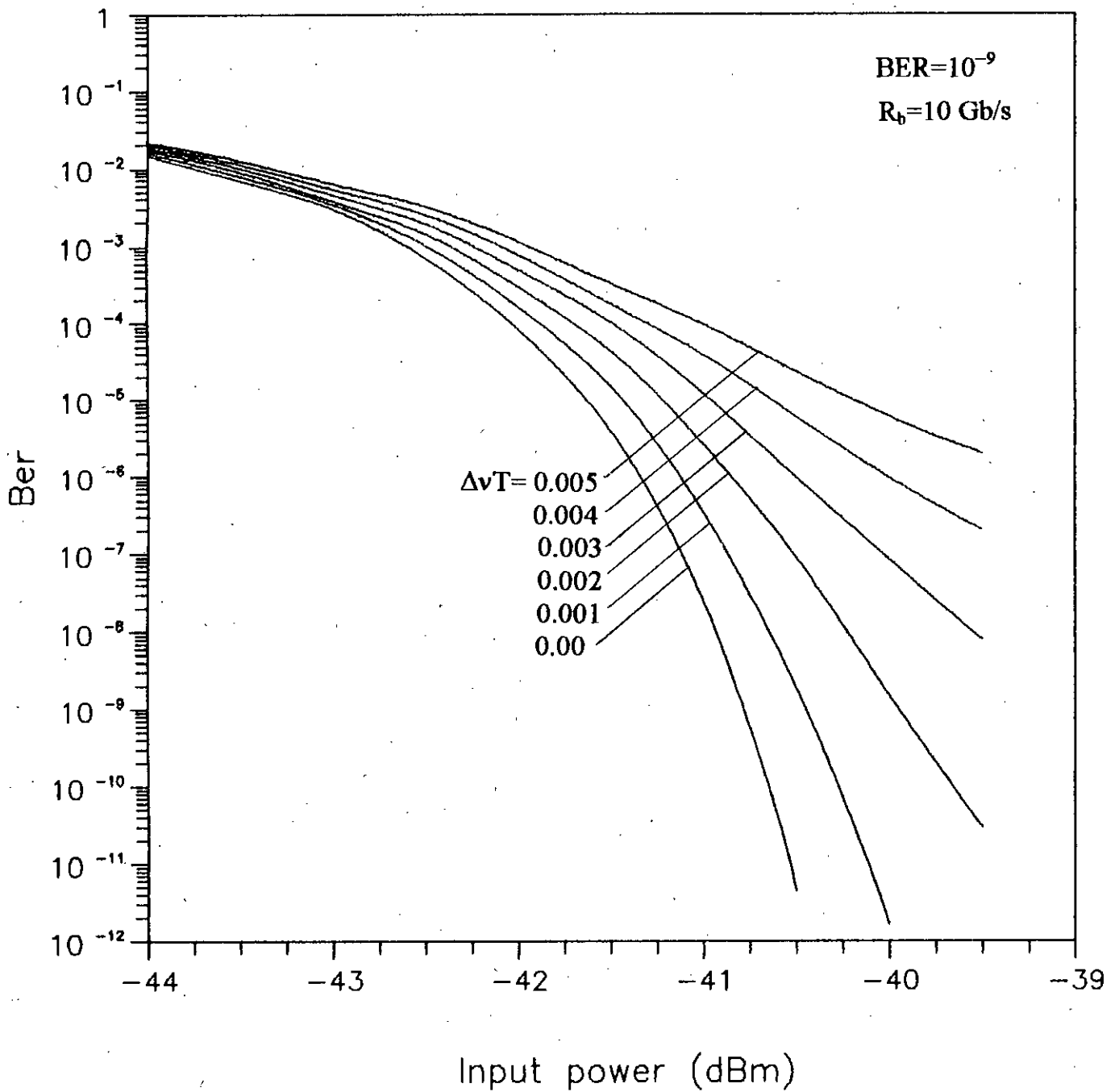


Fig. 3.8 Bit error rate vs. receiver input power of optical heterodyne DPSK transmission system at a bit rate of 10 Gb/s with fibre chromatic dispersion $D_c=1.0$ ps/Km.nm, fibre length $L=500$ Km, at an wavelength $\lambda=1550$ nm for several values of normalized laser linewidth $\Delta\nu T$.

When the dispersion coefficient D_c is increased to 3.0 ps/Km.nm, the bit error rate performance is shown in fig. 3.4 for several values of normalized laser linewidth $\Delta\nu T$. Compared to fig. 3.3, where $D_c=1.0$, it is evident that increased dispersion factor causes the system performance to be more degraded. For the same value of fibre length BER is plotted for higher value of dispersion coefficient in fig. 3.5. Similar conclusion can be drawn from fig. 3.5 when compared to fig. 3.2 and fig. 3.3. Bit error rate performance curves are plotted for $D_c=1$ ps/Km.nm, $\lambda=1550$ nm, $L=150$ Km, 200 Km and 500 Km in fig. 3.6 through fig. 3.8. From these figures, it is observed that, system performance is degraded with the increase in fibre length.

It is further observed that at increased value of $\Delta\nu T$, there occurs bit error rate (BER) floor at increased signal power, i.e. BER does not decrease with increase in signal power. As seen from fig. 3.4, the BER floor occurs around 3×10^{-9} corresponding to $\Delta\nu T=0.005$. Also, the BER floor goes upward for the same value of $\Delta\nu T$ when dispersion coefficient D_c is increased from 3 to 6 ps/Km.nm as is evident by comparing fig. 3.4 with fig. 3.5. Thus we can draw the conclusion that, the system suffers BER floor at larger values of the chromatic dispersion coefficient D_c and / or larger fibre length.

The bit error rate performance vs. input signal power for several values of dispersion coefficients are shown in fig. 3.9 through fig. 3.14 at an wavelength $\lambda=1300$ nm. From these figures, similar conclusions can be drawn as observed from the plots for $\lambda=1550$ nm.

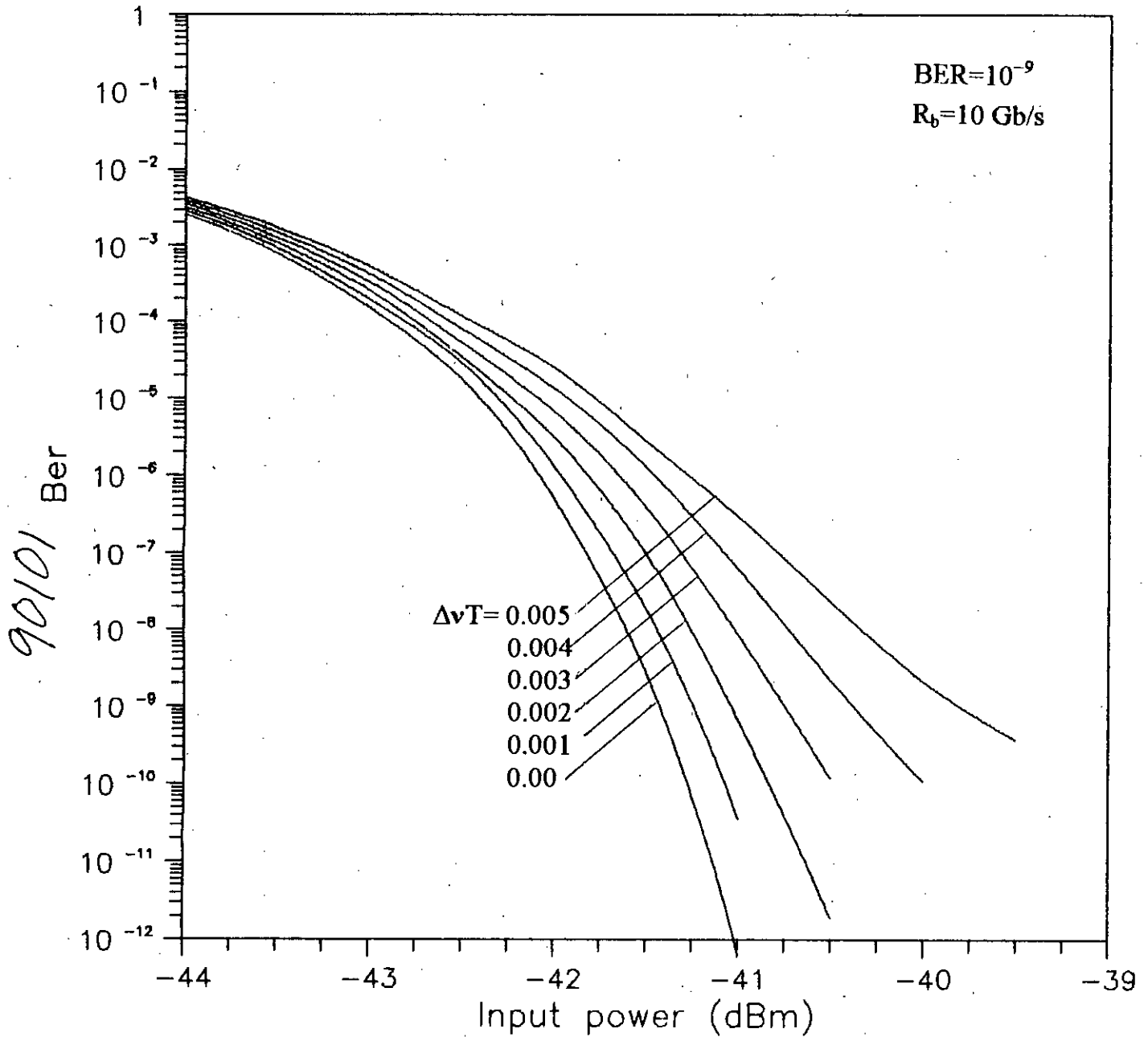


Fig. 3.9 Bit error rate vs. receiver input power of optical heterodyne DPSK transmission system at a bit rate of 10 Gb/s with fibre chromatic dispersion $D_c = 1.0 \text{ ps/Km.nm}$, fibre length $L = 100 \text{ Km}$, at a wavelength $\lambda = 1300 \text{ nm}$ for several values of normalized laser linewidth $\Delta\nu T$.

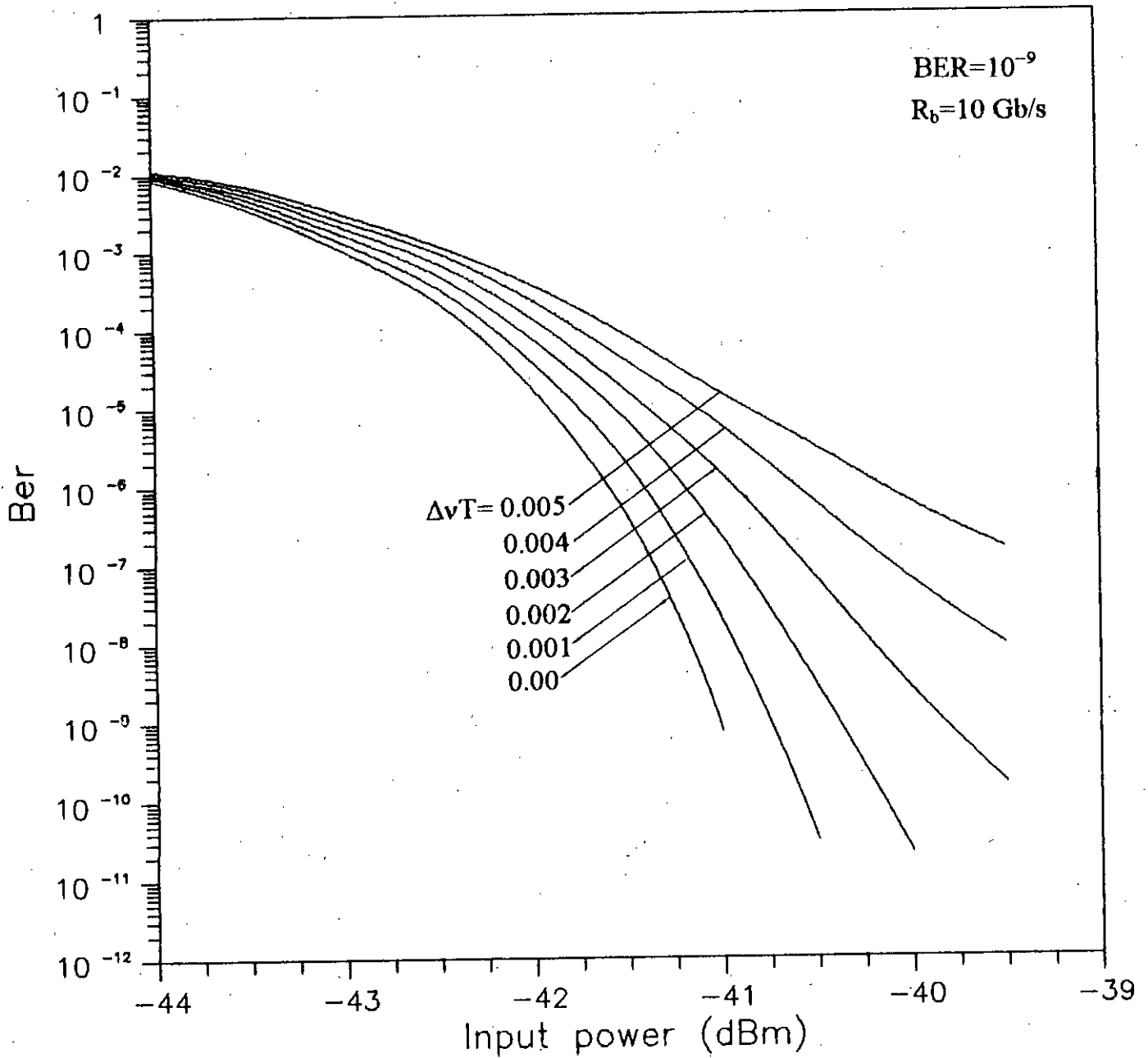


Fig. 3.10 Bit error rate vs. receiver input power of optical heterodyne DPSK transmission system at a bit rate of 10 Gb/s with fibre chromatic dispersion $D_c=3.0$ ps/Km.nm, fibre length $L=100$ Km, at an wavelength $\lambda=1300$ nm for several values of normalized laser linewidth $\Delta\nu T$.

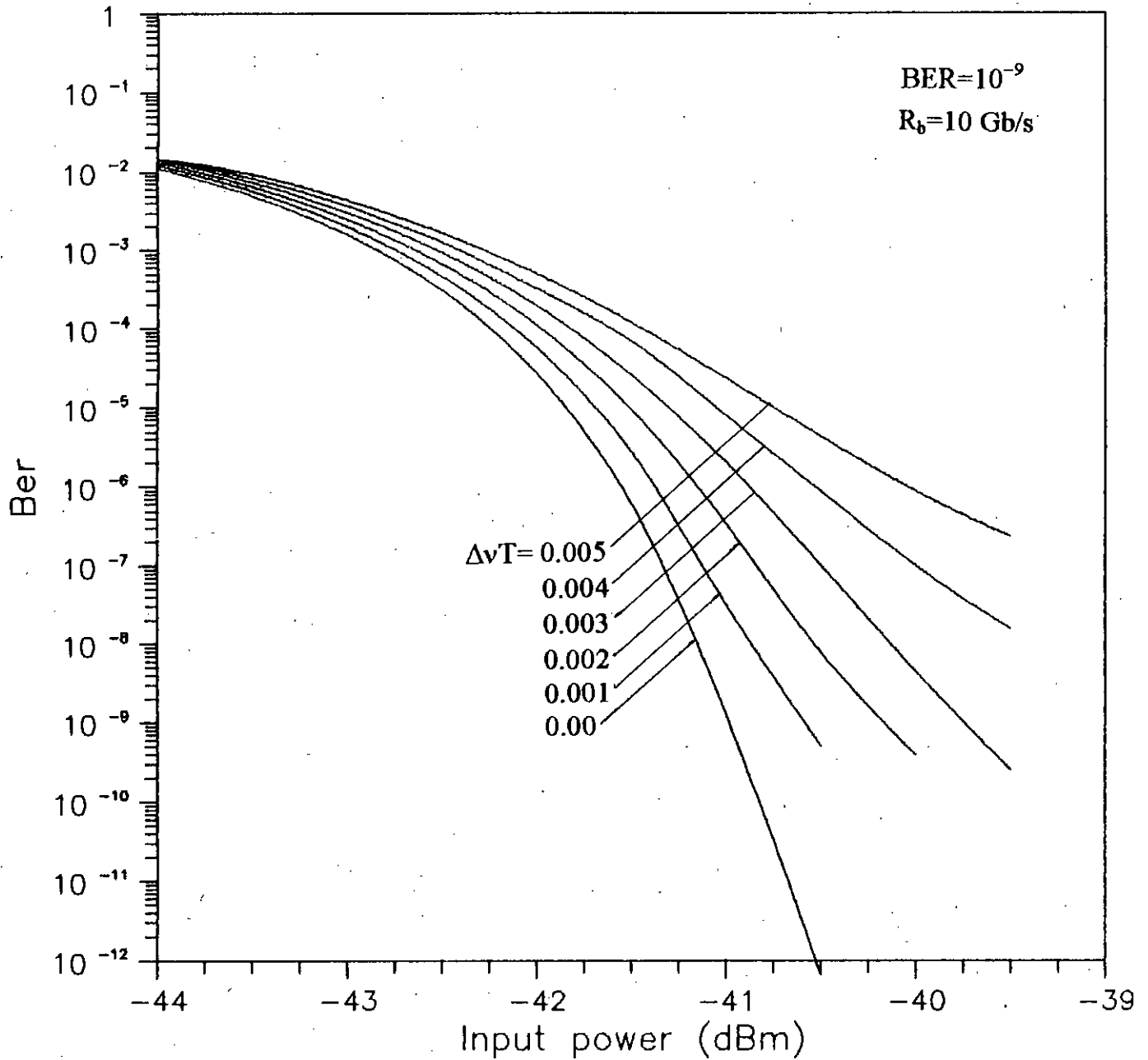


Fig. 3.11 Bit error rate vs. receiver input power of optical heterodyne DPSK transmission system at a bit rate of 10 Gb/s with fibre chromatic dispersion $D_c = 9.0$ ps/Km.nm, fibre length $L = 100$ Km, at an wavelength $\lambda = 1300$ nm for several values of normalized laser linewidth $\Delta\nu T$.

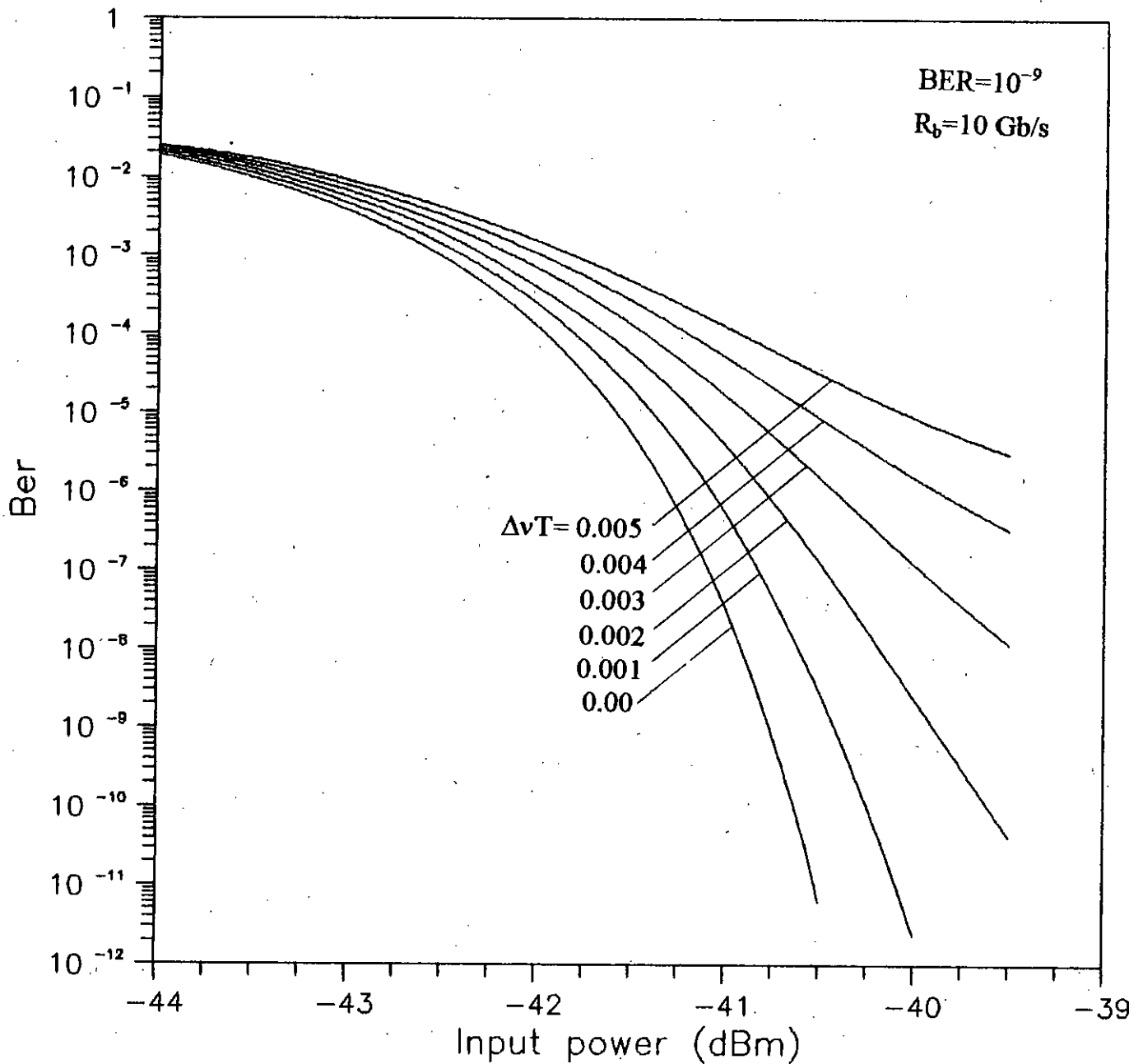


Fig. 3.12 Bit error rate vs. receiver input power of optical heterodyne DPSK transmission system at a bit rate of 10 Gb/s with fibre chromatic dispersion $D_c=15.0$ ps/Km.nm, fibre length $L=100$ Km, at an wavelength $\lambda=1300$ nm for several values of normalized laser linewidth $\Delta\nu T$.

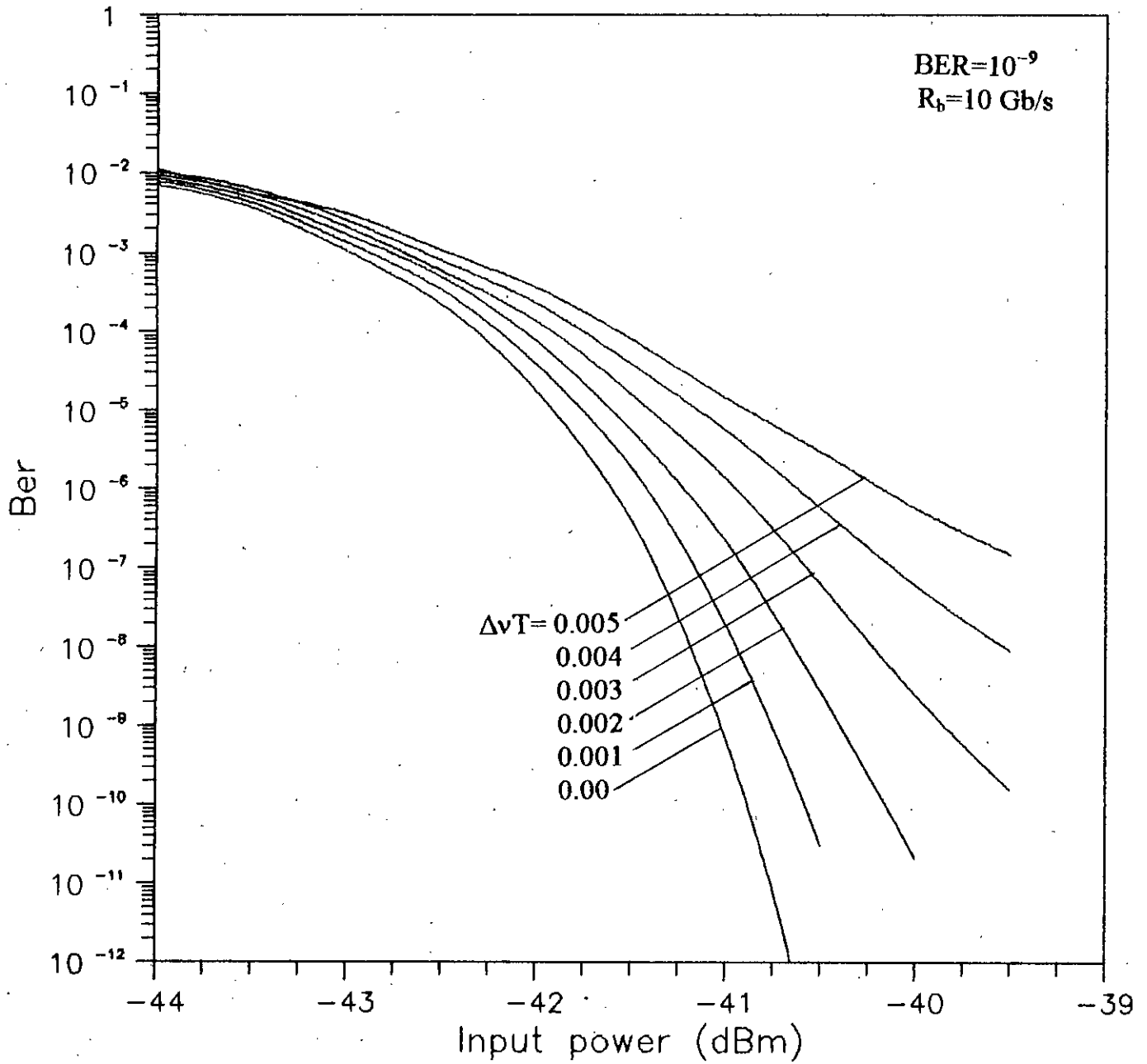


Fig. 3.13 Bit error rate vs. receiver input power of optical heterodyne DPSK transmission system at a bit rate of 10 Gb/s with fibre chromatic dispersion $D_c=1.0$ ps/Km.nm, fibre length $L=200$ Km, at an wavelength $\lambda=1300$ nm for several values of normalized laser linewidth $\Delta\nu T$.

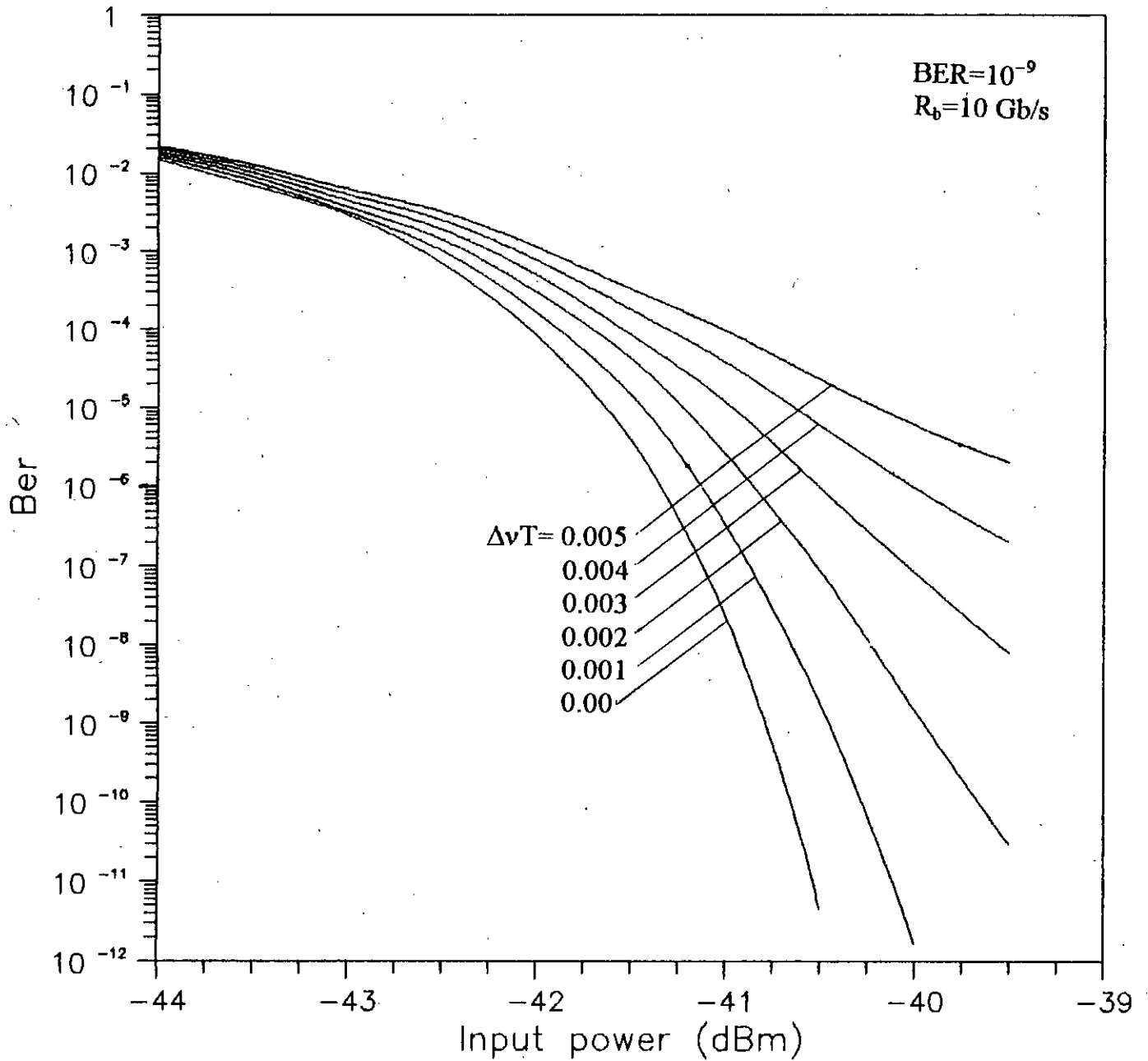


Fig. 3.14 Bit error rate vs. receiver input power of optical heterodyne DPSK transmission system at a bit rate of 10 Gb/s with fibre chromatic dispersion $D_c=1.0$ ps/Km.nm, fibre length $L=500$ Km, at an wavelength $\lambda=1300$ nm for several values of normalized laser linewidth $\Delta\nu T$.

The penalty in signal power suffered by the system due to the combined effect of laser phase noise and fibre chromatic dispersion are determined from bit error rate (BER) curves at $BER=10^{-9}$. The plots of power penalty versus chromatic dispersion coefficient D_c (ps/Km.nm) are shown in fig. 3.15 (for $\lambda=1550$ nm) and in fig. 3.16 (for $\lambda=1300$ nm). From these figures, it is observed that penalty increases with increase in $\Delta\nu T$ and / or dispersion coefficient D_c .

To get more insight into the effect of dispersion on the system performance, the penalty in signal power at $BER=10^{-9}$ is plotted as a function of the normalized linewidth $\Delta\nu T$ with dispersion factor as a parameter in fig. 3.17 (for $\lambda=1550$ nm) and in fig. 3.18 (for $\lambda=1300$ nm). In the absence of dispersion ($\gamma=0.0$) i.e. when only laser phase noise is present, the penalty is significantly less compared to the case of non-zero value of γ . When $\Delta\nu T=0.0$, the penalty suffered by the system is only due to chromatic dispersion and for $\Delta\nu T>0.0$ and $D_c >0.0$, the penalty is due to the combined effect of dispersion and phase noise. From the figure, it is observed that, for a given linewidth, the penalty increases with increase in the value of dispersion factor γ . Thus we can say that, chromatic dispersion imposes restriction on the allowable laser linewidth for a specified system penalty at a given BER.

The variation of power penalty with dispersion factor γ is plotted in fig. 3.19 for different values of normalized linewidth $\Delta\nu T$. It is observed that the penalty increases with increasing values of dispersion factor γ and normalized linewidth $\Delta\nu T$. Further, we also notice that for a given $\Delta\nu T$, at $BER=10^{-9}$ there is an upper

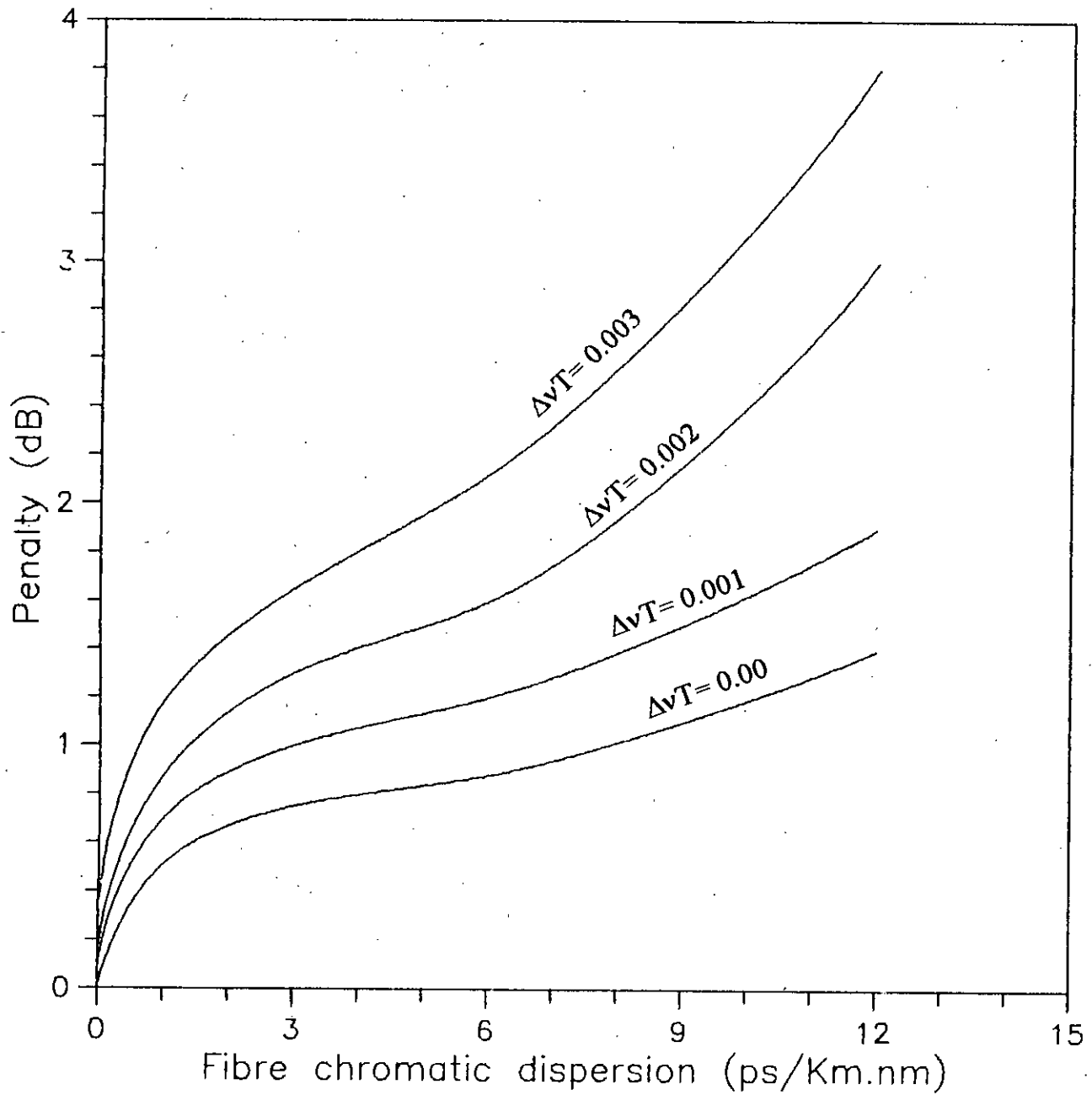


Fig. 3.15 Penalty in signal power due to combined effect of laser phase noise and fibre chromatic dispersion at $BER=10^{-9}$ versus dispersion coefficient D_c (ps/Km.nm) with fibre length $L=100$ Km and $\lambda=1550$ nm for several values of normalized laser linewidth $\Delta\nu T$.

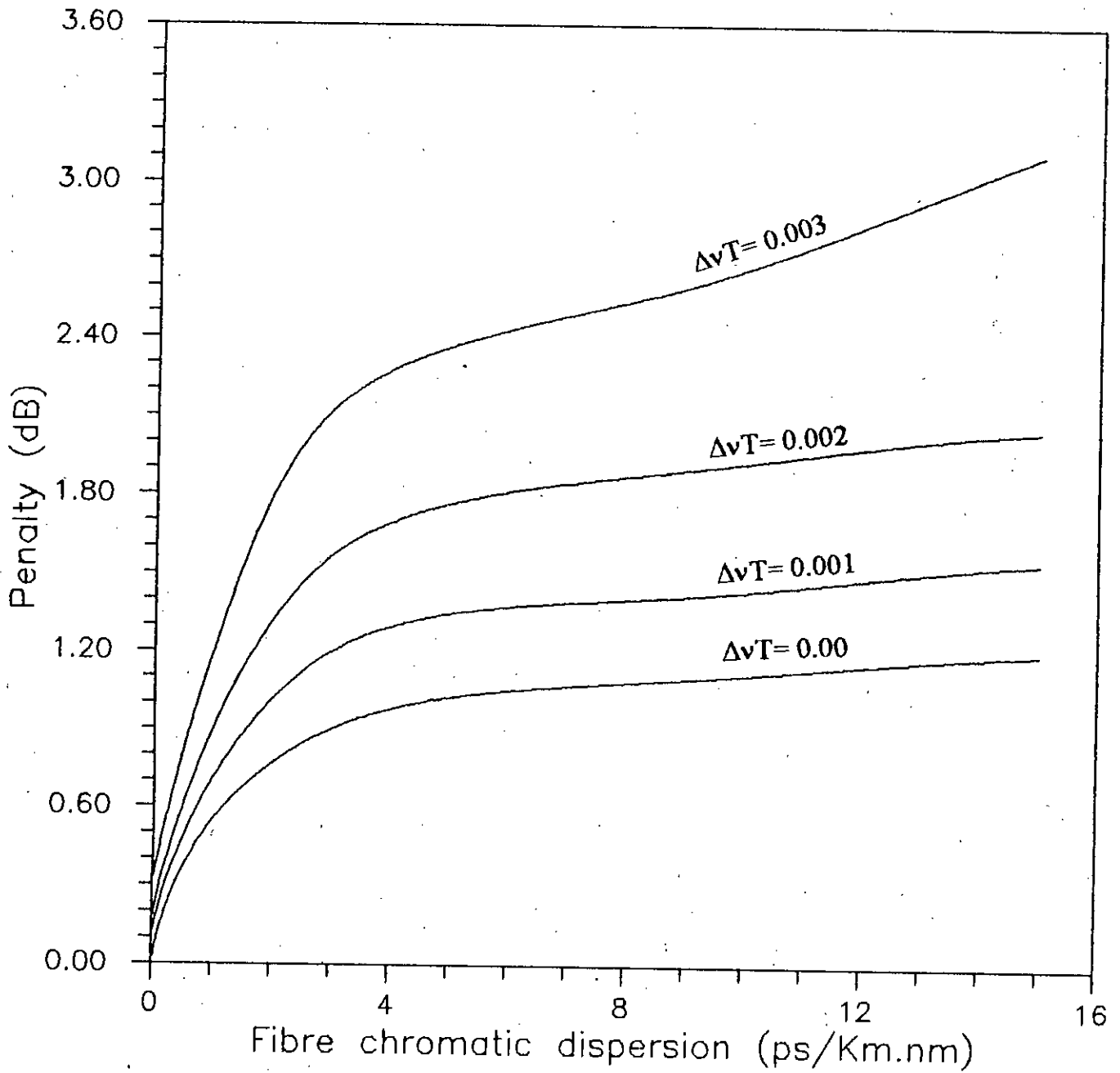


Fig. 3.16 Penalty in signal power due to combined effect of laser phase noise and fibre chromatic dispersion at $BER=10^{-9}$ versus dispersion coefficient D_c (ps/Km.nm) with fibre length $L=100$ Km and $\lambda=1300$ nm for several values of normalized laser linewidth $\Delta\nu T$.

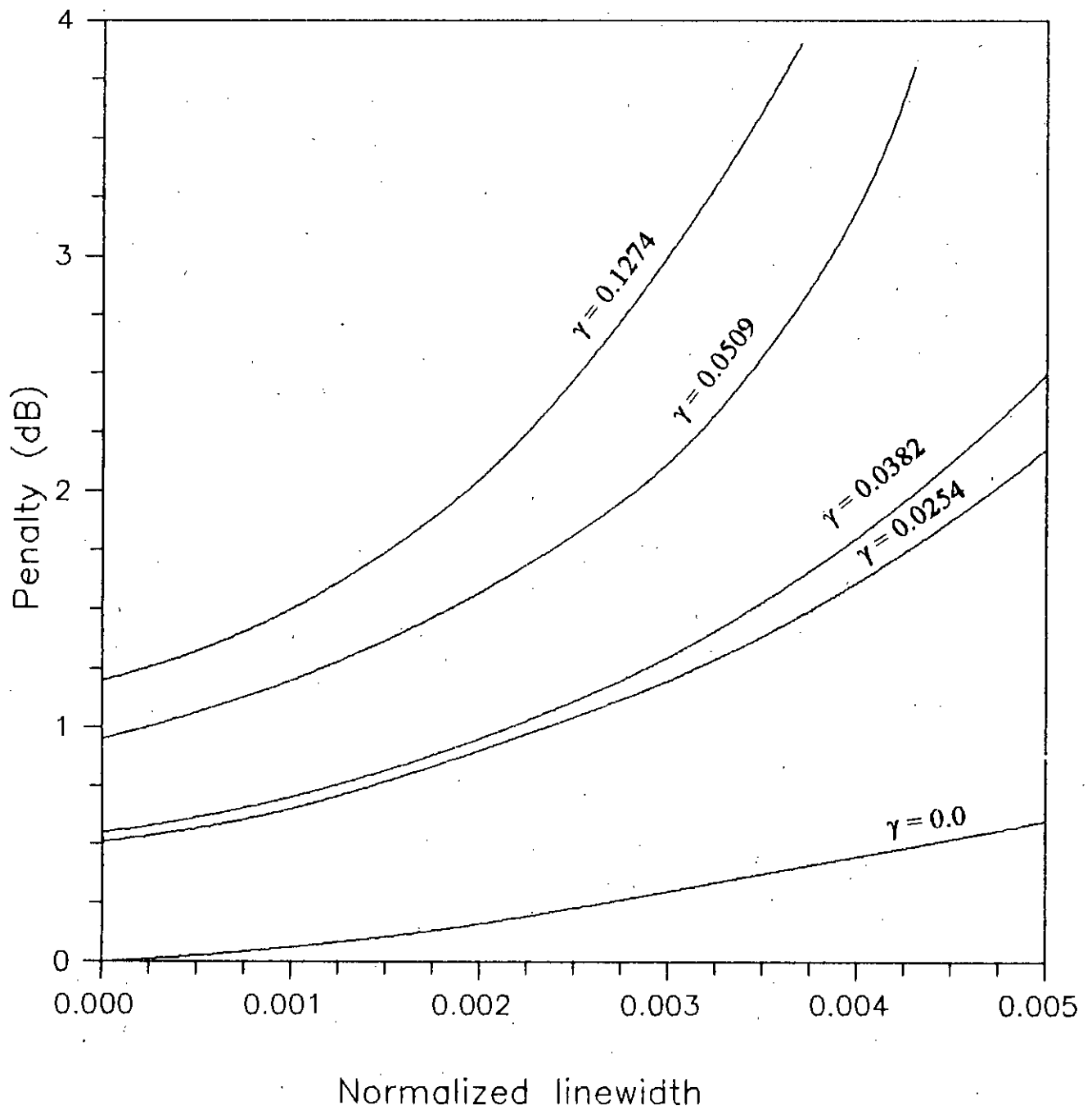


Fig. 3.17 Variation of power penalty (dB) due to combined effect of laser phase noise and fibre chromatic dispersion at $BER=10^{-9}$ with normalized laser linewidth $\Delta\nu T$ at $\lambda=1550$ nm for several values of dispersion factor γ .

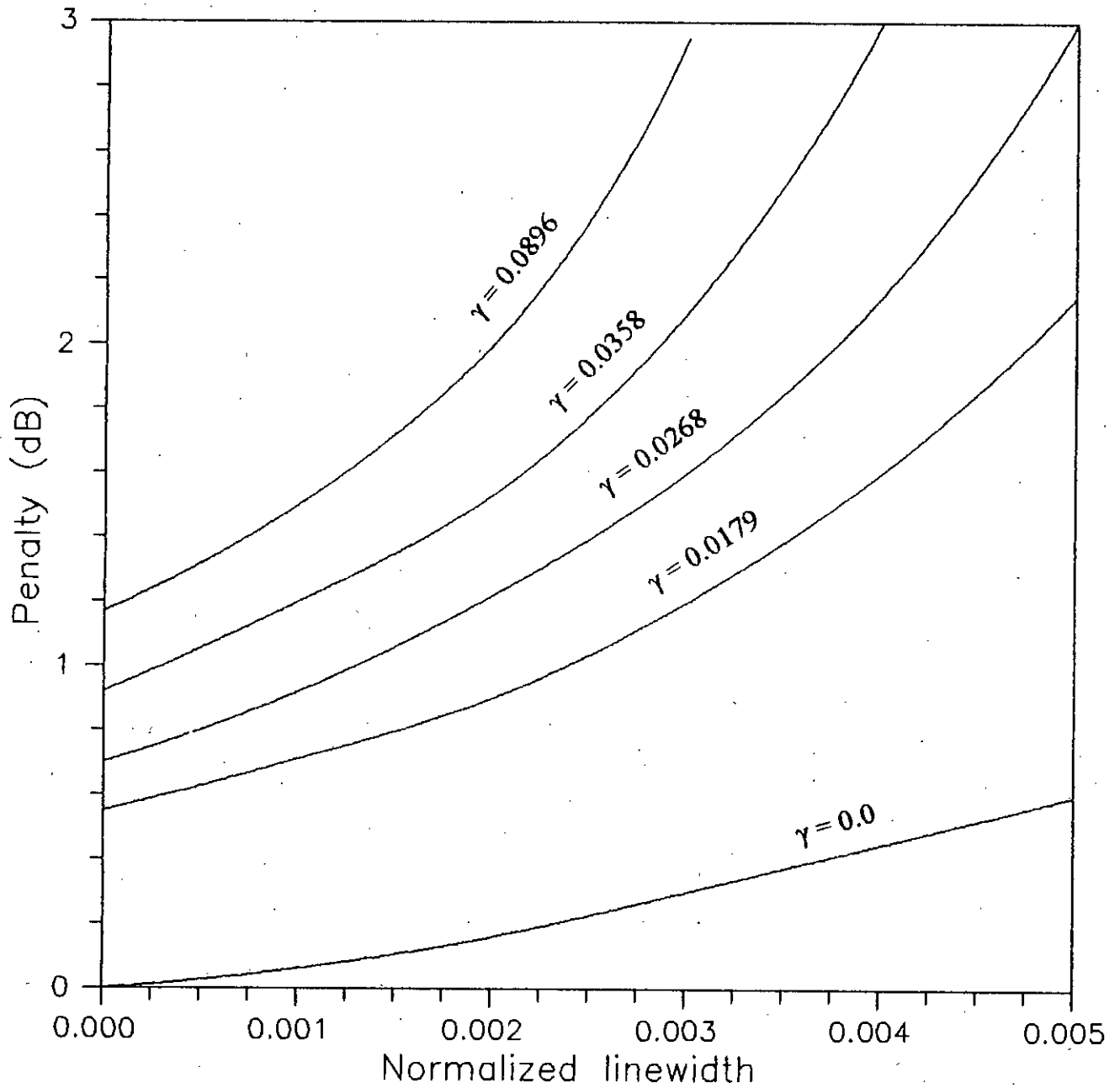


Fig. 3.18 Variation of power penalty (dB) due to combined effect of laser phase noise and fibre chromatic dispersion at $BER=10^{-9}$ with normalized laser linewidth $\Delta\nu T$ at $\lambda=1300$ nm for several values of dispersion factor γ .

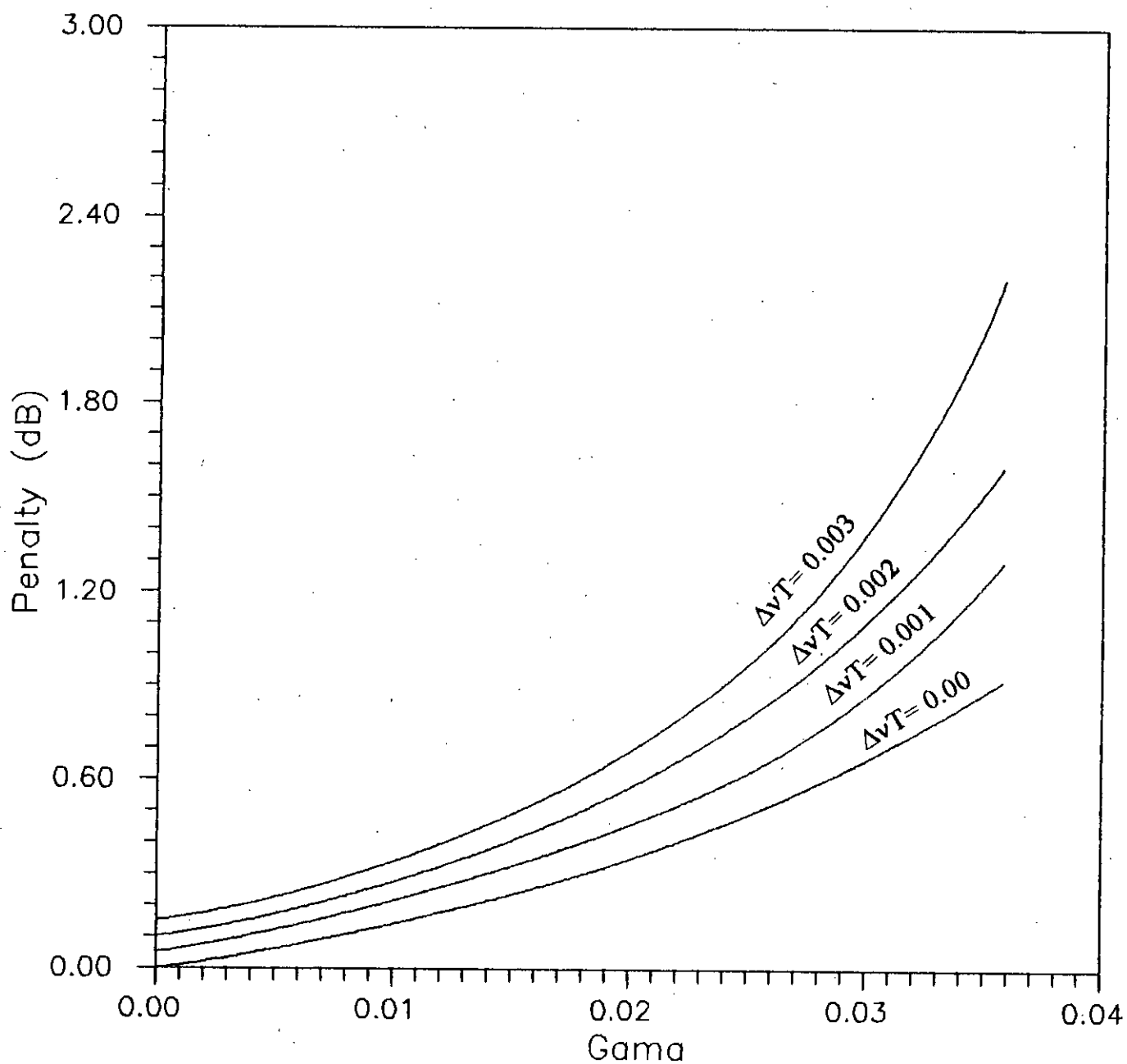


Fig. 3.19 Variation of power penalty (dB) due to combined effect of laser phase noise and fibre chromatic dispersion at $BER=10^{-9}$ with dispersion factor γ for several values of normalized laser linewidth $\Delta\nu T$.

limit on the dispersion factor γ for power penalty ≤ 1 dB. The upper limit or maximum allowable dispersion factor is less in the presence of phase noise and is significantly less at higher linewidth values. Corresponding to maximum allowable dispersion factor, we get an upper limit on the maximum fibre length for a given value of dispersion coefficient D_c corresponding to $BER=10^{-9}$ and penalty ≤ 1 dB.

For 1 dB power penalty at $BER=10^{-9}$, the allowable fibre length (Km) is plotted in fig. 3.20 as a function of normalized linewidth $\Delta\nu T$ for chromatic dispersion coefficient $D_c = 1.0, 2.0$ and 3.0 . It is observed that the allowable fibre length is about 170 Km when $\Delta\nu T=0.0$ and $D_c=1.0$. When chromatic dispersion coefficient D_c is increased to 2.0, the allowable fibre length reduces to around 85 Km and less than 60 Km for $D_c=3.0$. Further, the allowable fibre length exponentially decreases with increasing linewidth.

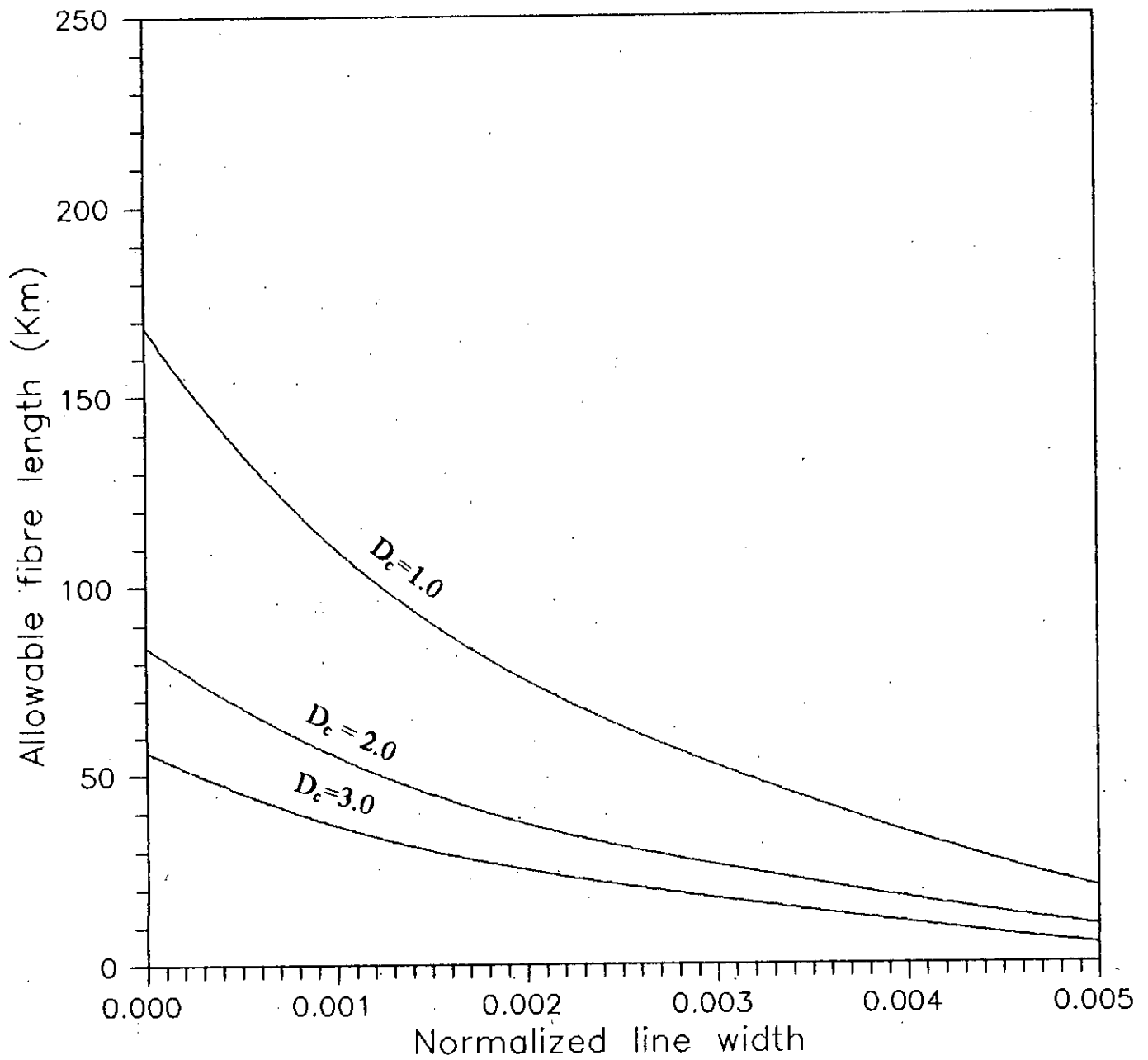


Fig. 3.20 Plots of allowable fibre length corresponding to 1 dB penalty at $BER=10^{-9}$ as a function of normalized laser linewidth $\Delta\nu T$ for dispersion coefficient $D_c = 1, 2$ and 3 ps/Km.nm.

CHAPTER 4

CONCLUSION AND SUGGESTIONS FOR FUTURE WORK

4.1 Conclusion

A theoretical analysis is provided for optical DPSK transmission system to evaluate the bit error rate (BER) performance with MZI based direct detection receiver in chapter 2. The analysis is carried out considering the effect of laser phase noise and fibre chromatic dispersion. Similar analysis is carried out for heterodyne optical DPSK system in chapter 3. Following the theoretical analysis, the bit error rate performance results are evaluated at a bit rate of 10 Gb/s with single-mode fibre at an wavelength of 1550 nm and 1300 nm for different values of receiver and fibre parameters.

The results show that in the absence of laser phase, the performance of DPSK system is highly degraded due to the effect of fibre dispersion. For small values of dispersion coefficient D_c and dispersion factor γ , the system suffers penalty in signal power at a specified BER of 10^{-9} compared to the case of no

dispersion. In the presence of laser phase noise, the system performance is more degraded and the penalty is higher. For example, in direct detection scheme, in the absence of laser phase noise ($\Delta\nu T=0.0$) the penalty suffered by the system at $BER=10^{-9}$ is approximately 0.1 dB for $D_c=1.0$, fibre span $L=50$ Km (from fig. 2.5). In presence of phase noise, when $\Delta\nu T=0.004$, the above penalty is found to be 0.7 dB (from fig. 2.5). It is observed that penalty is higher for coherent detection scheme. In coherent detection, in the absence of laser phase noise ($\Delta\nu T=0.0$) the penalty suffered by the system at $BER=10^{-9}$ is approximately 0.5 dB for $D_c=1.0$ and fibre span $L=100$ Km. In presence of laser phase noise, when $\Delta\nu T=0.004$, the above penalty is found to be 1.6 dB (from fig. 3.3). It is further noticed that the penalty is higher for higher values of dispersion coefficient D_c and fibre span L .

At increased value of normalized linewidth $\Delta\nu T$ and dispersion coefficient D_c , there occurs bit error rate floor which can not be lowered by increasing the signal power. Further, we also notice that for a given $\Delta\nu T$, at $BER=10^{-9}$, there is an upper limit on dispersion factor γ for power penalty ≤ 1 dB. The upper limit or maximum allowable dispersion factor is less in presence of phase noise and is significantly less at higher linewidth values. Corresponding to maximum allowable dispersion factor, we get an upper limit on the maximum fibre length for a given value of dispersion coefficient D_c , corresponding to $BER=10^{-9}$ and penalty ≤ 1 dB.

It is observed that in case of direct detection, the allowable fibre length corresponding to 1 dB penalty at $BER=10^{-9}$ is about 300 Km, when $\Delta\nu T=0.0$ and $D_c=1.0$. When chromatic dispersion D_c is increased to 2.0, the allowable fibre length reduces to around 175 Km and less than 100 Km for $D_c=3.0$. It is observed that in coherent detection scheme, the allowable fibre length is reduced for the same values of dispersion coefficient. In coherent detection, the allowable fibre length

corresponding to 1 dB penalty at $BER=10^{-9}$ is about 170 Km, when $\Delta\nu T=0.0$ and $D_c=1.0$. When chromatic dispersion D_c is increased to 2.0, the allowable fibre length reduces to around 85 Km and less than 60 Km for $D_c=3.0$. So we can draw the conclusion that the effect of laser phase noise and fibre chromatic dispersion is more in coherent detection than that of direct detection system.

Compared with the results of direct detection FSK reported earlier [34], we see that the effect of fibre chromatic dispersion is much less in case of direct detection DPSK. For example, for a given value of dispersion coefficient $D_c = 5.0$, the power penalty suffered by direct detection FSK is approximately 1.0 dB for $\Delta\nu T=0.002$ [34], whereas the same is 0.85 dB for direct detection DPSK. As a result, for a power penalty of 1 dB, the allowable fibre length is much higher for DPSK than for FSK.

4.2 Suggestions for future work

The present work has been carried out on single channel optical DPSK transmission system. Further work can be pursued on multi-channel optical DPSK transmission system. In multi-channel system, Mach-Zehnder interferometer can be employed as an optical frequency discriminator with a number of stages. The performance degradation of multi-channel transmission due to nonlinear effects of optical fibres, namely, chromatic dispersion, can be investigated. Further study can be carried out to evaluate the effect of four-wave mixing on optical frequency division multiplexing (OFDM) system.

Further works can be carried out to determine dispersion compensation techniques to reduce the power penalty due to fibre chromatic dispersion so as to

increase the repeaterless transmission distance in single/multi channel transmission systems with single-mode fibres. Further works can also be carried out to evaluate the impact of fibre dispersion on the performance of wavelength division multiplexed (WDM) optical FSK/DPSK transmission systems. The maximum number of wavelength channels, optimum channel separation, maximum fibre span limited by the effect of fibre chromatic dispersion at a bit rate of 10 Gb/s or higher are to be determined. Further investigations can also be initiated to analyze the performance of optical FSK/DPSK systems with fibre having nonuniform chromatic dispersion along the fibre.

The above work can be expanded to an optical network with bus or star topology and the optimum system parameters can be evaluated. A detail computer simulation for the optical system/network can also be carried out to validate the theoretical performance results.

REFERENCES

- [1] T.H.Maiman, "Stimulated optical radiation in ruby," *Nature*, Vol. 187, August 1960, pp. 493-494.
- [2] C.K.Kao and G.A.Hockman, "Dielectric-fibre surface waveguides for optical frequencies," *Proc.IEE*, Vol. 113, 1966, pp. 1151-1158.
- [3] Tingye Li, "Optical Fibre Communication-The State of the Art," *IEE Trans.Commun.* Vol. COM-26, no. 7, July 1978, pp. 946-954.
- [4] Heinrich Keil and Helmut Pascher, "Communications enter a new era with fibre optics," *Telecom report special issue "optical communications,"* Vol. 6, 1983, p.4.
- [5] K.Iwashita and T.Matsumoto, "Modulation and detection characteristics of optical continuous phase FSK transmission system," *J.Lightwave Technology*, Vol. LT-5, April 1987, pp. 461-468.
- [6] J.R.Pierce, "Optical Channels: Practical Limits with Photon Counting," *IEEE Trans. Comm.*, Vol. COM-26, No. 12, December 1978, pp. 1819-1821.
- [7] Ian Garrett, "Introduction to the effect of phase noise on coherent optical system," *Proc. of Fourth Tirrenia International workshop on Digital Comm.*, Tirrenia, Italy, September 19-23, 1989, pp. 103-116.
- [8] S.Saito, Y.Yamamoto and T.Kimura, "S/N and Error Rate Evaluation for an Optical FSK Heterodyne Detection System Using Semiconductor Lasers," *IEEE J.Quantum Electron.*, Vol. QE-19, 1983, pp. 180-193.

- [9] S.P.Majumder, "Theoretical and Simulation Studies on Some Relevant Modulation Schemes in Direct Detection and Coherent Optical Communication Systems," Ph.D.Dissertation, Indian Institute of Technology, Kharagpur (India), November 1991.
- [10] D.M.Spirit and L.C.Blank, "10 Gb/s, 28.5 Km distributed erbium fibre transmission with low signal power excursion," in Proc. Opt. Fibre Commun. Conf. OFC'91.
- [11] R.S.Tucker, "High-speed modulation of Semiconductor Laser," Journal of Lightwave Technology, Vol. LT-3, 1985, pp.1180-1192.
- [12] R.S.Vodhanel, A.S.Eltefaic, M.Z.Iqbal, R.E.Wagner, L.Gimett and S.Tsuji, "Performance of Directly Modulated DFB Laser in 10 Gb/s ASK, FSK and DPSK Lightwave System," Journal of Lightwave Technology, Vol. 8, no. 9, September 1990, pp. 1379-1385.
- [13] A.F.Elrefaic, R.E.Wagner, D.A.Atlas and D.G.Daut, "Chromatic dispersion limitations in coherent lightwave transmission system," Journal of Lightwave Technology, Vol. 6, May 1988, pp. 704-709.
- [14] A.R.Charplyvy, R.W.Tkach, L.L.Buhl and R.C.Alterness, "Phase modulation to amplitude conversion of CW Laser light in optical fibre," Electron Lett. Vol. 22, February 1986, pp. 409-411.
- [15] K.Tajima, "Self amplitude modulation in PSK coherent optical transmission system," in Conf. Proc. (Venice Italy) October 1985, pp. 351-354.
- [16] H.Toba, K.Oda and K.Nosu, "Design and performance of FSK direct detection scheme for optical FDM systems," Journal of Lightwave Technology, Vol. 9, no. 10, November 1991, pp.1335-1343.
- [17] Y.Yamamoto, "Receiver performance evaluation of various digital optical modulator-demodulator systems in 0.5-1.0 μm wavelength region," IEEE. J.Quantum Electron, Vol. QE-16, November 1980, pp. 1251-1259.

- [18] D.J.Malyon and W.A.Stallard, "565 Mb/s FSK direct detection system operating with four cascaded photonic amplifiers," *Electron. Lett.*, Vol. 25, no. 8, 1989, pp. 495-496.
- [19] C.Rolland, R.S.Moore, F.Shepherd and G.Hillier, "10 Gb/s, 1.56 μm multiquantum well InP/InGaAsP Mach-Zehnder optical modulator," *Electron.Lett.*, Vol. 29, no. 5, March 1993, pp. 471-472.
- [20] N.Takato, T.Kominato, A.Sugita, K.Jinguji, H.Toba and M.Kawachi, "Silica based integrated optic Mach-Zehnder Multi/demultiplexer with channel spacing of 0.01-250 nm," *IEEE. J. on selected areas in Comm.*, Vol. 8, no. 6, August 1990, pp. 1120-1127.
- [21] Faizul Alam, "Study of optical direct detection scheme using Mach-Zehnder discriminator," M.Sc.Engg. thesise submitted to EEE dept. of BUET, Dhaka, March 1994.
- [22] E.Bedrosian and S.O.Rice, "Distortion and cross-talk of linearly filtered angle-modulated signals," *Proc. IEEE*, Vol. 56, January 1968, pp.2-13.
- [23] Joao J.O.Pires, Jose R.F.da Rocha, "Performance analysis of direct detection optical DPSK system using dual detector optical receiver," *SPIE*, Vol.1579, *Advanced Fiber Communications Technologies*, 1991.
- [24] Md.Muzammel Haque Tarafder, "Effects of Fiber chromatic dispersion on optical FSK and DPSK transmission systems," M.Engg. Project, Dept. of EEE, BUET, Dhaka, 1994.
- [25] Chris P.Kaiser, Peter J.Smith and Mansoor Shafi, "An Improved Optical Heterodyne DPSK Receiver to Combat Laser Phase Noise," *Journal of Lightwave Technology*, Vol. 13, no. 3, March 1995, pp. 525-532.
- [26] Chris P.Kaiser, Mansoor Shafi and Peter J.Smith, "Analysis Methods for Optical Heterodyne DPSK Receivers Corrupted by Laser Phase Noise," *Journal of Lightwave Technology*, Vol. 11, no. 11, November 1993, pp. 1820-1829.

- [27] J.Salz, "Coherent lightwave communications," AT & T Technol. J., Vol. 64, December 1985, pp. 2153-2209.
- [28] G.Nicholson, "Probability of error for optical heterodyne DPSK system with quantum phase noise," Electron.Lett., Vol.20, November 1984, pp. 1005-1007.
- [29] G.Jacobsen and I.Garrett, "Theory for optical heterodyne DPSK receivers with postdetection filtering," J. Lightwave Technology, Vol. LT-5, April 1987, pp. 478-484.
- [30] G.Jacobsen, B.Jensen, I.Garrett and J.B.Waite, "Bit error rate floors in coherent optical systems with delay demodulation," Electron.Lett., Vol. 25, October 1989, pp. 1425-1427.
- [31] E.Patzak and P.Meissner, "Influence of 1F-filtering on bit error rate floor in coherent optical optical DPSK systems," IEE Proc. J., Vol. 135, October 1988, pp.355-357.
- [32] S.Haykin, Communication systems, 2nd ed. New York: 1983.
- [33] R.W.Lucky, J.Salz and E.J.Weldon, Jr., Principles of Data Communication. New York: McGraw-Hill, 1968.
- [34] Md. Abdul Moqaddem, "Performance analysis of direct detection optical FSK in the presence of fibre chromatic dispersion," M.Sc.Engg. thesis submitted to EEE dept. of BUET, Dhaka, June 1996.

Appendix A

Expressions of $w_{\phi}^c(f)$ and $w_{\phi}^I(f)$

$$\Gamma(f) = e^{-j\alpha f^2}$$

$$\Gamma(\rho) = e^{-j\alpha \rho^2}$$

$$\Gamma(f+\rho) = e^{-j\alpha(f+\rho)^2} = e^{-j\alpha(f^2+2f\rho+\rho^2)}$$

$$\begin{aligned} \Gamma(f)\Gamma(\rho)\Gamma(f+\rho) &= e^{-j\alpha f^2} e^{-j\alpha \rho^2} e^{-j\alpha(f^2+2f\rho+\rho^2)} \\ &= e^{-j2\alpha(f^2+f\rho+\rho^2)} \end{aligned}$$

$$\begin{aligned} W_{\phi}^c(f) &= 2W_{\phi}(f) \int_{-\infty}^{\infty} d\rho W_{\phi}(\rho) \{ \text{Re} \Gamma(f)\Gamma(\rho)\Gamma(-f-\rho) - |\Gamma(\rho)|^2 |\Gamma(f)|^2 \} \\ &= 2W_{\phi}(f) \int_{-\infty}^{\infty} d\rho W_{\phi}(\rho) [\text{Re}(e^{-j2\alpha(f^2+f\rho+\rho^2)}) - 1] \\ &= 2W_{\phi}(f) \int_{-\infty}^{\infty} W_{\phi}(\rho) [\cos\{2\alpha(f^2+f\rho+\rho^2)\} - 1] d\rho \end{aligned}$$

$$W_{\phi}^I(f) = \frac{1}{6} \int_{-\infty}^{\infty} d\rho \int_{-\infty}^{\infty} d\sigma W_{\phi}(\rho) W_{\phi}(\sigma) W_{\phi}(f-\rho-\sigma) |X(f)|^2$$

where,

$$X(f) = 2\Gamma(f)\Gamma(\sigma)\Gamma(f-\rho-\sigma) - \Gamma(f-\rho-\sigma)\Gamma(\rho+\sigma) - \Gamma(\rho)\Gamma(f-\rho) - \Gamma(\sigma)\Gamma(f-\sigma) + \Gamma(f)$$

$$\Gamma(\rho)\Gamma(f-\rho) = e^{-j\alpha\rho^2} e^{-j\alpha(f-\rho)^2} = e^{-j\alpha[f^2+2\rho^2-2f\rho]}$$

$$\Gamma(\sigma)\Gamma(f-\rho) = e^{-j\alpha\sigma^2} e^{-j\alpha(f-\sigma)^2} = e^{-j\alpha[f^2+2\sigma^2-2f\sigma]}$$

$$\Gamma(\rho) = e^{-j\alpha\rho^2}$$

$$\Gamma(f) = e^{-j\alpha f^2}$$

$$\Gamma(\sigma) = e^{-j\alpha\sigma^2}$$

$$\begin{aligned}\Gamma(\rho)\Gamma(\sigma)\Gamma(f-\rho-\sigma) &= e^{-j\alpha\rho^2} e^{-j\alpha\sigma^2} e^{-j\alpha(f^2+\rho^2+\sigma^2-2f\rho+2\rho\sigma-2f\sigma)} \\ &= e^{-j\alpha[f^2+2\rho^2+2\sigma^2-2f\rho+4\rho\sigma-2f\sigma]}\end{aligned}$$

Therefore,

$$\begin{aligned}X(f) &= 2\Gamma(f)\Gamma(\sigma)\Gamma(f-\rho-\sigma) - \Gamma(f-\rho-\sigma)\Gamma(\rho+\sigma) - \Gamma(\rho)\Gamma(f-\rho) - \Gamma(\sigma)\Gamma(f-\sigma) + \Gamma(f) \\ &= 2e^{-j\alpha[2\rho^2+2\sigma^2+f^2-2f\rho+2\rho\sigma-2f\sigma]} - e^{-j\alpha[f^2+2\rho^2+2\sigma^2-2f\rho+4\rho\sigma-2f\sigma]} \\ &\quad - e^{-j\alpha[f^2+2\rho^2-2f\rho]} - e^{-j\alpha[f^2+2\sigma^2-2f\sigma]} + e^{-j\alpha f^2} \\ &= 2e^{-j\alpha a} - e^{-j\alpha b} - e^{-j\alpha c} - e^{-j\alpha d} + e^{-j\alpha e}\end{aligned}$$

where,

$$a = 2\rho^2 + 2\sigma^2 + f^2 - 2f\rho + 2\rho\sigma - 2f\sigma$$

$$b = f^2 + 2\rho^2 - 2f\rho$$

$$c = f^2 + 2\rho^2 - 2f\rho$$

$$d = f^2 + 2\sigma^2 - 2f\sigma$$

$$e = f^2$$

Therefore,

$$\begin{aligned}|X(f)|^2 &= \left| 2e^{-j\alpha a} - e^{-j\alpha b} - e^{-j\alpha c} - e^{-j\alpha d} + e^{-j\alpha e} \right|^2 \\ &= [2\cos(\alpha a) - \cos(\alpha b) - \cos(\alpha c) - \cos(\alpha d) + \cos(\alpha e)]^2 \\ &\quad + [2\sin(\alpha a) + \sin(\alpha b) + \sin(\alpha c) + \sin(\alpha d) - \sin(\alpha e)]^2 \\ &= |X_1(f)|^2 + |X_2(f)|^2\end{aligned}$$

where,

$$\begin{aligned}|X_1(f)|^2 &= 4\cos^2(\alpha a) + \cos^2(\alpha b) + \cos^2(\alpha c) + \cos^2(\alpha d) + \cos^2(\alpha a) + \cos^2(\alpha e) \\ &\quad - 4\cos(\alpha a)\cos(\alpha b) - 4\cos(\alpha a)\cos(\alpha c) - 4\cos(\alpha a)\cos(\alpha d) + 4\cos(\alpha a)\cos(\alpha e) \\ &\quad + 2\cos(\alpha b)\cos(\alpha d) - 2\cos(\alpha b)\cos(\alpha e) + 2\cos(\alpha b)\cos(\alpha c) + 2\cos(\alpha c)\cos(\alpha d) \\ &\quad - 2\cos(\alpha c)\cos(\alpha e) - 2\cos(\alpha d)\cos(\alpha e)\end{aligned}$$

and,

$$\begin{aligned}
|X_2(f)|^2 &= 4 \sin^2(\alpha a) + \sin^2(\alpha b) + \sin^2(\alpha c) + \sin^2(\alpha d) + \sin^2(\alpha a) + \sin^2(\alpha e) \\
&\quad + 4 \sin(\alpha a) \sin(\alpha b) + 4 \sin(\alpha a) \sin(\alpha c) + 4 \sin(\alpha a) \sin(\alpha d) + 4 \sin(\alpha a) \sin(\alpha e) \\
&\quad + 2 \sin(\alpha b) \sin(\alpha d) + 2 \sin(\alpha b) \sin(\alpha e) + 2 \sin(\alpha b) \sin(\alpha c) + 2 \sin(\alpha c) \sin(\alpha d) \\
&\quad + 2 \sin(\alpha c) \sin(\alpha e) + 2 \sin(\alpha d) \sin(\alpha e)
\end{aligned}$$

Therefore,

$$\begin{aligned}
|X(f)|^2 &= |X_1(f)|^2 + |X_2(f)|^2 \\
&= 4 \{ \sin^2(\alpha a) + \cos^2(\alpha a) \} + \{ \sin^2(\alpha b) + \cos^2(\alpha b) \} + \{ \sin^2(\alpha c) + \cos^2(\alpha c) \} \\
&\quad + \{ \sin^2(\alpha d) + \cos^2(\alpha d) \} + \{ \sin^2(\alpha e) + \cos^2(\alpha e) \} - 4 \{ \cos(\alpha a) \cos(\alpha b) - \sin(\alpha a) \sin(\alpha b) \} \\
&\quad - 4 \{ \cos(\alpha a) \cos(\alpha c) - \sin(\alpha a) \sin(\alpha c) \} - 4 \{ \cos(\alpha a) \cos(\alpha d) - \sin(\alpha a) \sin(\alpha d) \} \\
&\quad + 4 \{ \cos(\alpha a) \cos(\alpha e) + \sin(\alpha a) \sin(\alpha e) \} + 2 \{ \cos(\alpha b) \cos(\alpha d) + \sin(\alpha b) \sin(\alpha d) \} \\
&\quad - 2 \{ \cos(\alpha b) \cos(\alpha c) - \sin(\alpha b) \sin(\alpha c) \} + 2 \{ \cos(\alpha b) \cos(\alpha c) + \sin(\alpha b) \sin(\alpha c) \} \\
&\quad + 2 \{ \cos(\alpha c) \cos(\alpha d) - \sin(\alpha c) \sin(\alpha d) \} - 2 \{ \cos(\alpha c) \cos(\alpha e) - \sin(\alpha c) \sin(\alpha e) \} \\
&\quad - 2 \{ \cos(\alpha d) \cos(\alpha e) - \sin(\alpha d) \sin(\alpha e) \} \\
&= 8 - 4 \cos \alpha (a + b) - 4 \cos \alpha (a + c) - 4 \cos \alpha (a + d) + 4 \cos \alpha (a - c) - 2 \cos \alpha (b - d) \\
&\quad - 2 \cos \alpha (b + e) + 2 \cos \alpha (b - c) + 2 \cos \alpha (c - d) - 2 \cos \alpha (c + e) - 2 \cos \alpha (d + c)
\end{aligned}$$

